UNIVERSITY OF CALIFORNIA, MERCED

Anthropogenic Sources of Carbonyl Sulfide: Implications for inverse analysis of process-level carbon cycle fluxes

A dissertation submitted in partial satisfaction of the requirements for the degree of Doctor of Philosophy

In

Environmental Systems

by

Andrew Lee Zumkehr

2017

Committee in charge:

Professor J. Elliott Campbell, Chair
Professor Teamrat A. Ghezzehei
Professor Wolfgang F. Rogge
Professor Mukesh Singhal

The Dissertation of Andrew Lee Zumkehr is approved, and it is acceptable in quality and form for publication on microfilm and electronically:

Professor Teamrat A. Ghezzehei

Professor Wolfgang F. Rogge

Professor Mukesh Singhal

Professor J. Elliott Campbell (Chair)

University of California, Merced

2017

Table of Contents

List of Tables

List of Figures

Acknowledgements

This work was supported by the U.S. Department of Energy, Office of Science, and Office of Terrestrial Ecosystem Sciences. Monthly coal consumption data was provided by K. Gurney.

I would like to thank my advisor Professor J. Elliott Campbell for his support and guidance through my graduate studies. I have had an excellent experience working in his lab where I gained many valuable technical and professional skills.

I would like to thank Professor Teamrat A. Ghezzehei, Professor Wolfgang F. Rogge and Professor Mukesh Singhal for their constructive input and guidance throughout my research at the University of California, Merced.

I would like to thank Dr. Le Kuai, Dr. Steve Smith, and Dr. John Worden for their support in collaboration of my research and my colleagues of the Campbell Lab at the University of California, Merced who directly supported various parts of my research: Dr. Timothy Hilton, James Stinecipher and Dr. Mary Whelan.

I would like to thank my friends and colleagues that I met during undergraduate research for their continued advice and support: Dr. Otto Alvarez, Jacob Flanagan, and Dr. Yanjun Su. Also, I would like to thank my undergraduate research advisor Professor Qinghua Guo for encouraging me to pursue graduate research.

I would also like to thank Professor James T. Randerson and his lab group for their hospitality while I was visiting the University of California, Irvine for one year.

Portions of Chapter 2 are a reprint of research as it appears in "Gridded anthropogenic emissions inventory and atmospheric transport of carbonyl sulfide in the U.S." in *Journal of Geophysical Research: Atmospheres*. Chapter 3 contains a figure obtained from "Estimate of carbonyl sulfide Tropical oceanic surface fluxes using Aura Tropospheric Emission Spectrometer observations" in *Journal of Geophysical Research: Atmospheres*. Permission to use copyrighted material in this dissertation has been granted by John Wiley and Sons.

I would also like to thank my family, especially my wife Joannee Zumkehr and my mother Janet Zumkehr, for all their invaluable encouragement and support.

Curriculum Vita

Andrew Lee Zumkehr

7301 Virtuoso – Irvine, CA 92620 – (209) 756-7049

andrewzumkehr@gmail.com

EDUCATION

Ph.D. – Environmental Systems (August, 2017), University of California, Merced

M.S. – Environmental Systems (2013), University of California, Merced

B.S. – Computer Science & Engineering (2011), University of California, Merced

PEER-REVIEWED PUBLICATIONS (* Under Review)

Campbell JE, Whelan M, Berry J, Hilton T, **Zumkehr** A, Stinecipher J, Lu Y, Kornfeld A, Seibt U, Dawson T, Montzka S (In Review). Coast redwood sink of atmospheric carbonyl sulfide provides a new biogeochemical tracer for coastal fog-mediated processes. *Journal of Geophysical Research: Biogeosciences.*

Zumkehr A, Hilton T, Whelan M, Smith S, Campbell JE (2017). Gridded anthropogenic emissions inventory and atmospheric transport of carbonyl sulfide in the U.S. *Journal of Geophysical Research: Atmospheres*. DOI: 10.1002/2016JD025550

Hilton T, Whelan M, **Zumkehr A**, Kulkarni S, Berry J, Baker I, Montzka S, Sweeney C, Miller B, Campbell, JE (2017). Peak growing season gross uptake of carbon in the USA is largest in the Midwest region. *Nature Climate Change.*

Zumkehr A & Campbell JE (2015). The potential of local croplands to meet food demand in the United States. *Frontiers in Ecology and the Environment* 13(5): 244-248. **News:** Capital Public Radio**,** Washington Post**,** NPR

Hilton T, **Zumkehr A**, Kulkarni S, Berry J, Whalen M, Campbell E (2015). Large variability in ecosystem models explains a critical parameter for quantifying GPP with carbonyl sulfide. *Tellus B.* 67.

Zumkehr A & Campbell JE (2013). Historical U.S. cropland areas and the potential for bioenergy production on abandoned croplands. *Environmental Science & Technology* 47(8): 3840-3847.

Campbell JE, Lobell DB, Genova RC, **Zumkehr A** & Field CB (2013). Seasonal energy storage using bioenergy production from abandoned croplands. *Environmental Research Letters* 8(035012): 7-13

SKILLS SUMMARY

Languages: Python, R, Fortran, GrADS, SQL, shell scripting, html

Software/OS: Windows, Linux, ESRI products, QGIS, SAGA GIS, Zope, GrAds, PostgreSQL

Instrumentation: LAI, hyper-spectral sensor, Garmin and Trimble GPS devices, laser and sonar range finders

PROFESSIONAL EXPERIENCE

***Graduate Researcher**, University of California and Merced* **2011 - Present**

- Investigating atmospheric COS concentrations to constrain estimates of terrestrial plant carbon interactions using Fortran-based atmospheric transport modeling, data mining, GIS spatial analysis, python scripting and by creating spatial data sets and cartography products.
- Investigating the water-food nexus, sustainable agriculture and water recycling.
- Conducting a feasibility analysis of the installation of solar panels over aqueducts and testing the proposed benefits by conducting a GIS analysis of potential evaporative savings from shading California canals and aqueducts. Also, conducting in a net present value cost analysis of the project. Presented findings to members of California Legislature in Sacramento.
- Researching the potential for the U.S. to feed its population locally using several local food system scenarios by developing python-based cropland allocation optimization models. This work was

presented to the Global Food Initiative and generated publications in several media outlets including the National Public Radio and the Washington Post.
- Researched the energy storage need required by intermittent renewable energy sources in a 100% renewable energy scenario in the U.S. and estimated the potential of biomass energy to meet the energy storage requirement using spatial analysis and python scripting techniques.
- Modeled historic U.S. cropland and abandoned cropland distributions and estimated U.S. biomass energy potential on abandoned cropland. Created a python-based land-use change model, cartography products and spatial data sets.

GIS Analyst (Contractor)**, Professor/Author Paul Almeida* ***2012
- Created cartography products for publication use in *Mobilizing Democracy* by Paul Almeida.
- Pre-processed and analyzed GIS data.
- Mentored client in the use of ESRI products and basic spatial analysis techniques.

GIS Analyst/Programmer**, Sierra Nevada Research Institute* ***2009 - 2011
- Overlay analysis, cartography productions, synthesis of spatial data sets, scripted GIScience data processing and data conversions.
- Compared the accuracy of niche modeling algorithms implemented in the ModEco software to similar implementations within the statistical computing language R.
- Conducted field work for the collection of ground-true measurements used to validate LIDAR products. Instrumentation: LAI, hyper-spectral sensor, Garmin and Trimble GPS devices, laser and sonar range finders.

GIS Web Developer**, Sierra Nevada Research Institute* ***2009 - 2010
- Managed and maintained websites written with JavaScript, html and python for the Sierra Nevada Research Institute, the National Critical Zone Observatory and the Southern Sierra Critical Zone Observatory.
- Mentored other SNRI webpage developers.
- Created cartography products for webpages visualization.
- Used Google Maps API to display research locations.

AWARDS

Environmental Systems Summer Fellowship ($3,100)	**2017**
UCOP Global Food Initiative Fellowship ($8,000)	**2015**
UC Merced's Global Food Initiative Fellowship ($2,500)	**2014**
Environmental Systems Summer Fellowship ($7,000)	**2014**
Environmental Systems Graduate Bobcat Fellowship ($6,000)	**2014**
Environmental Systems Summer Fellowship ($7,000)	**2013**
Environmental Systems Graduate Bobcat Fellowship ($6,000)	**2013**

Abstract

Anthropogenic Sources of Carbonyl Sulfide: Implications for inverse analysis of process-level carbon cycle fluxes

by
Andrew Zumkehr
Doctor of Philosophy in Environmental Systems
University of California, Merced, 2017
Prof. J. Elliott Campbell, Chair

Carbonyl sulfide (COS or OCS) is emerging as a potentially important tracer of terrestrial biological carbon fluxes. Anthropogenic sources of atmospheric COS are a first order uncertainty for utilizing COS as a tracer of the carbon cycle. As anthropogenic COS is a confounding source of atmospheric COS when interpreting COS observations, incorrect estimates of anthropogenic COS sources can introduce large interpretation bias when attempting to infer carbon cycle fluxes. However, the current gridded estimate of anthropogenic sources of atmospheric COS is largely derived from data over three decades old and therefore is not likely to be representative of current atmospheric conditions. Here I address this critical knowledge gap by providing a new gridded estimate of anthropogenic COS sources derived from the most current industry activity and emissions factor data available and employ a more sophisticated approach for the spatial distribution of sources than presented in previous work. This new data set results in a very different picture of the spatial distribution of anthropogenic sources of COS and in a large upward revision in total global sources than estimated in previous work. The large missing source of atmospheric COS needed to balance the global budget of atmospheric COS has largely been attributed to an unknown ocean source in previous work. However, considering the large upward revision of anthropogenic COS sources estimated here, I present the hypothesis that anthropogenic sources may be a key component of the missing source of atmospheric COS. I present subsequent modeling scenarios to test this hypothesis and show that anthropogenic COS sources can explain observations of atmospheric COS as well as or better than enhanced ocean sources. Therefore, the data set of anthropogenic sources of COS presented here emerges as a key component of reducing interpretation bias when inferring carbon cycle fluxes using COS and for explaining the missing source of atmospheric COS and balancing the global COS budget (which has previously not been considered).

Chapter 1: Introduction

This work is a study of the current understanding of anthropogenic sources of atmospheric carbonyl sulfide (COS or OCS) and the implications that revisions to estimates of the anthropogenic source of atmospheric COS has for inverse analysis of process-level carbon cycle fluxes and for understanding the global total atmospheric budget of COS.

COS, a trace gas with typical atmospheric concentrations close to 500 parts per trillion (ppt) and a total atmospheric lifetime of approximately 1.5 to 3 years[*Montzka et al.*, 2007; *Campbell et al.*, 2008], has been of increasing interest to studies related to carbon-climate, carbon cycle, atmospheric composition and trace gas remote sensing retrieval studies [*Kjellstrom*, 1998; *Kettle et al.*, 2002; *Montzka et al.*, 2004, 2007; *Suntharalingam et al.*, 2008; *Blake et al.*, 2008; *Campbell et al.*, 2008, 2013; *Blonquist et al.*, 2011; *Maseyk et al.*, 2012; *Berry et al.*, 2013; *Kuai et al.*, 2014, 2015; *Billesbach et al.*, 2014; *Hilton et al.*, 2017; *Launois et al.*, 2015; *Glatthor et al.*, 2015; *Hilton et al.*, 2015; *Lee and Brimblecombe*, 2016; *Du et al.*, 2016; *Anthony Vincent and Dudhia*, 2017; *Zumkehr et al.*, 2017]. A key motivation for increased interest in COS stems from the hypothesis that COS may be useful as an atmospheric tracer of the carbon cycle at leaf to regional scales [*Montzka et al.*, 2007; *Blake et al.*, 2008; *Campbell et al.*, 2008].

Terrestrial biological carbon fluxes are a key component to future climate projections [*Arneth et al.*, 2010; *Intergovernmental Panel on Climate Change*, 2014]. Terrestrial biological carbon fluxes are largely controlled by photosynthetic CO_2 uptake (gross primary production, GPP) and respiration; however, there currently exists large uncertainties and variability in estimates of these fluxes [*Friedlingstein et al.*, 2006, 2014; *Huntzinger et al.*, 2012; *Hilton et al.*, 2015, 2017]. Therefore, the hope that COS can be used as an atmospheric tracer of the carbon cycle to constrain these uncertainties has led to a quick intensification in COS research.

It is hypothesized that COS can be used as a powerful tracer of the carbon cycle because over 80% of the global COS sink participates in an analogous biogeochemical process to the photosynthesis of carbon dioxide (CO_2), however COS is not respired by plants [*Montzka et al.*, 2007; *Campbell et al.*, 2008; *Anthony Vincent and Dudhia*, 2017]. This allows for measurement based differentiation between terrestrial photosynthetic and respiration fluxes in the atmosphere at large spatial scales. Like CO_2, COS passes through plant stomata during photosynthesis where a one way reaction with carbonic anhydrase in the presence of water occurs to produce both CO_2 and hydrogen sulfide [*Protoschill-Krebs et al.*, 1996; *Anthony Vincent and Dudhia*, 2017]. Therefore, COS is not respired by plants, unlike CO_2. Furthermore, experimentation has established a strong relationship between the uptake of COS and CO_2 during photosynthesis, allowing the COS tracer approach to be used to infer the CO_2 flux into plants [*Stimler et al.*, 2010].

However, for COS to be confidently used as a tracer of the carbon cycle, two key concepts must be demonstrated: 1) that the uncertainty in the relationship between the plant uptake of COS and CO_2 is less uncertain than the range of terrestrial ecosystem models the COS tracer approach is trying to improve, and 2) that confounding sources of atmospheric COS can be quantified. The first was demonstrated by Hilton et al. (2015) while the second is an ongoing problem where the dominant sources and sinks of COS (oceans, anthropogenic activity, soils, plants) are continually being evaluated [*Watts*, 2000; *Kettle et al.*, 2002; *Berry et al.*, 2013; *Campbell et al.*, 2015].

The uncertainty in the confounding anthropogenic source is the key motivation for the research presented here. Anthropogenic COS sources have received relatively little attention from the scientific community. The currently available gridded anthropogenic COS emissions data set consists of input data over three decades old [*Kettle et al.*, 2002]. Yet, this data is still being used in current modeling studies [*Campbell et al.*, 2008; *Suntharalingam et al.*, 2008; *Berry et al.*, 2013; *Launois et al.*, 2014].

Chapter 2, "Gridded Anthropogenic Emissions Inventory and Atmospheric Transport of Carbonyl Sulfide in the U.S.", begins this body of work by reevaluating anthropogenic COS sources in the U.S., using the most current industry activity, emissions factor and spatial distribution data available as a case study to determine the need/usefulness of revising global anthropogenic COS sources and what implications might arise pertaining to carbon-climate studies. The U.S. was chosen for the spatial extent of this first study because 1) a high concentration of National Oceanic and Atmospheric Administration (NOAA) COS air monitoring sites are located in North America [*Montzka et al.*, 2007] and, 2) the U.S. rayon industry (rayon production is one of the largest indirect sources of anthropogenic COS [*Watts*, 2000]) has been in sharp decline suggesting a very different picture of anthropogenic COS sources in the U.S. than currently available data sets would suggest. The new data set of U.S. anthropogenic sources of COS presented in this study shows interestingly different estimates, in both magnitude and spatial distribution. These differences suggest that using the currently available data set could lead to considerable interpretation bias of COS observations at NOAA monitoring sites pertaining to using COS as a tracer of the carbon cycle.

Chapter 3 "Global Gridded Anthropogenic Emissions Inventory of Carbonyl Sulfide" is a follow-up to Chapter 2, using what was learned in revising the U.S. anthropogenic COS source estimates and adapting the methodology to a global extent. The result of this chapter is a new inventory of global anthropogenic COS sources with a finer spatial resolution, longer study period, more sophisticated spatial scaling strategy and the most comprehensive composition of sources ever presented before in a gridded inventory of anthropogenic COS sources. Similar to the U.S. inventory from Chapter 2, the global inventory from Chapter 3 presents a very different picture of anthropogenic COS sources, both in magnitude and spatial distribution, than presented by previous gridded estimates [*Kettle et al.*, 2002]. An intriguing and unexpected result of the global update to anthropogenic COS sources was the large magnitude of the upward revision (more than

double) of total global anthropogenic sources of COS in comparison to previous work and the concentration of these sources in China.

Total global, annual tropospheric measurements of COS concentrations show little variability over the past decade, suggesting that COS sources and sinks are similar in magnitude [*Kettle et al.*, 2002; *Montzka et al.*, 2007; *Kuai et al.*, 2015]. However, while previous estimates of global COS sources are balanced, a recent large upward revision in the global plant sink of COS in conjunction with the stability in atmospheric observations of COS concentrations suggests a large missing source of COS [*Sandoval-Soto et al.*, 2005; *Montzka et al.*, 2007]. While previous work has hypothesized that the missing source could be due to a large photochemical ocean enhancement of COS emissions [*Berry et al.*, 2013; *Glatthor et al.*, 2015; *Kuai et al.*, 2015], other recent studies cast doubt on the missing ocean source hypothesis [*Lennartz et al.*, 2016].

Chapter 4 "Anthropogenic Sources as an Explanation of the Missing Source of Atmospheric Carbonyl Sulfide" tests two possible explanations of the missing source of atmospheric COS: 1) the anthropogenic source hypothesis (developed in this study), and 2) the ocean source hypothesis (developed in previous work). The test is conducted by driving an atmospheric transport model with different sources and sinks of atmospheric COS characterized by the competing anthropogenic and ocean hypotheses and comparing the resulting simulated atmospheres to observations of atmospheric COS. Favorable representation of the atmosphere derived from increased anthropogenic sources in comparison to observations suggests that anthropogenic sources of COS are an important component to the missing source of atmospheric COS.

Three key results are demonstrated in the following chapters: 1) new estimates of anthropogenic COS sources based on the newest input data available and more sophisticated spatial distribution methods produce a very different picture of anthropogenic sources of COS than previous estimates (which are still being used in modeling studies today); 2) using outdated anthropogenic COS sources in modeling studies has the potential to introduce large bias when making interpretations of COS observations; 3) anthropogenic COS is a strong candidate as an alternative or complementary explanation to ocean sources for closing the COS budget; an assertion that has not previously been demonstrated or proposed before.

Chapter 2: Gridded Anthropogenic Emissions Inventory and Atmospheric Transport of Carbonyl Sulfide in the U.S.

2.1 Abstract

COS is the most abundant sulfur-containing gas in the troposphere and has recently emerged as a potentially important atmospheric tracer for the carbon cycle. Atmospheric inverse modeling studies may be able to use existing tower, airborne, and satellite observations of COS to infer information about photosynthesis. However, such analysis relies on gridded anthropogenic COS source estimates that are largely based on industry activity data from over three decades ago. Here we use updated emission factor data and industry activity data to develop a gridded inventory with a 0.1° resolution for the U.S. domain. The inventory includes the primary anthropogenic COS sources including direct emissions from the coal and aluminum industries as well as indirect sources from industrial carbon disulfide emissions. Compared to the previously published inventory, we found that the total anthropogenic source (direct and indirect) is 47% smaller. Using this new gridded inventory to drive the Sulfur Transport and Deposition Model/Weather Research and Forecasting atmospheric transport model, we found that the anthropogenic contribution to COS variation in the troposphere is small relative to the biosphere influence, which is encouraging for carbon cycle applications in this region. Additional anthropogenic sectors with highly uncertain emission factors require further field measurements.

2.2 Introduction

A key component of climate change modeling is characterizing the carbon-climate feedbacks driven by photosynthesis and respiration carbon fluxes [*Cox et al.*, 2000; *Friedlingstein et al.*, 2006; *Field et al.*, 2007]. Regional-scale measurements of these carbon fluxes are needed to improve the understanding of these highly uncertain feedback mechanisms. While observations of atmospheric CO_2 concentrations provide regional information on the net effect of photosynthesis and respiration surface fluxes [*Gurney et al.*, 2002], additional approaches are needed to partition the regional net flux into the photosynthesis and respiration components for a better understanding of carbon-climate feedbacks.

COS is being investigated as a means to address this critical knowledge gap as a regional-scale tracer of photosynthetic CO_2 uptake (gross primary production, GPP) [*Montzka et al.*, 2007; *Campbell et al.*, 2008]. Terrestrial plant uptake has been shown to be the dominant continental sink for atmospheric COS in a process that is closely related to GPP [*Campbell et al.*, 2008]. Unlike CO_2, COS does not have a large ecosystem source at regional scales. The dominant global COS source is in the tropical oceans [*Berry et al.*, 2013; *Launois et al.*, 2014; *Glatthor et al.*, 2015; *Kuai et al.*, 2015]. Because the dominant COS sink is strongly related to GPP and the dominant COS source is spatially separated from the sink,

there is potential for inverse analysis of atmospheric COS observations to be used to infer regional GPP. While some canopy-scale observations have detected ecosystem COS sources at times, regional-scale evidence demonstrates that COS plant uptake dominates the variation observed in large-scale continental measurements [*Montzka et al.*, 2007; *Campbell et al.*, 2008; *Berry et al.*, 2013; *Maseyk et al.*, 2014a; *Commane et al.*, 2015; *Wang et al.*, 2016; *Whelan et al.*, 2016]. Fortunately the photosynthetic relationship between COS and CO_2 uptake by terrestrial plants is relatively stable across a variety of vegetation types [*Sandoval-Soto et al.*, 2005; *Stimler et al.*, 2010; *Hilton et al.*, 2015]. Furthermore, this variability imposes relatively small variations in atmospheric COS [*Hilton et al.*, 2015]. The use of regional COS analysis to infer GPP relies on comprehensive budgets of COS sources and sinks. Aside from the plant sink and ocean source, the most significant budget component is anthropogenic activity [*Campbell et al.*, 2015]. Previous atmospheric COS models that interpret atmospheric COS measurements rely on the gridded anthropogenic COS inventory from Kettle et al. (2002). The Kettle inventory is a spatial extrapolation of a global estimate that was largely derived from industry activity data that are at least three decades old and emission factors that are known to be biased [*Campbell et al.*, 2015]. An updated gridded inventory is now needed to support COS tracer applications.

A recent inventory of anthropogenic COS sources provided an update to the global source estimate [*Campbell et al.*, 2015]. While the inventory methods from that study were used for global, historical estimates, these methods could also be applied to create spatially explicit, gridded inventories that are needed for regional COS analysis. Here we use these methods to develop a gridded inventory for U.S. emissions. The U.S. domain is of particular interest because it has the highest density of COS air-monitoring data globally which makes regional COS analysis possible in this domain [*Montzka et al.*, 2007]. We also used our new estimate of gridded anthropogenic fluxes as input to a regional atmospheric chemical transport model to explore the significance of using our revised inventory in comparison to the Kettle inventory. Our gridded 0.1° resolution inventory is available online to the scientific community at http://portal.nersc.gov/project/m2319/.

2.3 Methods

2.3.1 Inventory Modeling

An inventory of U.S. anthropogenic COS sources was constructed on a 0.1° resolution grid for the three dominant sectors previously considered in the Kettle inventory: direct emissions from coal combustion, direct emissions from aluminum smelting, and indirect sources from anthropogenic carbon disulfide (CS_2) emissions that are rapidly oxidized to COS in the atmosphere. We also created estimates for additional sectors that were either minor sources in the Kettle inventory or not included in the Kettle inventory. These additional sectors include the pigment industry, transportation, sulfur recovery, and the pulp and paper industry. Emissions are estimated as the product of emission factors (mass of emission per unit of anthropogenic activity) and spatially and temporally explicit U.S. industry activity data. Detailed emission factor information is provided in Campbell et al.

(2015) which was shown to provide a significant update to the outdated emission factor data applied in the Kettle inventory. The emission factor approach from Campbell et al. (2015) is also summarized below along with the data we used for U.S. industry activity. The approach from the Kettle inventory is also briefly summarized below for comparison. Our results for each of the COS sources described below are summarized in Table 2-1.

Table 2-1. Summary of direct and indirect COS anthropogenic sources (Gg S y^{-1} as COS) in the U.S. from this study and from the Kettle inventory.[a]

Source	**This Study**	**Kettle**
Rayon CS_2	0	23 ± 12
Other Industry CS_2	6.1 ± 3.1	NA
Agriculture CS_2 Application	5.9 ± 3.0	NA
Coal, Direct COS	2.9 ± 1.2	3.6 ± 1.8
Aluminum, Direct COS	1.3 ± 0.4	7.7 ± 3.9
Pigment Industry		
Carbon Black, Direct COS	0.1 - 8.5	NA
Carbon Black, Indirect via CS_2	0.2 - 20.5	NA
TiO_2, Direct COS	9.9 ± NA	NA
Sulfur Recovery		
Direct COS	0.3 - 12.7	0.2 ± 0.1
Indirect via CS_2	0.1 - 5.5	NA
Pulp and paper		
Direct COS	15.2 ± NA	NA
Indirect via CS_2	9.9 ± NA	NA
Tires		
Direct COS	2.0 ± NA	NA
Indirect via CS_2	2.3 ± NA	NA
Total	56 - 103	34 ± 17

[a]NA indicates not available. Ranges for pigment and sulfur recovery assume emission sources are controlled for minimum and uncontrolled for maximum.

2.3.1.1 Coal Combustion

The inventory for the U.S. coal COS source utilizes updated emission factors from the NASA North American Intercontinental Chemical Transport Experiment airborne campaign which revealed that the single emission factor observation used in Kettle inventory underestimated the U.S. emission factor by a factor of 2 [*Blake et al.*, 2008]. Based on these data, we used an emission factor of 2.3 and 6.0 ppt COS ppm CO_2^{-1} for the western and eastern U.S. regions, respectively. The industry activity was based on year 2010 national coal consumption [*U.S. Energy Information Administration*, 2003]. We extrapolated this estimate in space and time using U.S. county-level coal consumption data

which was available for the year 2002 [*U.S. Energy Information Administration*, 2003]. The industry activity approach for the Kettle inventory was based on the global coal consumption in year 1989 which was spatially and temporally extrapolated using year 1985, 1° gridded anthropogenic SO_2 emissions.

2.3.1.2 Aluminum Smelting

Aluminum emission factors have been examined for a range of anode sulfur contents, emission control devices, and smelter types (prebake and Söderberg smelters) [*Kimmerle and Noel*, 1997; *Utne et al.*, 1998]. Based on these data, we used an emission factor of 0.9 kg S t Al^{-1}. The Kettle inventory overestimated the emission factor due to a failure to account for smelter types and the nonlinear relationship between anode sulfur content and COS emissions [*Utne et al.*, 1998]. Industry activity was based on individual production levels at each aluminum smelter in the U.S. for the year 2012 [*U.S. Geological Survey*, 2013]. The industry activity approach for the Kettle inventory was based on the global aluminum production in year 1995 which was spatially and temporally extrapolated using year 1985, 1° gridded anthropogenic SO2 emissions.

2.3.1.3 Industrial CS_2 Applications

Global anthropogenic COS sources are dominated by the indirect source from industrial CS_2 emissions during rayon production [*Campbell et al.*, 2015; *Lee and Brimblecombe*, 2016]. The emitted CS_2 is rapidly oxidized to COS in the troposphere [*Chin and Davis*, 1993]. Atmospheric oxidation of CS2 to COS has a molar conversion efficiency that has been estimated at 81% [*Chin and Davis*, 1993]. In the U.S., rayon production has been in decline beginning in the 1970s and is no longer produced in the U.S. using CS_2 [*Blagoev and Funada*, 2011; *Fiber Economics Bureau*, 2014]. Thus, our inventory does not include rayon emissions. However, the Kettle inventory includes a large rayon source in the U.S. because it uses a map of 1985 anthropogenic SO_2 emissions to scale the global rayon source in space.

Atmospheric emissions of CS_2 have also been reported from other applications including solvents and agriculture chemicals [*Peyton et al.*, 1978; *Blagoev and Funada*, 2011]. To estimate emissions from these categories, we use year 2010 U.S. consumption data of 20,000 t for agriculture CS_2 application and 21,000 t for other industrial applications [*Blagoev and Funada*, 2011]. We assume that 80% of these applications are emitted to the atmosphere as CS_2 due to high volatility and low solubility in water [*Chin and Davis*, 1993]. We scale the industrial applications in space using EDGAR v4.2 fields of N_2O, and we scale the agriculture applications using a U.S. cropland map [*Joint Research Centre*, 2011; *Zumkehr and Campbell*, 2013]. We use the 81% molar conversion efficiency for this and all subsequent CS_2 emissions.

Future measurements may allow the differentiation of emission factors by crop types, management, and industrial applications. Nevertheless, our approach using U.S. specific data represents an advance over the Kettle inventory which relied on an estimate of the

year 1984 consumption of rayon which was spatially and temporally extrapolated using year 1985, 1° gridded anthropogenic SO_2 emissions.

2.3.1.4 Additional Sources

We also estimated sources from sectors that were either minor sources in the Kettle budget or not included in that inventory. The pigment industry has been noted to emit COS and CS_2 but was not accounted for in the Kettle inventory. First, we consider the pigment carbon black which includes sources of COS and CS_2. For carbon black, emission factors are 10 kg COS/Mg carbon black produced and 30 kg CS_2/Mg carbon black produced [*Blake et al.*, 2004]. Previous work noted that the emission factors were reduced by 99% in developed countries due to emission controls [*Blake et al.*, 2004]. We used the controlled and uncontrolled emission factors to provide a lower and upper range for this source. As with all indirect emissions from CS_2, we use the molar oxidation conversion factor from CS_2 to COS of 81%. For industry activity, we use the U.S. carbon black production in year 2015 of 1.6 × 106 t. Production of the pigment TiO_2 results in direct emissions of COS. We used an emission factor of 14.7 g COS/kg of TiO_2 produced [*Blake et al.*, 2004] and industry activity of 1.26 × 106 t for the year 2014 [*Lee and Brimblecombe*, 2016].

For the tire wear source, which were not included in the Kettle inventory, we base our emission factor on the following emission data: 1.17 kg rubber emitted/car/yr, 1.6% sulfur content of rubber, and a fraction of sulfur emissions as 43% COS and 57% CS2 [*Pos and Berresheim*, 1993; *Lee and Brimblecombe*, 2016]. The activity for the tire emissions is 253 million U.S. vehicles.

Next we estimate emissions from sulfur recovery which were a minor source in the Kettle inventory. Previous inventories have used an emission factor of 0.263 g COS/kg sulfur recovered [*Peyton et al.*, 1978]. However, more recent reports for U.S. emission factors are 0.1 and 2.7 g COS/kg sulfur recovered for controlled and uncontrolled emissions, respectively, and 0.02 and 0.9 g CS_2/kg sulfur recovered for controlled and uncontrolled emissions, respectively. Here we use the more recent estimates to provide a lower and upper limit. For industry activity, we used 9 × 106 t of sulfur recovery in the year 2014 [*Apodaca*, 2015].

The global pulp and paper industry has previously been reported to result in 97 Gg S-COS/yr and 79 Gg S-CS_2/yr [*Lee and Brimblecombe*, 2016]. Here we scale this global estimate to U.S. emissions based on the ratio of U.S. to global pulp and paper production (16%). This sector was not included in the Kettle inventory. At present, the emission factor data are highly speculative for these additional sources. Thus, we included estimates of these sources in our national estimates for comparison with other sectors (Table 2-1), but we did not include these additional sources in our gridded inventory.

2.3.2 Atmospheric Transport Modeling

We used our gridded anthropogenic COS inventories and the Kettle inventory as input to the Sulfur Transport and Deposition Model (STEM) with meteorological fields provided by the Weather Research and Forecasting version 2.2 (WRF) model. STEM has been widely applied for analysis of anthropogenic and biosphere exchange with the atmosphere for U.S. and other regional domains [*Carmichael et al.*, 1991; *Campbell et al.*, 2007; *D'Allura et al.*, 2011; *Kulkarni et al.*, 2014]. STEM is a mesoscale, 3-D Eulerian model that employs a finite difference numerical approach to solve the chemical continuity equation. The WRF and STEM simulations were completed for July and August in year 2008 and have a 60 km horizontal resolution and 22 vertical levels. While simulations of the seasonal cycle are an important next step for future studies, the growing season focus of the present study is useful because this is the time period when the COS tracer approach is most likely to yield information on GPP due to the peak growing season conditions. For comparison, we simulated the atmospheric signature of the biosphere using plant uptake fluxes from Hilton et al. (2015).

2.4 Results

The U.S. total emissions for our estimates and the Kettle inventory are compared in Table 2-1. In total, U.S. anthropogenic sources of COS, from our estimate, are only 47% of the Kettle source estimate when only comparing the sources considered in the Kettle inventory. Including other sectors leads to a much larger anthropogenic source, but these sectors are based on speculative emission factors.

While the coal source of COS was found to be similar in magnitude in both estimates, the updated inventory for the aluminum source of COS is 17% of the previous estimates and the industrial CS_2 inventory is 52% of the previous estimates. The difference for aluminum is due to the recent data showing a lower emission factor, and the difference for CS_2 is largely due to the decline of the U.S. rayon industry.

The large difference in the industrial CS_2 source estimate between our inventory and the Kettle inventory is due to the fact that the Kettle inventory is based on a global, gridded SO_2 emission inventory as a proxy for spatial scaling. While SO_2 emissions may be useful as a preliminary spatial scalar of anthropogenic activity, they lead to large regional biases in COS emission estimates because industrial CS_2 activity has a very different spatial distribution than SO_2 emissions. The Kettle emissions result in a large CS_2 source in the U.S., but our industry-specific data show that CS_2 emissions in the U.S. are relatively small.

The differences between the detailed U.S. inventory in this study and the preliminary U.S. inventory from Campbell et al. (2015) are due to several factors. First, this study estimates a smaller coal source because of differentiation of emission factors for the eastern and western U.S. while Campbell et al. (2015) assumed a constant national emission factor. Second, we estimate a larger CS_2 source because we account for CS_2

use reported from multiple industrial and agriculture activities while Campbell et al. (2015) focused on rayon. Finally, we find a smaller aluminum source because we assume that smelters are evenly split between prebake and Söderberg smelters while Campbell et al. (2015) assumed that the fraction was the same as the global mix (90% of smelter are prebake).

Emission factors and industry activity data both contribute to the differences found in our estimate compared to previous work. Our coal emissions are based on a larger set of measurements that suggest an emission factor that is double the rate assumed in the Kettle inventory [*Blake et al.*, 2008]. Furthermore, our spatial scaling is based on recent U.S. county-level coal consumption data which provides a different level of industry activity than assumed by the SO_2 scaling approach in the Kettle inventory. Although new industry activity data and emissions factors are used here, our estimate for the magnitude of the coal source remains similar to that of the Kettle inventory because the increased emissions factor offsets the smaller industry activity totals.

We also report large sources for other sectors that were either minor sources in the Kettle inventory or not included (Table 2-1). When considering these additional sources that are not taken into account in the Kettle inventory, our estimate becomes approximately 1.6 to 3 times larger than that of the Kettle inventory. These additional sources could be much larger than the CS_2 application, coal, and aluminum sources described above. However, these estimates are based on highly uncertain emission factor data in comparison to the emission factor data available for CS_2 application, coal, and aluminum. The upper limit for the total source of 103 Gg S yr^{-1} seems particularly unlikely given the persistent drawdown of tropospheric COS observed over North America during the growing season [*Campbell et al.*, 2008].

While the national-scale source from coal is similar for our estimate and the Kettle inventory, the spatial variation is different. Comparison of emissions maps (Figure 2-1, left) shows a high concentration of the coal COS source in the northeast for the Kettle inventory but a more widely dispersed source in our estimates. The surface enhancement in atmospheric COS mixing ratios in the boundary layer as simulated by STEM/WRF can exceed 10 ppt in regions of anthropogenic activity (Figure 2-1, right).

While the Kettle inventory uses the same spatial scaling for all anthropogenic sectors, our emissions inventory uses industry-specific data for the spatial scaling of each sector. The aluminum emissions were based on aluminum smelting data, giving the locations of individual smelting plants, and are mapped in Figure 2-2. The revised aluminum estimates also show a wider distribution than the Kettle emissions, particularly in the midcontinent, southeast, Texas, and northwest.

Figure 2-3 shows the spatial distribution of anthropogenic CS_2 sources of anthropogenic COS for industrial activity (top) and agriculture applications (bottom). While Kettle used the same spatial scaling based on SO_2 for all sources of COS (Kettle CS_2 distribution could look identical to Figure 2-1 (top row, left), but with a higher magnitude), our distribution

based on cropland locations and industrial N_2O provide a much different spatial representation of the CS_2 sector. We find emissions of modest magnitude spread over large areas for sources derived from agriculture CS_2 applications and intense hot spots from the industrial CS_2 sector.

The wider spatial distribution in our estimates includes regions where NOAA air-monitoring sites are located (Figures 2-1 and 2-3) [*Montzka et al.*, 2007]. In particular, our emissions show that some NOAA sites are located within hot spots of anthropogenic COS emissions. While the plant uptake is generally thought to be much larger than the anthropogenic source [*Campbell et al.*, 2008], these revised emission estimates may be useful in reducing the uncertainty associated with interpreting COS observations at the colocated sites.

To this end, we examined the influence of anthropogenic emissions on the NOAA sites that are located within regional hot spots of anthropogenic emissions. STEM/WRF simulations that were driven by only plant uptake show a widely dispersed and large sink that is characteristic of ecosystem fluxes (Figure 2-4). These simulations are consistent with the large plant uptake flux in the Corn Belt region and the prevailing westerly winds that result in low tropospheric COS mixing ratios in the midcontinent region. We extracted simulated vertical profiles from three STEM/WRF runs that were driven by plant uptake, our coal emissions, and the Kettle coal emissions (Figure 2-5). We considered the NOAA airborne monitoring stations at HIL (Homer, Illinois, USA) and SCA (Charleston, South Carolina, USA).

Two metrics are compared at these monitoring sites: average July concentrations and the day of peak anthropogenic mixing ratio enhancement. The peak anthropogenic day is solely due to transport because there is no daily variation in our anthropogenic emission estimate. Even in these emission hot spots, the simulated biosphere signal is roughly twice the anthropogenic signal for the average monthly vertical profile (Figure 2-5, top row). This is due to the large spatial extent of the biosphere sink. However, for the peak anthropogenic day, the anthropogenic signal can be similar in magnitude to the biosphere signal on that same day (Figure 2-5, bottom row). This suggests that the climatological analysis of air-monitoring data will be less sensitive to anthropogenic emissions, but a more time-resolved analysis of these data will benefit from the improved emissions inventory presented here.

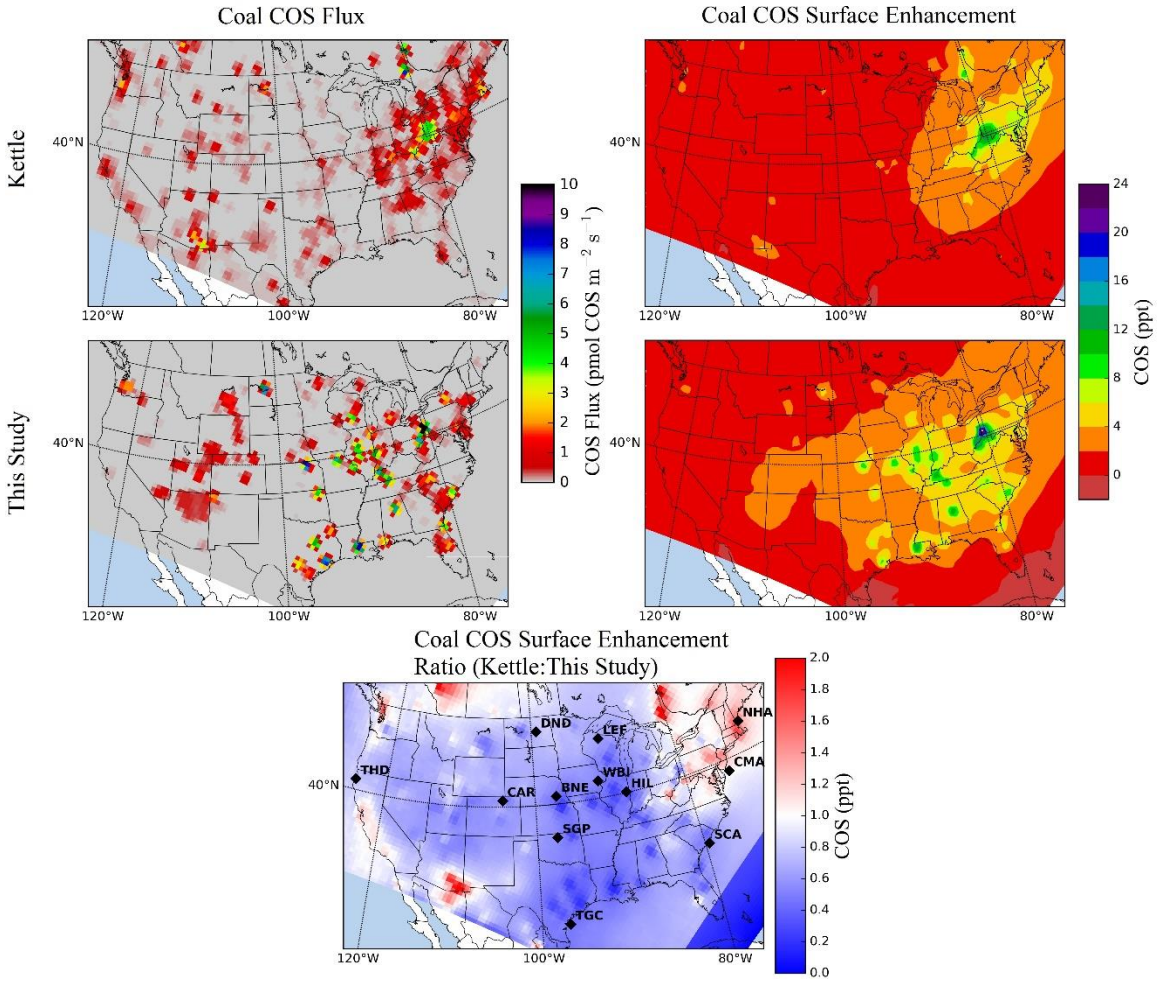

Figure 2-1. Comparison of coal COS sources from the Kettle inventory (top row) and our updated inventory (middle row) and the ratio of the surface enhancements from the previous COS inventory and from this study (bottom). Modeled surface enhancement is for July and August (mean difference between free troposphere and boundary layer mixing ratios).

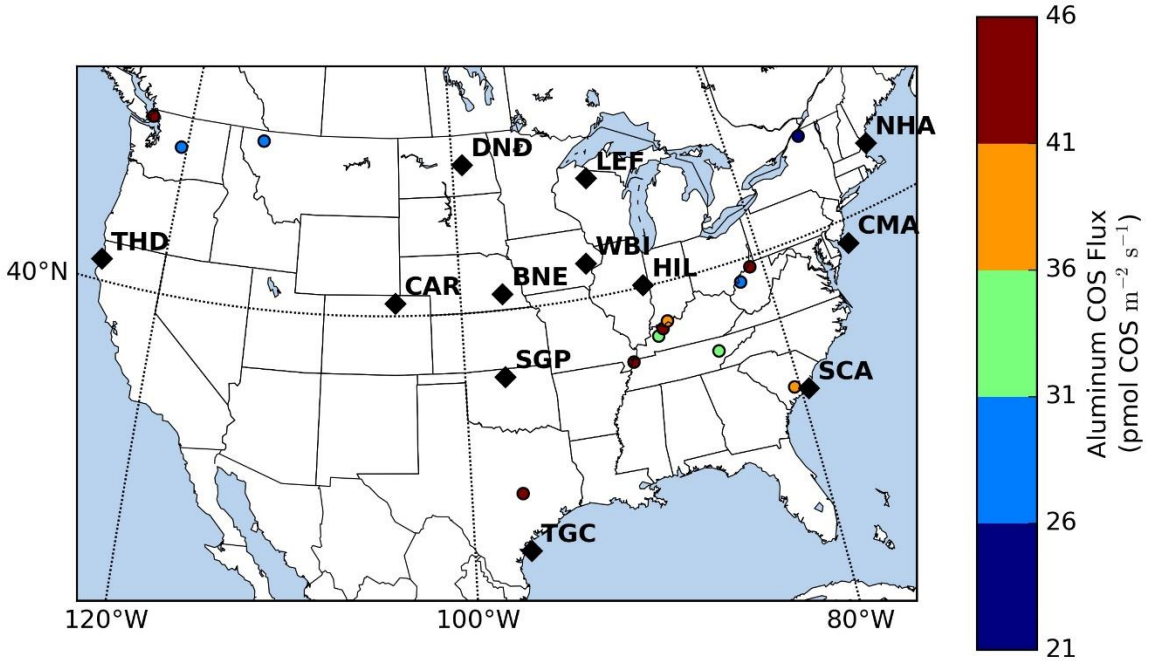

Figure 2-2. COS flux from aluminum smelting in the U.S. for 2012 (circles) and locations of NOAA air-monitoring sites that measure atmospheric COS from airborne platforms in the U.S. (diamonds). Additional surface sites not shown here but are presented in Montzka et al. (2007).

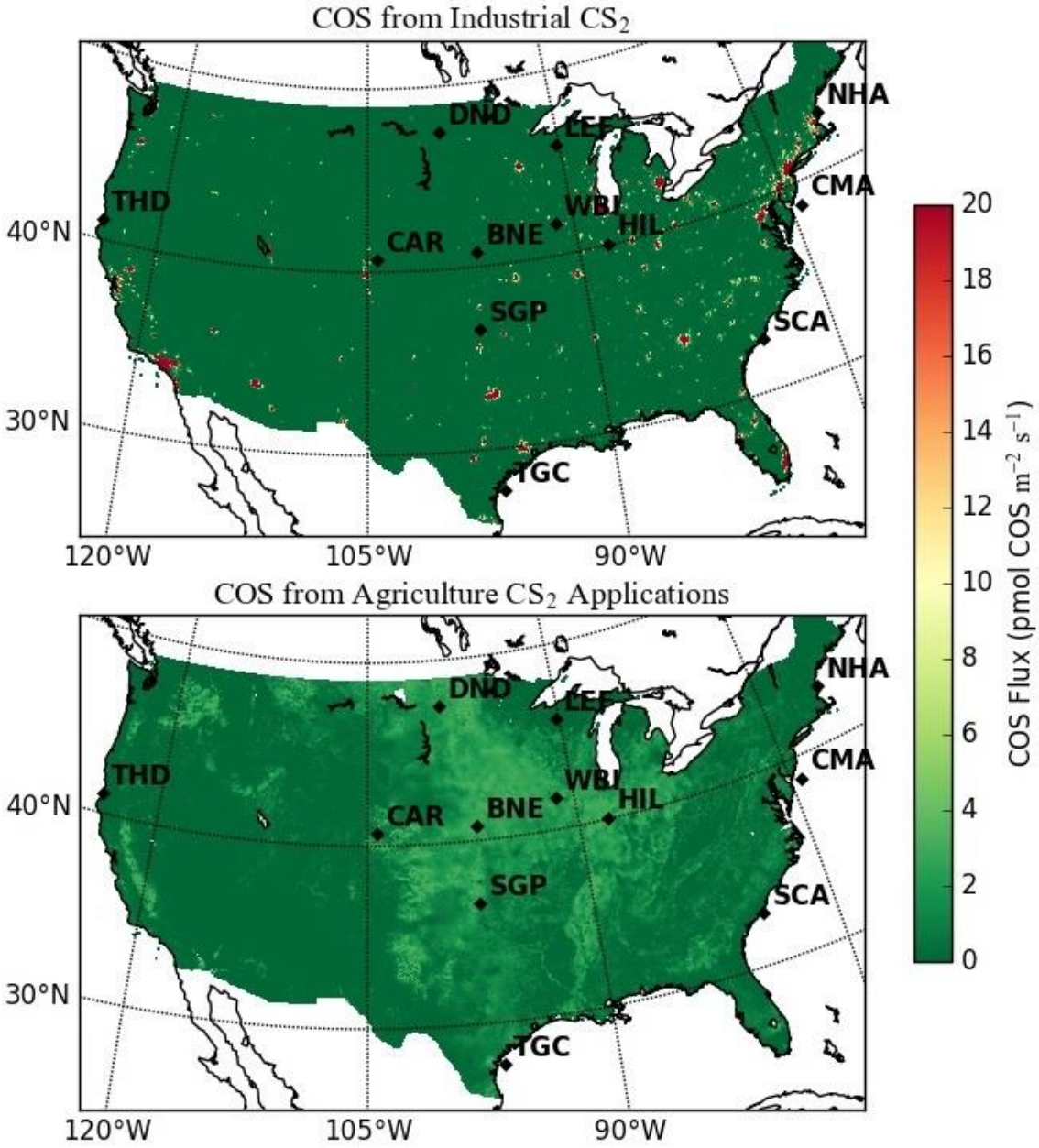

Figure 2-3. COS sources from anthropogenic CS_2 applications to (top) industrial processes and (bottom) agriculture CS_2 applications.

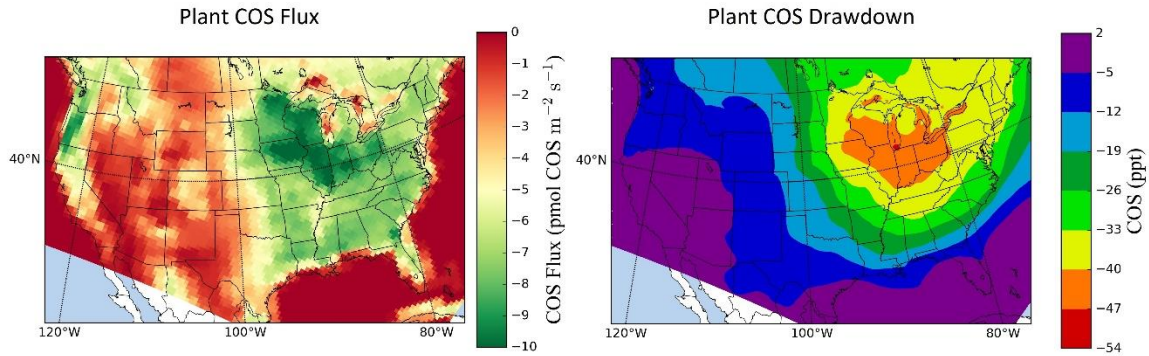

Figure 2-4. CASA GFED-3 (left) plant COS flux and the average (right) plant COS tropospheric vertical drawdown for July and August 2008, simulated by the STEM/WRF atmospheric transport model with CASA GFED-3 COS plant surface fluxes.

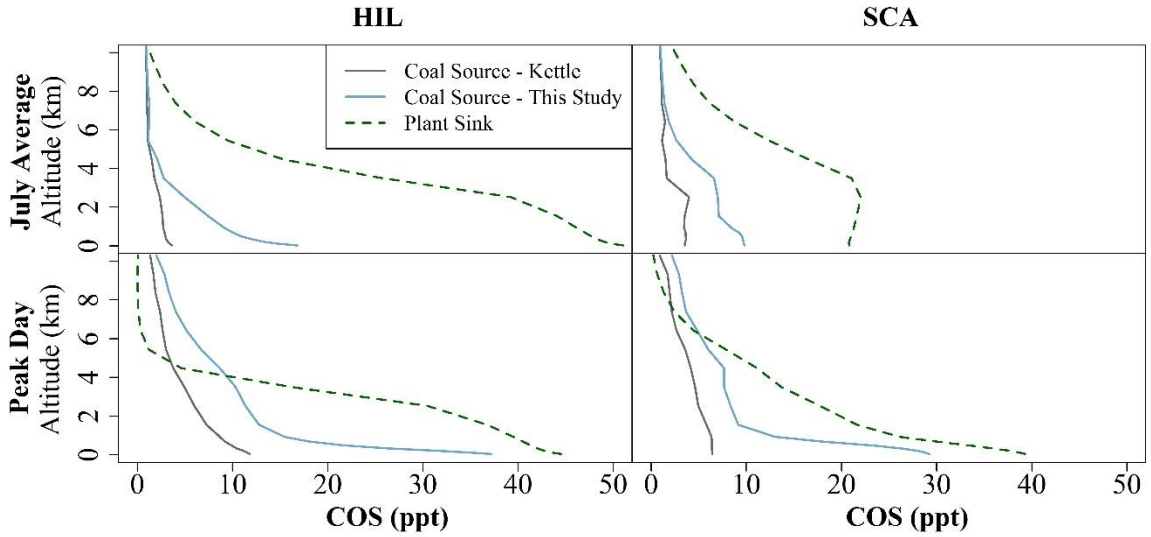

Figure 2-5. A comparison of the average coal COS surface enhancement from this study (blue), from the Kettle inventory (grey) and plant COS drawdown from CASA GFED-3 (dashed green line) at the Homer, Illinois (HIL), and Charleston, South Carolina (SCA), NOAA airborne monitoring sites for July and August and the peak coal COS enhancement day. The x axis shows the absolute value of the vertical profile (both the biosphere drawdown and anthropogenic enhancement are plotted as positive on the x axis) to allow for visual comparison of the biosphere and anthropogenic activity.

2.5 Discussion

Here we have demonstrated that updated anthropogenic COS inventories based on more recent industrial activity and emissions factors data have significantly different magnitudes and spatial distributions than previous inventories that were based on a smaller subset of emission factor data and outdated industry activity data. Additionally, we demonstrated that the simulated impact on the atmosphere based on this new anthropogenic COS emissions inventory can have very different spatial signatures (including the coal sector,

despite similar magnitudes) (Figure 2-1). It follows that interpretations of observations using these simulations could be similarly biased, especially if the study area or observation site is near anthropogenic COS hot spots.

The analysis presented here includes multiple sources of uncertainty in the emission estimates and the transport simulations. The uncertainty in the atmospheric transport simulations is a result of uncertain meteorological data, numerical integration, and subgrid processes. STEM model accuracy has been demonstrated in previous work [*Campbell et al.*, 2007, 2008; *D'Allura et al.*, 2011]. However, these uncertainties will have similar effects on all three transport simulations presented in this paper and should not influence our conclusions regarding the comparison of the three cases.

The main sources of uncertainty for the magnitude of the anthropogenic emissions depend largely on the emissions factors. The industry activity data, on the other hand, are likely to be more accurate due to the economic importance of tracking these data. The estimated uncertainty for the magnitudes of anthropogenic COS sources from this study are ±30% for aluminum and ±40% for coal. CS_2 uncertainty is represented here as an upper estimate due to source data limitations where the lower estimate is based on an emissions factor previously applied to a study in Japan that used an emissions factor that was half of what was used here [*Blake et al.*, 2004].

The spatial pattern of the coal COS source is based on county-level coal consumption data which is sufficient for regional analysis that is the intended application of this inventory. However, for applications that require Aluminum emissions are more easily resolved spatially as there are relatively few smelting plants and the location and production share are known for each [*U.S. Geological Survey*, 2013].

The atmospheric transport simulations presented in this study were conducted to examine the sensitivity of atmospheric COS profiles to the industrial source relative to the biosphere sink. Such simulations may also provide a framework for a top-down assessment of our anthropogenic inventory when combined with atmospheric measurements. This top-down assessment would require atmospheric observations for times (e.g., winter) and locations (e.g., western U.S.) in which the industrial source may be dominant and the biosphere sink relatively small. Future field campaigns would be needed to support such an assessment. However, even without a top-down assessment, our updated inventory provides a significant advance over the previous Kettle inventory which was based on a small subset of the published emission factor data and outdated industry activity data.

Chapter 3: Global Gridded Anthropogenic Emissions Inventory of Carbonyl Sulfide

3.1 Abstract

COS is the most abundant sulfur containing gas in the troposphere and is currently being considered as a possible atmospheric tracer of the carbon cycle. However, a high-resolution, contemporary inventory of global anthropogenic sources of atmospheric COS is needed for interpreting these modeling studies but is not available. The currently available gridded data, which is being used in atmospheric transport modeling studies, is based on input data that is over three decades old and is likely not representative of current conditions. This study proposes a new, higher-resolution (0.1° latitude × 0.1° longitude) data set of global anthropogenic COS sources that includes more sources than previously available and uses the most current emissions factors and industry activity data as input. Additionally, the inventory is provided as annually varying estimates from 1980 to 2012 and employs a source specific spatial scaling procedure. Significant differences in both magnitude and spatial patterns of anthropogenic COS sources are found in comparison to previous work. The new global source estimate of 406 Gg S y^{-1} is about twice as large as the previous gridded inventory and is highly concentrated in China

3.2 Introduction

Measurement based estimates of regional-scale carbon fluxes are needed to improve our understanding of carbon-climate feedbacks. These feedbacks are driven by photosynthesis and respiration fluxes and are key components in climate change modeling [*Cox et al.*, 2000; *Friedlingstein et al.*, 2006; *Field et al.*, 2007; *Glatthor et al.*, 2015]. While measurements of CO_2 over terrestrial vegetation are useful for quantifying the net exchange of carbon during photosynthesis and respiration [*Gurney et al.*, 2002], they are not useful for differentiating photosynthesis and respiration fluxes.

An emerging approach for solving this problem, is the use of regional and global COS observations to estimate the underlying GPP sink [*Montzka et al.*, 2007; *Campbell et al.*, 2008, 2015].
The dominant COS sink at regional scales is uptake by terrestrial vegetation in a process that is closely related to GPP [*Sandoval-Soto et al.*, 2005; *Campbell et al.*, 2008]. The COS plant sink is largely controlled by stomatal conductance which in turn is closely related to GPP, particularly for regional COS observations [*Hilton et al.*, 2017]. Furthermore, experimentation has established a strong relationship between the uptake of COS and CO_2 during photosynthesis, allowing the COS tracer approach to be used to infer the CO_2 flux into plants [*Stimler et al.*, 2010]. Thus, the absence of COS respiration by plants makes detecting changes in COS concentrations over terrestrial vegetation a means of quantifying

regional scale photosynthetic activity and partitioning the photosynthetic and respiration fluxes. Existing observations of COS concentrations, including TES, TRACE-P and NOAA Airborne and tower monitoring networks, can be utilized to drive the COS tracer approach [*Montzka et al.*, 2007; *Glatthor et al.*, 2015; *Kuai et al.*, 2015; *Wang et al.*, 2016].

The major source of atmospheric COS is derived from oceans [*Berry et al.*, 2013; *Kuai et al.*, 2014; *Launois et al.*, 2014; *Glatthor et al.*, 2015]. This spatial and temporal separation of the major ocean source from the dominant sink of COS by terrestrial vegetation allows for most locations to be strongly suited for the COS tracer approach. However, some confounding sources of COS exist at certain locations. These additional sources must be known for the COS tracer approach to be applied with confidence. The most significant confounding COS source component is the anthropogenic source of COS [*Campbell et al.*, 2015].

Previous estimates of anthropogenic sources of COS suffer from various limitations that weaken their suitability for use in the COS tracer approach. This approach involves the use of gridded inventories as input to 3-D atmospheric transport models to constrain the influence of anthropogenic activities on COS observations [*Berry et al.*, 2013]. The Kettle inventory, while a global and gridded data set, is now quite dated as it is composed of industry activity data from over three decades ago [*Kettle et al.*, 2002]. The Kettle inventory also does not provide any yearly trends and has a relatively course spatial resolution of 1° latitude × 1° longitude [*Kettle et al.*, 2002]. The age of the input data brings into question the data set's ability to represent current anthropogenic processes that result in COS emissions. For example, the Kettle inventory reports a large source of anthropogenic COS from rayon production in the U.S., however current reports show that this industry has largely shifted to China [*Fiber Economics Bureau*, 2014]. Additionally, the Kettle inventory does not differentiate between the spatial distributions of the various components of the anthropogenic COS source but instead distributes them all according to global industrial SO_2 fields [*Kettle et al.*, 2002]. A more recent estimate of historical global anthropogenic COS sources was made for the years 1850 to 2013 using the most current industry activity data and emissions factors but does not explore methodology for spatially distributing the inventory into a gridded format suitable for spatially explicit modeling studies. Additionally, high-resolution regional gridded data has been developed, but these inventories do not provide historical estimates and they are limited to the U.S. and Asia [*Blake et al.*, 2004; *Zumkehr et al.*, 2017].

Previous work has identified a large missing source of atmospheric COS from around 230 to as much as 800 Gg Sulfur per year, which has generally been attributed to a missing oceanic source [*Suntharalingam et al.*, 2008; *Berry et al.*, 2013; *Glatthor et al.*, 2015; *Kuai et al.*, 2015; *Lennartz et al.*, 2016]. However, recent work finding under-saturation of ocean surface waters with respect to COS and low global annual direct emissions of COS from oceans suggest that it is unlikely that the missing source is coming from oceans [*Lennartz et al.*, 2016]. Additionally, there is evidence presented in recent work for considering larger anthropogenic COS emissions than previously accepted [*Lee and Brimblecombe*, 2016]. However, this evidence cannot be incorporated into the analysis of COS observations

because the estimates are not gridded and in some cases are not based on emissions data [*Lee and Brimblecombe*, 2016]. Therefore, this study proposes that a revision of global estimates of anthropogenic COS sources could reveal an anthropogenic explanation of a large portion of the missing source of atmospheric COS. Furthermore, this hypothesized upward revision in anthropogenic sources of COS could result either through increased industrial activity or by introducing new anthropogenic sources that have been largely neglected in previous work.

Given the limitations of the Kettle gridded inventory and the recent advances in understanding anthropogenic source [*Campbell et al.*, 2015; *Lee and Brimblecombe*, 2016], we have developed a new global gridded inventory of the primary emission sectors. The inventory has a 0.1° spatial resolution and uses the most current emission factors and industry activity data as input. The inventory is provided as annually varying estimates from years 1980 to 2012 and employs a source specific spatial scaling procedure.

3.3 Methods

The inventory developed here includes direct and indirect anthropogenic sources. Indirect sources of COS result from anthropogenic carbon disulfide (CS_2) emissions which are rapidly oxidized to COS in the atmosphere [*Watts*, 2000; *Wang et al.*, 2001; *Kettle et al.*, 2002]. The atmospheric oxidation of CS_2 to COS has a molar conversion rate of 87% [*Barnes et al.*, 1994]. Source estimates reported in the study (results section 4) are the sum of direct and indirect sources.

The anthropogenic sources of COS considered in this study are: agricultural chemicals, aluminum smelting, carbon black production, industrial and residential coal consumption, pulp & paper industries, rayon production, industrial solvent applications, titanium dioxide production and tire wear [*Watts*, 2000; *Campbell et al.*, 2015; *Du et al.*, 2016; *Lee and Brimblecombe*, 2016]. Industrial coal consumption includes manufacturing and electricity production. We did not include biomass burning (e.g. open burning, agriculture waste, biofuel) because this source is generally modeled with a separate inventory [e.g. Berry et al., 2013]. Furthermore, soil emissions from managed lands are not included here as they are typically modeled separately using soil flux models that account for concurrent soil sinks and sources [*Hilton et al.*, 2017].

Table 3-1. Input data for the anthropogenic sources of COS considered in this study.

Source	Industry Activity	Emissions Factor	Sub-Country Spatial Scaling	Temporal Scaling
Agricultural Chemicals	Country-level consumption of CS_2 (CEH agricultural chemicals category)[a]	Proportion of CS_2 emitted to atmosphere: 80%[b]; Molar conversion to COS: 87%[c]	Agriculture land[d]	Yearly consumption of CS_2 and average growth rates of CS_2 consumption[a]
Aluminum Smelting	Country-level primary aluminum production[e]	0.6 kg COS/Mg Al for prebake[f], 1.2 for Söderberg	Industrial CO_2[g]	Yearly country-level aluminum primary production[e]
Industrial Coal	Country-level coal consumption[h]	4.7 to 6.8 µmol COS mol CO_2 $^{-1}$ [i]; Scaled by SO_2 emissions	Energy industry and waste incinerator SO_2[g]	Yearly country level-coal SO_2 emissions[h]
Residential Coal	Country-level residential coal consumption[j]	0.47 to 1.75 g COS kg^{-1} coal consumed [k]	Energy for buildings SO_2[g]	Yearly residential coal consumption[j]
Industrial Solvents	Country-level consumption of CS_2 (CEH other category)[a]	solvent CS_2: 80% is emitted to atmosphere, 87% molar conversion to COS[b,a]	Industrial N_20[g]	Yearly consumption of CS_2 and average growth rates of CS_2 consumption[a]
Carbon Black	Global estimates of carbon black production for select years[l,m n,o,p,q,r]; global production share[m,n]	10 g OCS kg^{-1} carbon black produced; 30g CS_2 kg^{-1} carbon black produced; 99% removal from developed countries[t]	Chemical industry NH_3[g]	Linear interpolation of industry activity data
Titanium Dioxide	Country-level production[u]	14.7 g COS kg^{-1} titanium dioxide produced[t]	Chemical industry NH_3 [g]	Yearly production[u]
Pulp & Paper	Country-level production[v,w]	Emissions scaled from previous work by industry activity data[x]	Manufacturing industry CO_2[g]	Yearly production[v,w]
Rayon Yarn	Country-level cellulosic fiber production[y]	0.25 g CS_2 g^{-1} yarn[z]	Industrial N_2O[g]	Yearly cellulosic fiber production[y]
Rayon Staple	Country-level cellulosic fiber production[y]	0.12 g CS_2 g^{-1} staple (year ≤ 2000)[z]; 0.07g CS_2 g^{-1} staple (year > 2000)[aa]	Industrial N_2O[g]	Yearly cellulosic fiber production[y]
Tires	Cars in use (years ≥ 2004)[ab]; Cars 1000 population^{-1} (yeas < 2004)[ab,bc]	1.17kg rubber y^{-1} vechicle$^{-1,}$ 43% COS, 57% CS_2[ad]; 1.6% rubber released as sulfur[ae]	Transportation CO_2[g]	Yearly cars in use (years ≥ 2004)[ac]; Product of population by vehicle ownership (yeas < 2004)[ab,ac,af]

[a][*Blagoev and Funada*, 2011], [b][*Chin and Davis*, 1993], [c][*Barnes et al.*, 1994], [d][*Ramankutty et al.*, 2008], [e][*U.S. Geological Survey*, 2012], [f][*Kimmerle and Noel*, 1997], [g][*Joint Research Centre*, 2011], [h][*Smith et al.*, 2011], [i][*Blake et al.*, 2008], [j][*United Nations Statistics Division*, 2016a], [k][*Du et al.*, 2016], [l][*IARC - World Health Organization*, 1984], [m][*IARC - World Health Organization*, 2010],

[n][Büchel et al., 2000], [o][Crump, 2000], [p][Gandhi, 2005], [q][ICBA, 2016a], [r][Lee and Brimblecombe, 2016], [s][U.S. Environmental Protection Agency, 2003], [t][Blake et al., 2004], [u][U.S. Geological Survey, 2015], [v][Food and Agriculture Organization, 2010], [w][United Nations Statistics Division, 2016b], [x][EPA Office of Air Quality Planning and Standards and EPA Office of Air and Radiation, 2012], [y][Fiber Economics Bureau, 2014], [z][U.S. Environmental Protection Agency, 2003], [aa][Dodd et al., 2013], [ab][Dargay et al., 2007], [ac][OICA, 2016], [ad][Pos and Berresheim, 1993], [ae][Susa and Haydary, 2013], [af][The World Bank, 2016]

Table 3-1 Continued.

For each source, four pieces of data are required to estimate the magnitude of the source and then to distribute the source spatially and through time: industry activity data, emissions factors, sub-country spatial scaling models and temporal scaling data. Often the industry activity data set also provides the information for temporal scaling. However, in some cases when data is sparse or emissions factors change through time, additional data are needed (see source specific sections below). Sub-country spatial scaling is performed by distributing country-level estimates to a grid based on a gridded proxy flux. The IPCC code associated with the gridded proxy flux is used as the criteria for identifying the flux that most closely describes the specific anthropogenic estimate that needs to be distributed. Table 3-1 summarizes the input data used in the creation of each of the anthropogenic sources of COS calculated in this study. Figure 3-1 is a flowchart of the process of creating the global anthropogenic COS sources inventory presented here. The following sections describe the specific methods and data used to create the estimates of direct or indirect emissions of anthropogenic COS for each source.

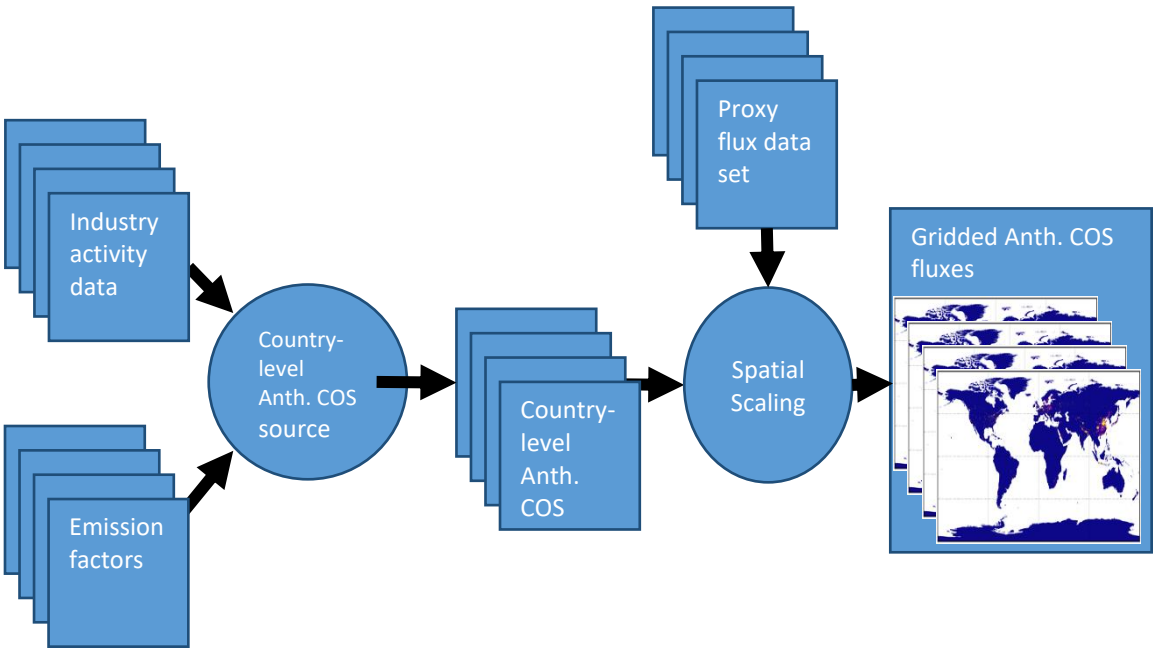

Figure 3-1. Process flowchart describing the input data and steps taken to arrive at the global anthropogenic (anth.) COS inventory created from this study. This process is repeated for each year and COS source. Rectangles represent a data set and ovals represent a processing step.

3.3.1 Agricultural Chemicals

Agricultural chemicals derived from CS_2 are an indirect source of COS. These agricultural chemicals are commonly used as insecticides and fumigants [*Hinds*, 1902]. A component of CS_2 used to form agricultural chemicals is released to the atmosphere and then oxidized to COS via tropospheric hydroxide [*Chin and Davis*, 1993; *Wang et al.*, 2001]. Thus, agricultural chemicals are likely a component COS source that are emitted over large areas of global agriculture lands.

Here we estimate the country-level consumption of agricultural chemicals by searching consumption reports for the total amount of CS_2 used specifically for agricultural chemical applications [*Blagoev and Funada*, 2011]. However, only a portion of the CS_2 used for non-cellulosic applications (such as agricultural chemicals) reaches the atmosphere [*Chin and Davis*, 1993]. We assume this emissions factor to be approximately 80% based on the assumptions of previous work [*Chin and Davis*, 1993]. Once the CS_2 has reached the atmosphere, the molar conversion efficiency of the CS_2 oxidation to COS is approximately 87% [*Barnes et al.*, 1994].

We convert our country-level emissions into a sub-country gridded map using maps of croplands as a spatial proxy [*Ramankutty and Foley*, 1999].

Data for agricultural chemicals for all years considered in this study are not available in the CEH report for all countries. However, average growth rates are presented in the CEH report and are used here to extrapolate the approximate amount of CS_2 used in agricultural chemicals for missing years [*Blagoev and Funada*, 2011]. A summary for the input data used to estimate the source of COS from agricultural chemicals can be found as part of Table 3-1.

3.3.2 Aluminum Smelting

Aluminum smelting is a significant source of atmospheric COS [*Harnisch et al.*, 1995; *Watts*, 2000]. There are two main methods used for aluminum smelting: Söderberg and prebake [*Kimmerle and Noel*, 1997]. Country-level primary production of aluminum is obtained from USGS reports [*U.S. Geological Survey*, 2012]. To obtain the COS emitted per mass of aluminum produced, the emissions factors of 0.6 and 1.2 kg COS Mg Al^{-1} are used for prebake and Söderberg, respectively [*Kimmerle and Noel*, 1997]. Prebake is a more efficient smelting technique, resulting in fewer emissions of many chemical species, including COS. Due to the lack of data describing these smelting techniques at the factory level and because these techniques result in significantly different emissions factors, a method for estimating the distribution and production share of each of these technologies must be developed. It is estimated that in the year 2012, 90% of the global aluminum production was produced through the prebake smelting process [*Campbell et al.*, 2015]. Therefore, we assume all countries in the year 2012 conform to this ratio of prebake to Söderberg smelting and that any reductions in smelting in previous years are subtracted

from prebake smelting to simulate the gradual adoption of the new prebake technology over time.

The COS source estimated for each country is proportionally distributed over EDGAR v4.2 industrial CO_2 emissions for the appropriate year [*Joint Research Centre,* 2011]. CO_2 is a major emission of aluminum smelting so industrial emissions are used as a constraining spatial proxy for aluminum smelting in the absence of a more robust option [*Harnisch et al.*, 1995]. A summary for the input data used to estimate the source of COS from aluminum smelting can be found as part of Table 3-1.

3.3.3 Coal Consumption

Coal consumption is traditionally considered as the largest direct source of anthropogenic COS [*Watts*, 2000; *Blake et al.*, 2008] where COS is emitted from coal combustion [*Watts*, 2000]. We consider two classes of coal consumption in this study: industrial coal consumption by power plants and residential coal consumption for cooking and heating. Typically, when coal is considered as an anthropogenic COS source in previous work, only the industrial component of power plant consumption is considered [*Watts*, 2000; *Kettle et al.*, 2002]. However, recent work suggests potentially large emissions of COS from residential coal consumption [*Du et al.*, 2016]. A summary for the input data used to estimate the sources of COS from coal can be found as part of Table 3-1. Sections 3.3.3.1 and 3.3.3.2 provide specific methods for the industrial and residential components, respectively.

3.3.3.1 Industrial Coal

Industrial coal combustion by power plants is a large direct source of atmospheric COS [*Watts*, 2000; *Kettle et al.*, 2002; *Campbell et al.*, 2015]. Country-level industry activity data of industrial coal consumption is readily available [*Smith et al.*, 2011]. However, the emissions factors for translating coal consumption to COS emissions are underdeveloped on a global scale.

While studies for the emissions factor for COS from coal consumption in the United States have been conducted [*Khalil and Rasmussen*, 1984; *Blake et al.*, 2008], varying combustion efficiencies, emissions controls and the sulfur content of coal in other countries suggests that the U.S. emissions factor may not be appropriate to apply globally without modification. To overcome this limitation, previous work has used the ratio of SO_2 emissions to coal consumption for each country to scale emissions factors [*Campbell et al.*, 2015]. This correction for estimating emissions factors is adopted in this.

For sub-country spatial scaling, industrial SO_2 emissions are used to proportionally distribute the estimated country-level COS estimates [*Joint Research Centre,* 2011]. SO_2 distributions are selected for constraining COS resulting from industrial coal consumption because SO_2 is a co-product of coal combustion [*Kettle et al.*, 2002].

3.3.3.2 Residential Coal

Emissions factors for residential coal consumption are obtained through laboratory coal stove experimentation and by taking measurements in a farmhouse in China [*Du et al.*, 2016]. The observed emissions factors were 0.57 ± 0.10 and 1.43 ± 0.32 g COS kg^{-1} of coal for the laboratory and farmhouse studies, respectively (suggesting residential coal emissions factors that are more than 50 times larger than from power plants) [*Du et al.*, 2016]. The emissions factors obtained from farmhouse and laboratory studies present a considerable range for possible emissions factors. Here, an average of the two emissions factors is assumed for the baseline scenario and the range presented in the two studies is imbedded in the uncertainty. Also, while these emissions factors are obtained from experimentation in China and different regions may result in different emissions factors, we assume the difference to be small and to be encompassed in the range of emissions factors found in China.

Country-level residential coal consumption can be found in the United Nations Statistics Division Energy Statistics Database [*United Nations Statistics Division*, 2016a]. This industry activity data is used for the spatial and temporal distribution of the residential coal source of COS at the country-level. Similar to the industrial coal source described in the previous section, SO_2 is used as the spatial proxy source for similar reasons but is limited to residential SO_2 for this application [*Joint Research Centre*, 2011].

3.3.4 Industrial Solvents

Like agricultural chemicals, many industrial solvents result in emissions of CS_2 which then oxidizes rapidly to form COS [*Chin and Davis*, 1993; *Wang et al.*, 2001]. Unfortunately, unlike agricultural chemicals, the CEH reports for CS_2 consumption do not specifically track CS_2 based industrial solvents [*Blagoev and Funada*, 2011]. To give an upper-limit estimate in the absence of data specific to the CS_2 solvent industry, we use the CEH CS_2 "other" category to constrain the industrial solvent source of COS [*Blagoev and Funada*, 2011].

Because CS_2 industrial solvents are non-cellulosic applications, approximately 80% of the CS_2 associated with the industrial solvents reaches the atmosphere and then oxidizes to form COS at an approximate molar conversion of 87% [*Chin and Davis*, 1993].

Data for the "other" category used here to provide an upper-estimate for industrial CS_2 solvent applications are not available in the CEH report for some countries for certain years. However, average growth rates are presented in the CEH report and are used to extrapolate the approximate amount of CS_2 used for industrial solvents in missing years [*Blagoev and Funada*, 2011]. A summary for the input data used to estimate the source of COS from industrial solvents can be found as part of Table 3-1.

3.3.5 Pigment Industry

The pigments industry has recently been identified as a potentially important source of anthropogenic COS [*Blake et al.*, 2004; *ICBA*, 2016b] but has not been included in global, gridded anthropogenic COS inventories. There are two pigments that show potential for being significant sources of anthropogenic COS: carbon black and titanium dioxide (TiO_2) [*Blake et al.*, 2004; *Lee and Brimblecombe*, 2016]. Carbon black, as its name suggests, is used for black pigments while titanium dioxide is used for creating white pigments. A summary for the input data used to estimate the source of COS from pigments can be found as part of Table 3-1. Sections 3.3.5.1 and 3.3.5.2 describe the specific methods for the carbon black and titanium dioxide components of the pigment source of COS.

3.3.5.1 Carbon Black

Industry activity data for carbon black is not available for all countries or years. Global carbon black production estimates could only be found for select years from various studies or reports [*IARC - World Health Organization*, 1984; *Büchel et al.*, 2000; *Crump*, 2000; *Gandhi*, 2005; *ICBA*, 2016a]. Years where an estimate for the total global production of carbon black was not available were approximated through linear interpolation of the available data.

However, country-level divisions of the global totals described above were not included. Two reports were found that provided estimates of the country-level contribution of carbon black production by percentage for the year 2000 [*Büchel et al.*, 2000] and for the year 2005 [*IARC - World Health Organization*, 2010]. The country-level proportions of carbon black production are assumed here to apply for the closest year of global carbon black production.

The emissions factors for black carbon are 10 g COS kg^{-1} and 30 g CS_2 kg^{-1} [*U.S. Environmental Protection Agency*, 2003]. The emissions factor for TiO_2 is 14.7 g COS kg^{-1} (no CS_2 emissions) [*Blake et al.*, 2004]. A reduction in the emission factor of 99% is applied to developed countries due to emissions controls [*Blake et al.*, 2004].

Chemical industry NH_3 is used as a spatial proxy flux for distributing carbon black sources [*Joint Research Centre*, 2011]. The spatial scaling for NH_3 falls under the IPCC code for chemical industry activity and carbon black and titanium dioxide share this IPCC code making NH_3 from the EDGAR v4.2 data set the closest spatial approximation available. Country-level carbon black estimates are proportionally distributed over the NH_3 grid.

3.3.5.2 Titanium Dioxide (TiO_2)

Unlike carbon black, titanium dioxide is not characterized by large emissions of CS_2 that would oxidize to COS [*Chin and Davis*, 1993; *Barnes et al.*, 1994]. Therefore, one emissions factor of 14.7 g COS kg^{-1} titanium dioxide is used here [*Blake et al.*, 2004].

Sub-country spatial scaling is handled identically to carbon black, simply adding to the magnitude of the gridded carbon black result in the absence of any subdivision of the IPCC code for the chemical industry in the EDGAR v4.2 data set.

3.3.6 Pulp and Paper Industry

Similar to the pigment industry, the pulp and paper industry is another potentially important source of anthropogenic COS that has not been included in gridded estimates of global anthropogenic COS emissions in the past [*Kettle et al.*, 2002]. Yearly, country-level industry activity data is available from the United Nations statistics database (UN Stats) up to the year 2007 and after 2007 by a separate United Nations (UN) report on the capacities of the pulp and paper industry [*Food and Agriculture Organization*, 2010; *United Nations Statistics Division*, 2016b]. Together, these resources make a complete data set of industry activity with yearly temporal scaling resolved for production quantities of pulp and paper by country.

Previous work estimated that current global emissions from the pulp and paper industry could be as much as 97.2 Gg S y^{-1} and 78.5 Gg S y^{-1} for COS and CS_2, respectively [*Lee and Brimblecombe*, 2016]. While the industry activity data provides production quantities, the emissions factor used for estimating CS_2 and COS emissions from pulp and paper plants in previous work requires that the furnace volume is known for pulp and paper industries in each country [*Lee and Brimblecombe*, 2016]. The UN data does not provide the furnace volume nor could this data be found in other reports. Furthermore, using UN Stats industry activity to spatially distribution the global pulp and paper emissions of previous work (97.2 Gg S y^{-1} and 78.5 Gg S y^{-1} for COS and CS_2, respectively) resulted in 23 Gg S y^{-1} for the U.S. in 2010. This is in stark contrast to the U.S. EPA estimates of pulp and paper emissions of 90 tons y^{-1} and 3 tons y^{-1} for CS_2 and COS (or less than 1 Gg S y^{-1} combined), respectively [*EPA Office of Air Quality Planning and Standards and EPA Office of Air and Radiation*, 2012]. The U.S. EPA estimate is assumed to be accurate for the U.S. for the year 2010 and industry activity data from UN Stats for is used for spatiotemporal scaling.

Sub-country spatial scaling is performed using CO_2 from combustion in the manufacturing industry as the proxy flux for emissions from pulp and paper production because the IPCC code describing this section of the EDGAR v4.2 data set also includes paper production [*Joint Research Centre*, 2011]. A summary for the input data used to estimate the source of COS from pulp and paper industries can be found as part of Table 3-1.

3.3.7 Rayon Production

Despite being an indirect source of COS through the emission of CS_2, rayon production is the most significant anthropogenic component of atmospheric COS [*Campbell et al.*, 2015]. Emissions of CS_2 from rayon production can be divided into two categories, rayon yarn and rayon staple, each having different emissions factors, and magnitudes of production. Country-level rayon production is reported in the Fiber Organon for both yarn and staple categories [*Fiber Economics Bureau*, 2014].

Yarn rayon has an emissions factor of 0.25 g CS_2 per gram of yarn produced, while staple rayon production has an emissions factor of 0.12 g CS_2 per gram of staple material produced [*U.S. Environmental Protection Agency*, 2003; *Campbell et al.*, 2015]. In recent years, improved technology for the production of staple rayon has reduced the emissions factor to 0.07 g CS_2 per gram of staple produced; however, the yarn emissions factor remains unchanged [*Dodd et al.*, 2013; *Campbell et al.*, 2015]. Here, the newer emissions factor for staple rayon production is used for any new production capacity occurring after the year 2000 and the older emissions factor is applied for all other capacity. Drops in capacity are subtracted from production using the older emissions factor because it is more likely that factories with older technology would be taken offline in times of reduced demand. Likewise, if the production capacity is replenished after a drop in demand, the replenished capacity is added back with the older emissions factor to simulate older factories that were not in use during times of lower rayon demand and are brought back online after the market recovered.

Because N_20 is also produced during rayon production, we use industrial N_2O estimates for sub-country scaling of both rayon yarn and staple production where country-level COS source estimates are proportionally distributed over the N_2O grid [*Joint Research Centre*, 2011; *Gullingsrud*, 2017]. A summary for the input data used to estimate the source of COS from rayon can be found as part of Table 3-1.

3.3.8 Tires

Automotive tire wear also emits COS and has been identified as a significant source of COS emissions for several decades [*Pos and Berresheim*, 1993; *Lee and Brimblecombe*, 2016]. However, little effort has been put into investigating tire emissions of COS and less still for creating global gridded data sets. Emission of COS from tires is also associated with a CS_2 emission as sulfur leaves tires.

Data for the approximate number of cars in use is available after the year 2004 [*OICA*, 2016] and for the years prior to 2004, country-level ownership rates (cars per 1000 population) are available. The latter is multiplied by yearly population data (thousands in population) to estimate total cars in use for earlier years [*Dargay et al.*, 2007; *The World Bank*, 2016].

An emissions rate per vehicle per year is calculated by assuming that the average automobile deposits 1.17 kg of tire rubber to the road each year and that the sulfur within the rubber (accounting for 1.6% of the rubber in the tires) is eventually released as either COS or CS_2 (57% as CS_2, 43% as COS), where CS_2 will oxidize to produce additional COS [*Chin and Davis*, 1993; *Pos and Berresheim*, 1993; *Susa and Haydary*, 2013].

Transportation CO_2 emissions are available in the EDGAR v4.2 data set providing a very appropriate spatial proxy data set for sub-country spatial scaling [*Joint Research Centre*,

2011]. A summary for the input data used to estimate the source of COS from tires can be found as part of Table 3-1.

3.4 Results

Total anthropogenic sources (indirect and direct) for the gridded inventories from Kettle and our inventory show large differences in both spatial distribution and total magnitude. The anthropogenic source from the Kettle inventory is relatively evenly distributed between Asia, North America, and Europe (Figure 1a). However, our inventory shows a concentration of emissions in Asia. We find that 45% of the global source is emitted by China and the remaining source is relatively evenly distributed between India, North America, and Europe. The anthropogenic source for our inventory relative to the Kettle inventory is 7 and 10 times larger in China and India, respectively. While earlier years in our inventory have lower emissions in Asia, there are no years in our inventory that resemble the dramatically lower Asian emissions suggested by the Kettle inventory.

In Figure 3-2 the Kettle inventory is compared to the estimates of anthropogenic COS sources from this study for the most recent year presented by each data set (Kettle: circa 1989, this study: 2012) [*Kettle et al.*, 2002]. The Kettle inventory uses data from a range of years with spatial scaling based on SO_2 emission grids from 1989. For sources of COS that are considered by both the Kettle inventory and in this study, Figure 3-2 shows that sources from this study are larger. Furthermore, this study provides additional sources of COS that were not considered in the Kettle inventory and serve to further widen the gap in total sources between the two inventories. This upward revision is in support of the supplementary hypothesis of this study: anthropogenic sources explain a large portion of the missing source of atmospheric COS. The total source of anthropogenic COS estimated in this study is 230 Gg Sulfur y^{-1} more than that of the Kettle inventory. 230 additional Gg of Sulfur per year is within the lower range of the estimated missing source of 230 to 800 Gg Sulfur per year and therefore potentially explains a large component of the missing source.

This study produces larger estimates of anthropogenic COS sources because of the inclusion of additional sources and because the Kettle inventory is based on data that no longer represents current industrial conditions. The increase in emissions from coal sources suggest that global coal consumption is outpacing emissions control regulations that may reduce emissions factors for COS [*Blake et al.*, 2008; *Smith et al.*, 2011]. The reduction of COS emissions from aluminum production is largely due to reduced emissions factors for aluminum production [*Kimmerle and Noel*, 1997]. The reduction in the emissions factor of COS from of aluminum production is largely due to prebake smelting replacing Söderberg smelting (prebake smelting accounted for 90% of aluminum production in 2012), with prebake smelting emitting roughly half the amount of COS per unit of aluminum produced [*Campbell et al.*, 2015].

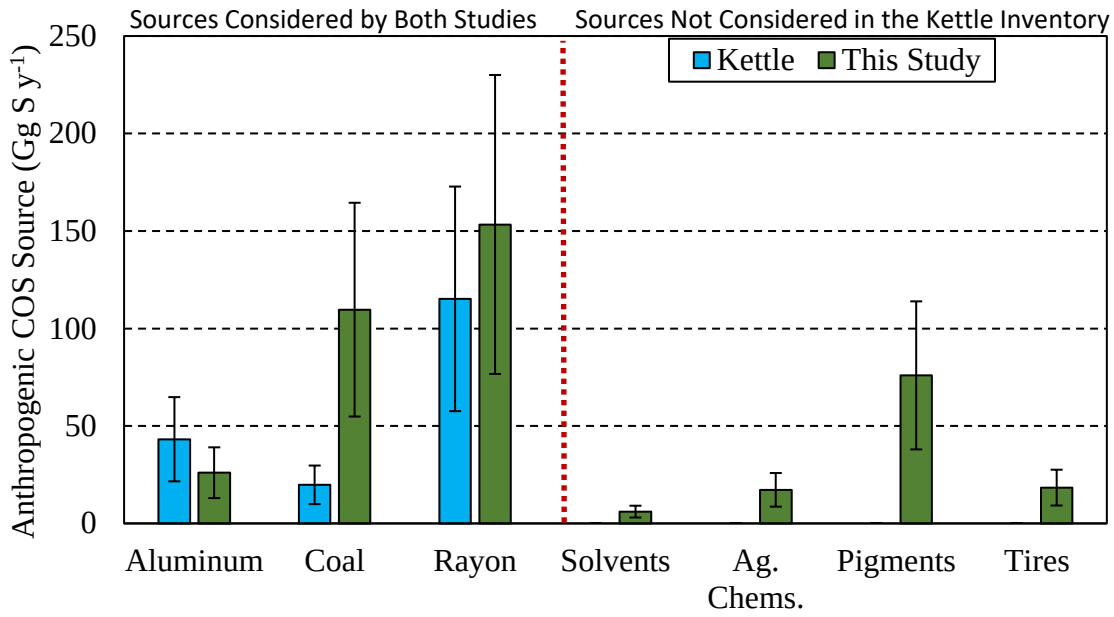

Figure 3-2. A comparison of annual global anthropogenic sources of COS (Gg S y^{-1}) from the Kettle inventory and from this study for the year 2012. Fluxes reporting zero for Kettle on the right-hand side of the red dotted line were not considered in the Kettle inventory. When referring to this study, the coal category includes combined residential and industrial sources; pigments include carbon black and titanium dioxide and rayon includes yarn and staple.

A time series of cumulative global anthropogenic sources of COS from this study is shown in Figure 3-3 as Gg Sulfur y^{-1}. Currently rayon (yarn and staple) production (red and yellow, respectively) is the dominant source. In earlier years, industrial coal and residential coal (orange and brown, respectively) were the largest source of anthropogenic COS. These results for corresponding sources are very similar to the global anthropogenic totals reported by Campbell et al. (2015) but the addition of the residential coal, carbon black, titanium dioxide, pulp and paper industries and tire wear sources suggest a larger anthropogenic source. Additionally, the spatial distribution of these results allows for the analysis of spatial patters of COS emissions through time.

For each source, Figure 3-4 displays the countries that are the top contributors of anthropogenic COS as a percentage of the total global source for 2012. Figure 3-5 shows the shares of the total source for dominant regions through time. In the recent past (2000 – 2012), China has been a dominant contributor of anthropogenic COS for most major anthropogenic sources: aluminum (1st place), carbon black (2nd place), industrial coal (1st place), rayon (1st place), residential coal (1st place), titanium dioxide (1st place) (Figure 3-4, 5). Furthermore, China continues to obtain a larger portion of the global anthropogenic COS sources, widening the gap between China's emissions share and other countries. This is largely due to increased industrial activity in China and the outsourcing of manufacturing to China by various other nations. Additionally, increased coal consumption to support growing energy needs for a growing population further contribute to this trend [*Blagoev*

and Funada, 2011; *Smith et al.*, 2011; *U.S. Geological Survey*, 2013; *Fiber Economics Bureau*, 2014]. The U.S. is currently the second largest contributor by a small margin over India; however, trends suggest that India, with a growing population and an increasing demand for energy, will soon surpass the U.S. because U.S. emissions are in decline [*U.S. Energy Information Administration*, 2013; *Central Intelligence Agency*, 2016]. While India will likely surpass the U.S. in COS emissions, the trends found in this study suggest that it is unlikely that Inia or any other country will be able to match Chinese sources of anthropogenic COS in the foreseeable future. Russia, Germany and Canada are also significant contributors to global anthropogenic COS sources, though these countries' emissions are declining as is the case with many developed countries.

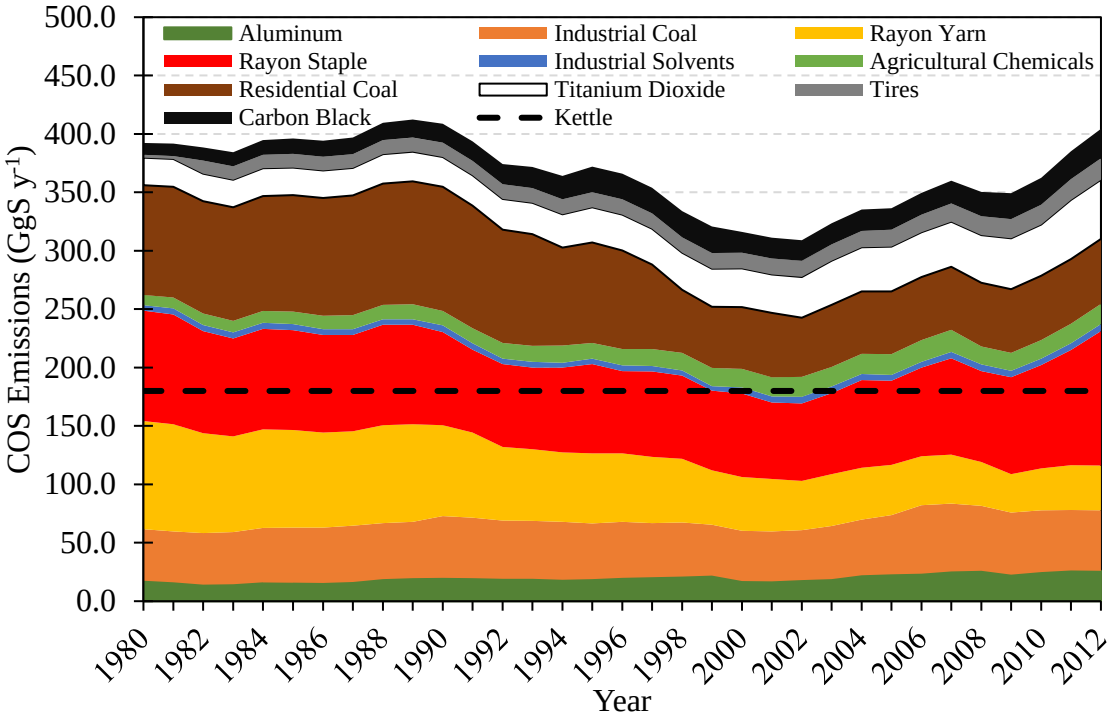

Figure 3-3. Time series of global anthropogenic COS sources, including direct and indirect emissions. The dashed black line represents the climatological estimate from the Kettle inventory. The pulp & paper source is omitted from this figure due to the insignificance of the estimated source.

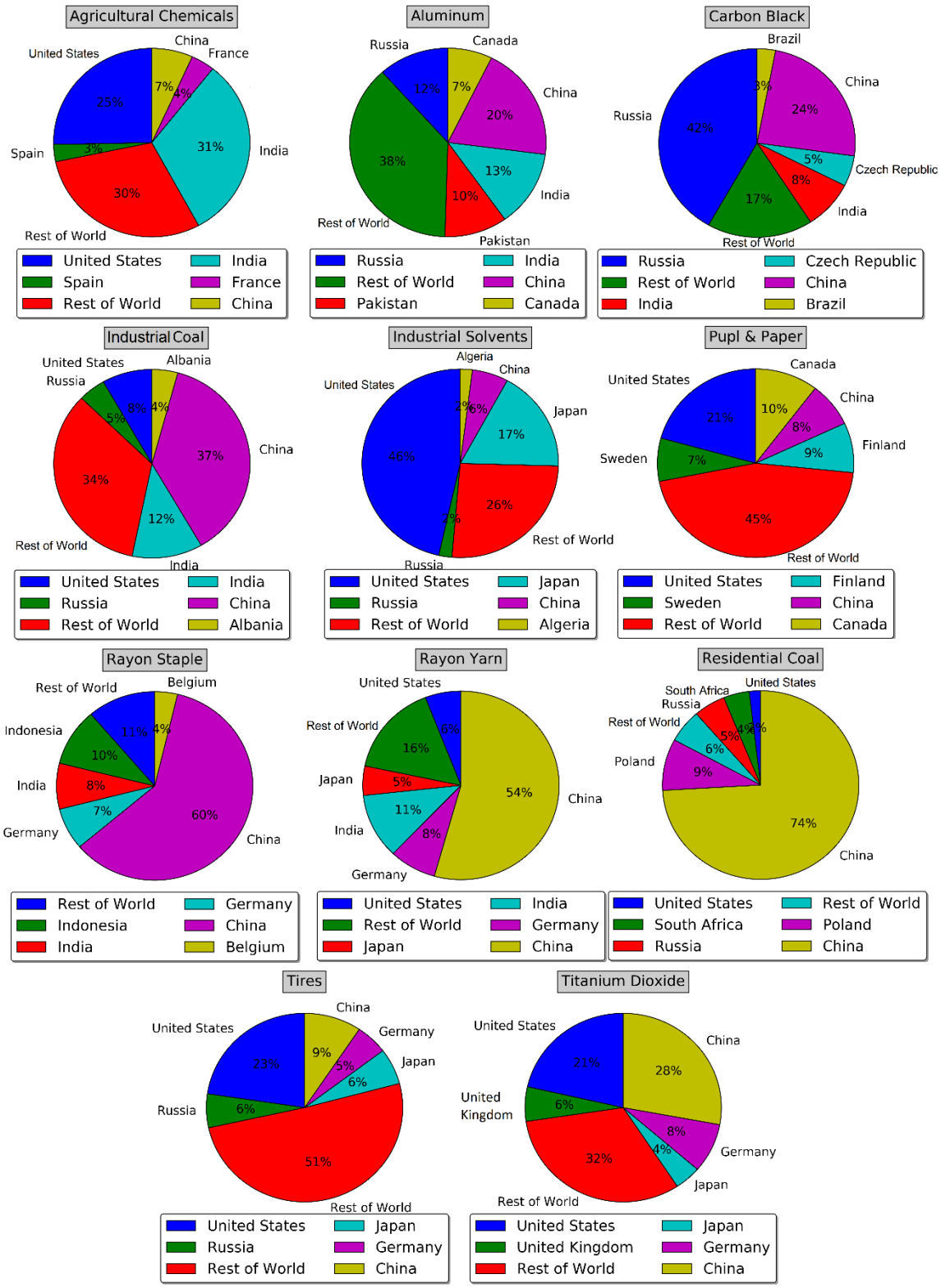

Figure 3-4. The share of global anthropogenic COS sources from the highest contributing countries by source for 2012. “Rest of World” data includes the contribution of all countries excluding the five countries listed in each legend.

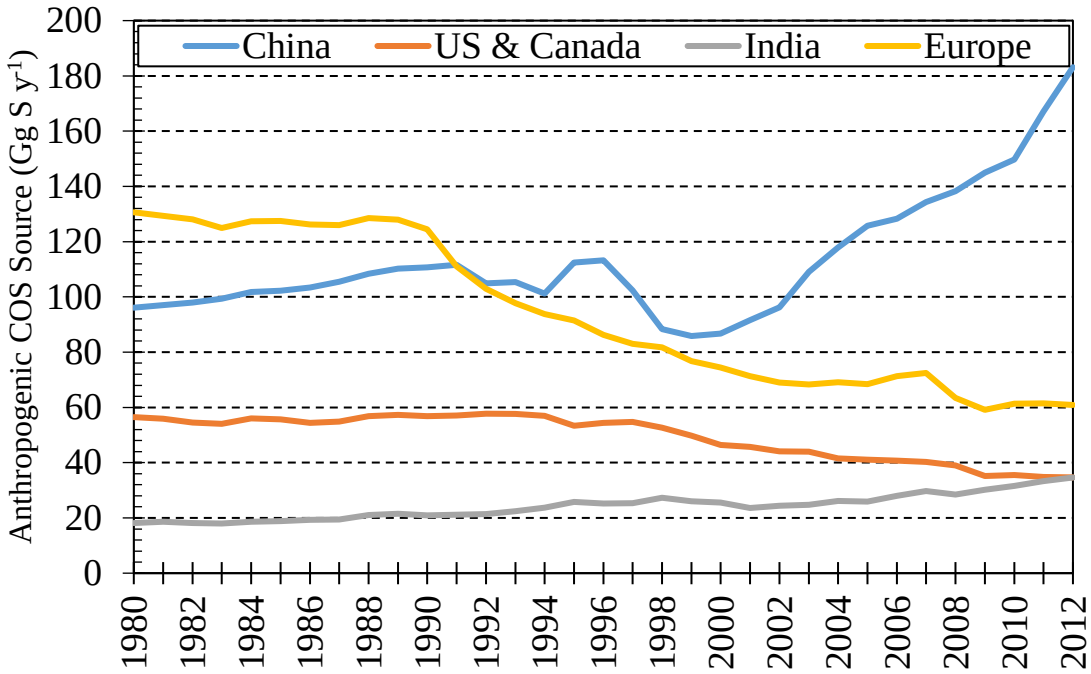

Figure 3-5. Time series of the total anthropogenic source of COS (Gg S y^{-1}) from the highest contributing regions.

Figure 3-6 and 3-7 also compare the Kettle inventory to the estimates from this study for the year 2012. Figure 3-6 shows the magnitude and spatial distribution of total anthropogenic COS sources for the Kettle inventory (top panel) and for this study (bottom panel). Figure 3-7 summarizes the totals of anthropogenic COS sources (Gg S y^{-1}) for select regions. In Southeast China, the Kettle inventory proposes a relatively weak anthropogenic COS signal while, in contrast, this study estimates that this region has highest anthropogenic COS contribution for 2012. In Europe, the spatial distribution is somewhat similar between data sets, however, the Kettle inventory proposes a smaller magnitude (Figure 3-6). In the U.S. & Canada, the Kettle inventory concentrates the COS flux in the southern and eastern U.S. In contrast, the fluxes proposed in this study are more point-source in nature and distributed over may parts of the U.S. The difference in the U.S. is largely due to a reduction in rayon production and the addition of several other sources of COS in this study. Like what was found for China, estimates from this study for India are strikingly different from the Kettle inventory. In Figures 3-6 and 3-7, the COS flux in India is nearly nonexistent in the Kettle inventory, while we estimate much larger anthropogenic contributions to atmospheric COS, making India one of the major contributors.

Figure 3-8 also shows regional anthropogenic COS sources, but provides estimates for the specific components of the anthropogenic total source from this study in 2012. In all regions, except for the U.S. & Canada, the rayon sources (yarn and staple) are dominant. In the U.S., the rayon industry went into decline, leaving pigment industries to dominate

the anthropogenic COS emissions in this region. While we estimate China to have several large sources, it is specifically the rayon (yarn and staple) and coal (industry and residential) sources that make China by far the dominant global contributor of anthropogenic COS. India dominates the agricultural chemicals source and Europe has a slight lead over China for the aluminum source.

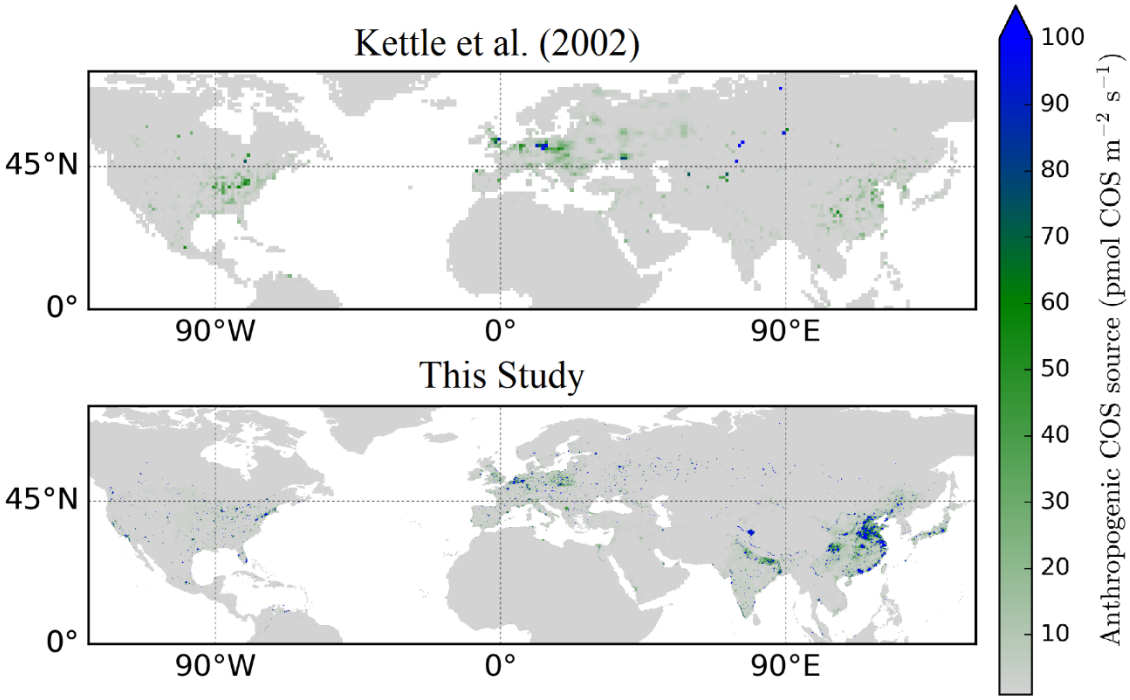

Figure 3-6. Comparison of the global gridded anthropogenic COS flux from the climatological Kettle inventory and this study for year 2012. These source inventories include direct emissions from COS and indirect sources from anthropogenic CS_2 emissions.

Figure 3-9 shows a time progression of the global anthropogenic COS emissions from this study. Like Figure 3-4 a slight decrease in European and North American anthropogenic COS emissions can be seen through the study period and a dramatic intensification of emissions can be seen in Asia, particularly in China. The more important feature to note is that at no point in this study do the spatial patterns in emissions estimates resemble that of the Kettle inventory; not even for the years that are most closely represented by the Kettle inventory (circa 1989). This difference between studies results from the source specific spatial scaling of this study and the addition of new sources. In contrast, the Kettle inventory used only global SO_2 emissions for the spatial scaling of all anthropogenic sources [*Kettle et al.*, 2002]. We assert that the spatial scaling used here is greatly improved and the addition of new sources provides a more comprehensive data set than previously available.

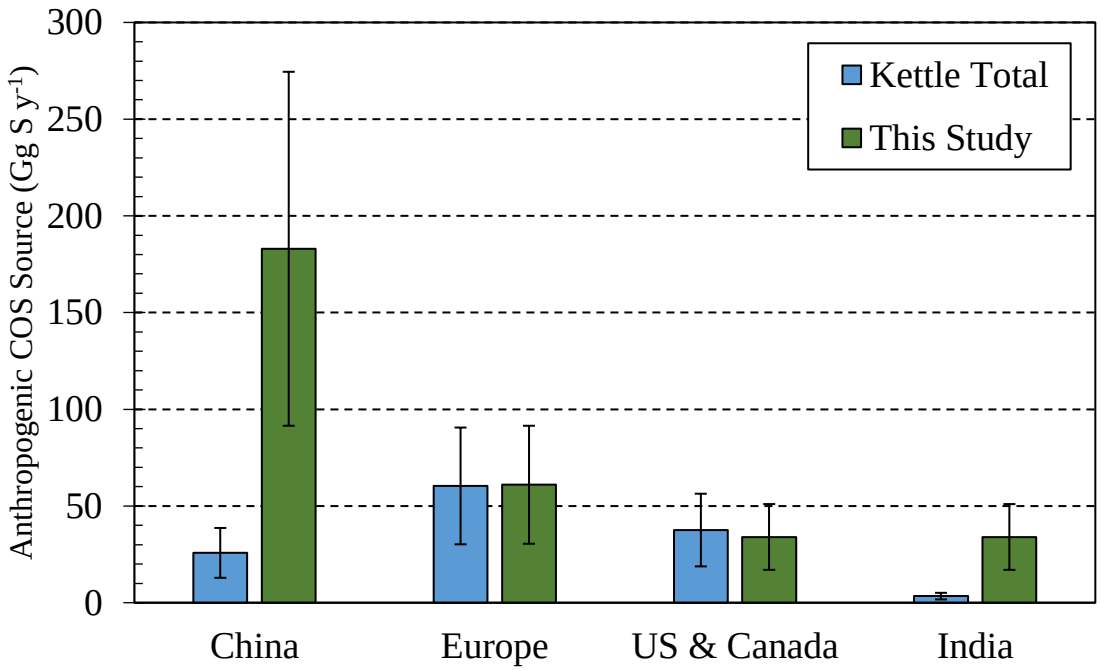

Figure 3-7. A comparison of regional total anthropogenic COS sources from the Kettle inventory (blue) and from this study, year 2012 (green).

Lee and Brimblecombe (2016) make estimates for many of the same anthropogenic sources of COS that are considered in this study: aluminum smelting, coal combustion, pigments, pulp and paper industries, rayon production and tire wear.

Lee and Brimblecombe (2016) adopt the global COS emission from aluminum smelting of 30 ± 7 Gg S y^{-1} from Campbell et al. (2015). In this study, we follow the methods from Campbell et al. 2015 and find good agreement with their estimate.

For the industrial coal source of COS, Lee and Brimblecombe (2016) again cite Campbell et al. (2015) for an estimate of 60 Gg S y^{-1}. In this study, we use similar emissions factors as Campbell et al. (2015) but scale them based on the SO_2 emissions to coal consumption ratio to simulate differences in emissions controls and the sulfur content of coal. With these adjustments to the methods, a slightly lower emission of COS from industrial coal of 54 Gg S y^{-1} is found. Lee and Brimblecombe (2016) do not provide a COS emissions estimate for the domestic use of coal.

For the pigments industry, Lee and Brimblecombe (2016) estimate 43 Gg S y^{-1} as COS and 205 Gg S y^{-1} CS_2 for carbon black and 31 Gg S y^{-1} for titanium dioxide. Using similar methods, but with different industry data that provided estimates of carbon black and titanium dioxide for multiple years, this study proposes the direct emission of COS from carbon black to be 8 Gg S y^{-1} and the emission of CS_2 to be 92 Gg S y^{-1} and 50.8 Gg S y^{-1} for titanium dioxide for the year 2012. The large difference in estimates of carbon black between studies is due to the removal of 99% of emissions from developed countries in

this study and, to a lesser extent, differences in industry activity data used [*Blake et al.*, 2004]. For titanium dioxide, we follow the same methods as Lee and Brimblecombe (2016); therefore, differences are solely a result of difference in industry activity data for titanium dioxide production.

Lee and Brimblecombe (2016) estimate the COS source from the pulp and paper industry to be 97 Gg S y^{-1} based on COS concentrations found in recovery boilers at pulp and paper plants. As mentioned in the methods section, insufficient data was found to duplicate the Lee and Brimblecombe (2016) methods for all countries or years. However, the EPA estimates for COS and CS_2 emissions from pulp and paper plants in the U.S. suggest much smaller emissions with extrapolated global direct and indirect sources totaling to <1 Gg S y^{-1} as COS. These findings suggest that the pulp and paper industry is not a significant source of direct or indirect COS in sharp contrast to Lee and Brimblecombe (2016). Therefore, the pulp and paper sources is omitted from Figures 3-3, 3-7 and 3-8 because estimates were too small to be visible.

For rayon, Lee and Brimblecombe (2016) take the annual global rayon production and using an emissions factor of 79 g S kg^{-1} propose a total rayon source of 395 Gg S y^{-1} as CS_2 based on 2017 projections made in 2011 [*Global Industry Analysts*, 2011]. Lee and Brimblecombe do not attempt an estimate of the COS source that would result from the oxidation of the 395 Gg S y^{-1} and do not differentiate between yarn and staple rayon. In this study, the combined CS_2 source from yarn and staple rayon is 450 Gg S CS_2 for 2012 [*Fiber Economics Bureau*, 2014].

For COS emissions from tires, similar methods are applied in this study and in Lee and Brimblecombe (2016) by assuming the average vehicle has tire wear of approximately 1.17 kg rubber y^{-1}, 1.6% of the rubber is released as sulfur (57% as CS_2 and the remainder as COS) [*Pos and Berresheim*, 1993; *Susa and Haydary*, 2013]. The similarity in methods leads to similar results between studies with Lee and Brimblecombe (2016) estimating 9.8 and 12.6 Gg S y^{-1} for as COS and CS_2, respectively, and 7.7 and 8.9 Gg S y^{-1} in this study as COS and CS_2, respectively. Differences in totals are due to the different sources used for the number of vehicles on the road. Whereas Lee and Brimblecombe (2016) used Oregon Independent Colleges Association (OICA) data for their estimate, we relied on a combination of data to acquire estimates of the number of vehicles in use to provide estimates for many years [*Dargay et al.*, 2007; *OICA*, 2016; *The World Bank*, 2016].

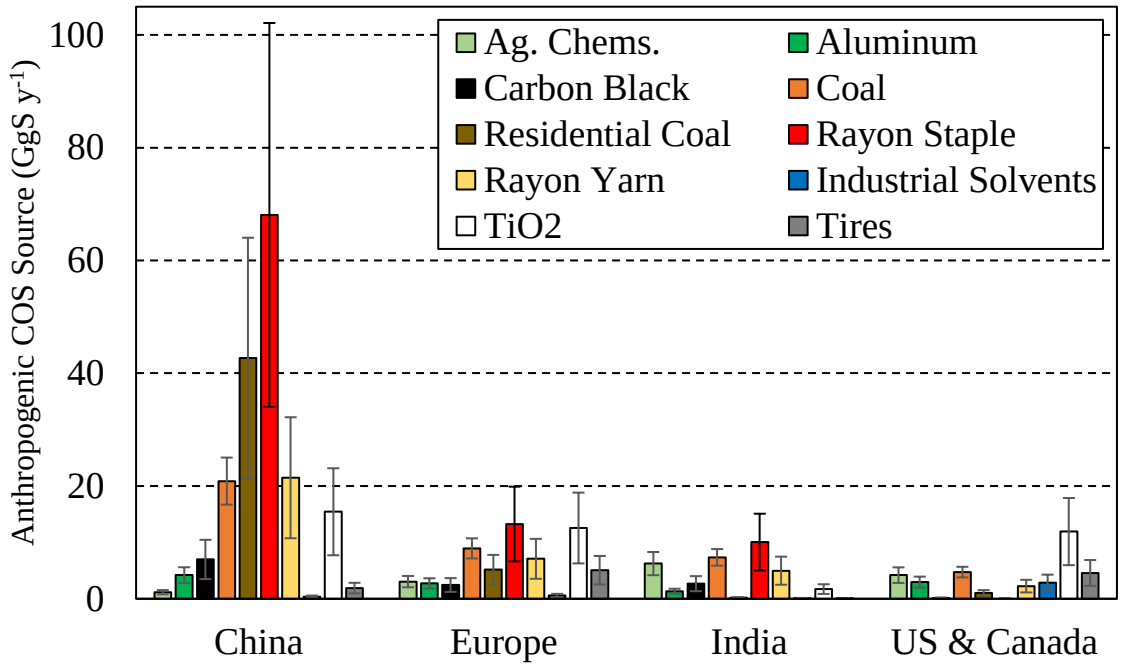

Figure 3-8. Individual sources of anthropogenic COS (Gg S y^{-1}) by region. The regions of China, Europe, U.S. & Canada and India are shown here because they are dominant source regions of atmospheric COS from anthropogenic activity. The pulp & paper source is omitted from this figure due to the insignificance of the estimated source.

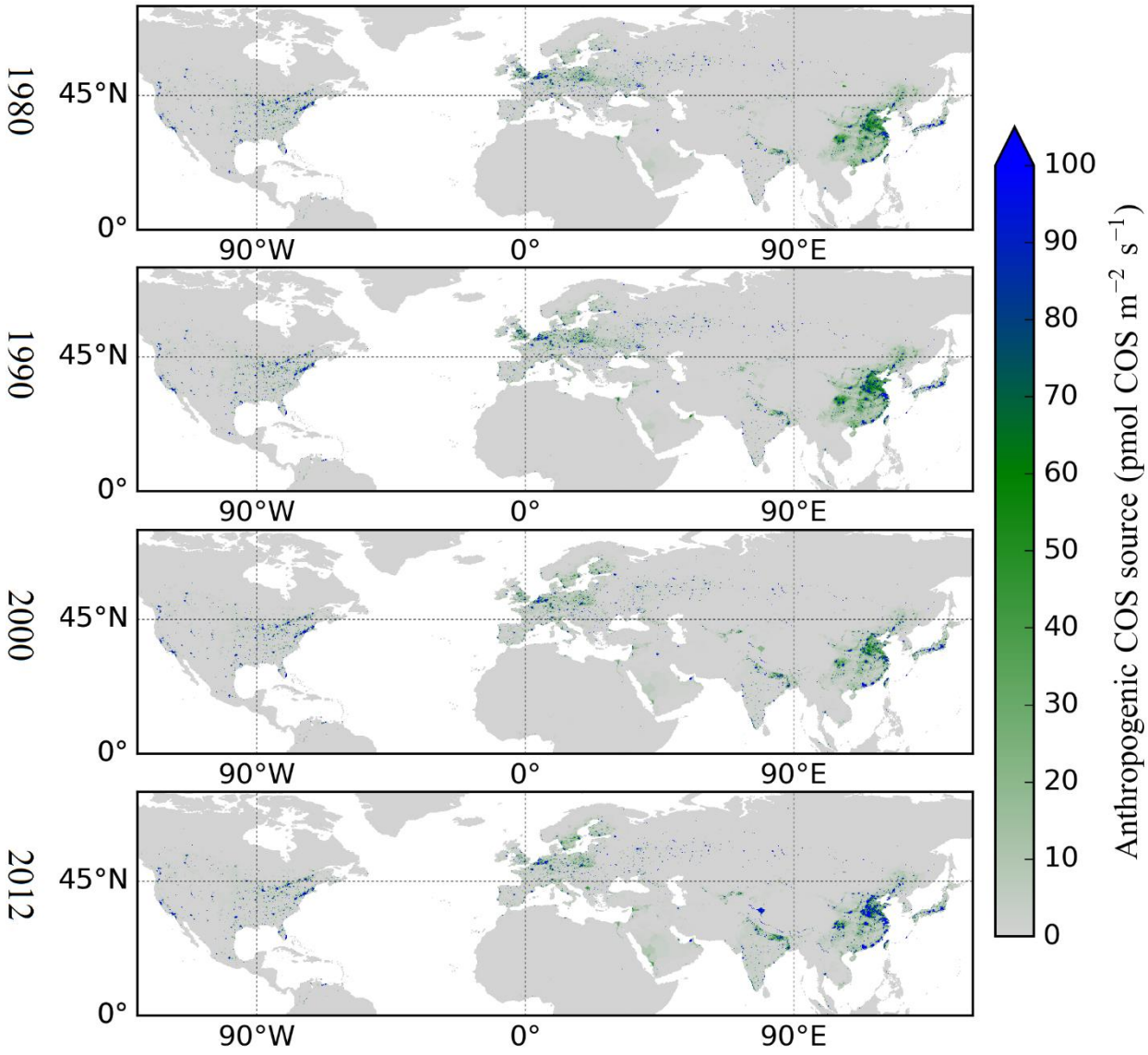

Figure 3-9. A comparison of the total anthropogenic COS flux (pmol m^{-2} s^{-1}) from all sources considered in this study for the years 1980, 1990, 2000 and 2012. Indirect sources from CS_2 are included as a surface flux of COS.

3.5 Discussion

Previous work extrapolated global estimates of COS emissions over SO_2 grids to provide a climatological inventory that became the standard for gridded anthropogenic COS sources [*Kettle et al.*, 2002]. However, this inventory was created over a decade ago, incorporates industry activity data from over three decades ago and uses outdated emissions factors. Recent work suggests that the Kettle inventory is not representative of current conditions[*Campbell et al.*, 2015]. In the absence of an updated inventory, the Kettle inventory is still being used in all modeling studies incorporating anthropogenic

atmospheric COS sources [*Campbell et al.*, 2008; *Suntharalingam et al.*, 2008; *Berry et al.*, 2013; *Launois et al.*, 2014]. The data set of anthropogenic COS sources resulting from this study provides estimates with a higher spatial resolution, more sophisticated spatial scaling, includes more component sources and more years of historical estimates than any other single data set while using the most current industry activity data and emissions factors as input.

While this study proposes that the sources presented here are a more contemporary and complete picture of anthropogenic COS sources, uncertainties persist. The emissions factors for the various components of the anthropogenic source of COS are the largest source of uncertainty for the magnitudes of emissions presented in this study. However, due to the economic importance of accurately tracking industry activity data, the values used to quantify anthropogenic activity that leads to emissions of COS (directly or indirectly) are likely accurate. Uncertainty estimates for indirect sources from industrial CS_2 emissions are based on half the range of the emissions factors and an atmospheric oxidation rate with a molar conversion efficiency of 87% to COS and assumed to be ± 50% [*Chin and Davis*, 1993; *Launois et al.*, 2015]. More detail is given for direct COS sources where ranges of emissions factors exist, suggesting a narrower uncertainty spread of approximately ±25% for industrial coal and ±33% for aluminum. These uncertainty ranges are reflected in Figures 3-2, 3-7 and 3-8.

The spatial domain of the input industry activity data is generally at the country-level. Spreading out a country's COS flux over its entire area limits the usefulness of the data set in modeling studies given the large spatial uncertainty of the flux. To reduce this spatial uncertainty, we rely on separate emissions data sets for other chemical species or croplands as spatial proxies for the COS flux. Proxy fluxes that would likely constrain the spatial distribution of the target COS flux are chosen. For example, in the case of the aluminum source of COS, industrial CO_2 emissions are chosen as the spatial proxy because a primary emission from aluminum smelting is CO_2 and therefore, aluminum smelting would most likely be constrained by the spatial distribution of the CO_2 flux (or would absolutely be constrained by the CO_2 flux if the proxy data set was without uncertainty). While this method, very likely, is still very generous with the spatial distribution of many of the sources explored here (especially point source emissions such as from aluminum smelting), large areas that are extremely unlikely to contain the associated COS flux are excluded. This exclusion and gridded spatial distribution increases the data set's suitability for modeling studies. Furthermore, this method has been used in previous work [*Kettle et al.*, 2002]; however, only one proxy flux was used to distribute the entire global flux from all sources. Here, country-level totals, as opposed to global totals, and source-specific proxy fluxes are used for each component of the anthropogenic COS flux instead of using one proxy flux for all sources.

This study was unable to replicate the Lee and Brimblecombe (2016) methods for estimating pulp and paper sources of COS because boiler COS concentrations were not found and Lee and Brimblecombe (2016) do not explain the process of the COS escaping the recovery boilers or if any emissions controls apply. Furthermore, Vainio et al. (2010)

give two estimates of the COS concentrations in the recovery boilers but Lee and Brimblecombe (2006) do not indicate which value is used. U.S. EPA estimates of COS emissions only provide an estimate for one year and so the spatiotemporal scaling used here will not reflect any changes in emissions factors, resulting in further uncertainty. However, at least in the U.S., COS is not mentioned as an emission that is controlled in U.S. EPA reports and CS_2 is stated explicitly as not controlled, suggesting minimal uncertainty resulting from emissions factors [*EPA Office of Air Quality Planning and Standards and EPA Office of Air and Radiation*, 2012]. While there is persistent uncertainty in emissions factors, the small estimated magnitude of COS and CS_2 emissions from pulp and paper from the U.S. EPA suggests that the underlying uncertainties persisting here would likely not significantly impact global totals of COS emissions [*EPA Office of Air Quality Planning and Standards and EPA Office of Air and Radiation*, 2012].

While uncertainty still remains, the level of uncertainty is likely within the functional range for regional-scale modeling efforts and, despite the remaining uncertainty, is an overdue update and an improvement to the inventory from 2002 [*Kettle et al.*, 2002].

While this study suggests that anthropogenic sources of COS account for a large share of the missing source of COS, other sources such as soils, biomass burning and oceans may also be contributing more COS to the atmosphere than previous estimates have suggested. More work is needed in these areas to further evaluate possible contributions of these sources to the missing source of COS. The leading hypothesis has been that oceans have been responsible for the missing source of COS in light of high concentrations of COS observed over tropical oceans by the Tropospheric Emissions Spectrometer (TES) (Figure 3-10 A)) [*Kuai et al.,* 2015]; however, recent work casts doubt on oceans as the missing source [*Lennartz et al.*, 2016]. Furthermore, the upward revision of COS sources in Asia found in this study (Figure 3-10 B)) suggests that anthropogenic sources might be the cause of the high COS concentrations observed by the TES satellite. An atmospheric transport modeling study could be performed to further explore this possibility. Reproduction of the concentration patterns through atmospheric transport modeling would suggest minimal unknown oceanic contributions while failing to reproduce concentration patterns would encourage deeper investigation of ocean processes or other sources that produce COS.

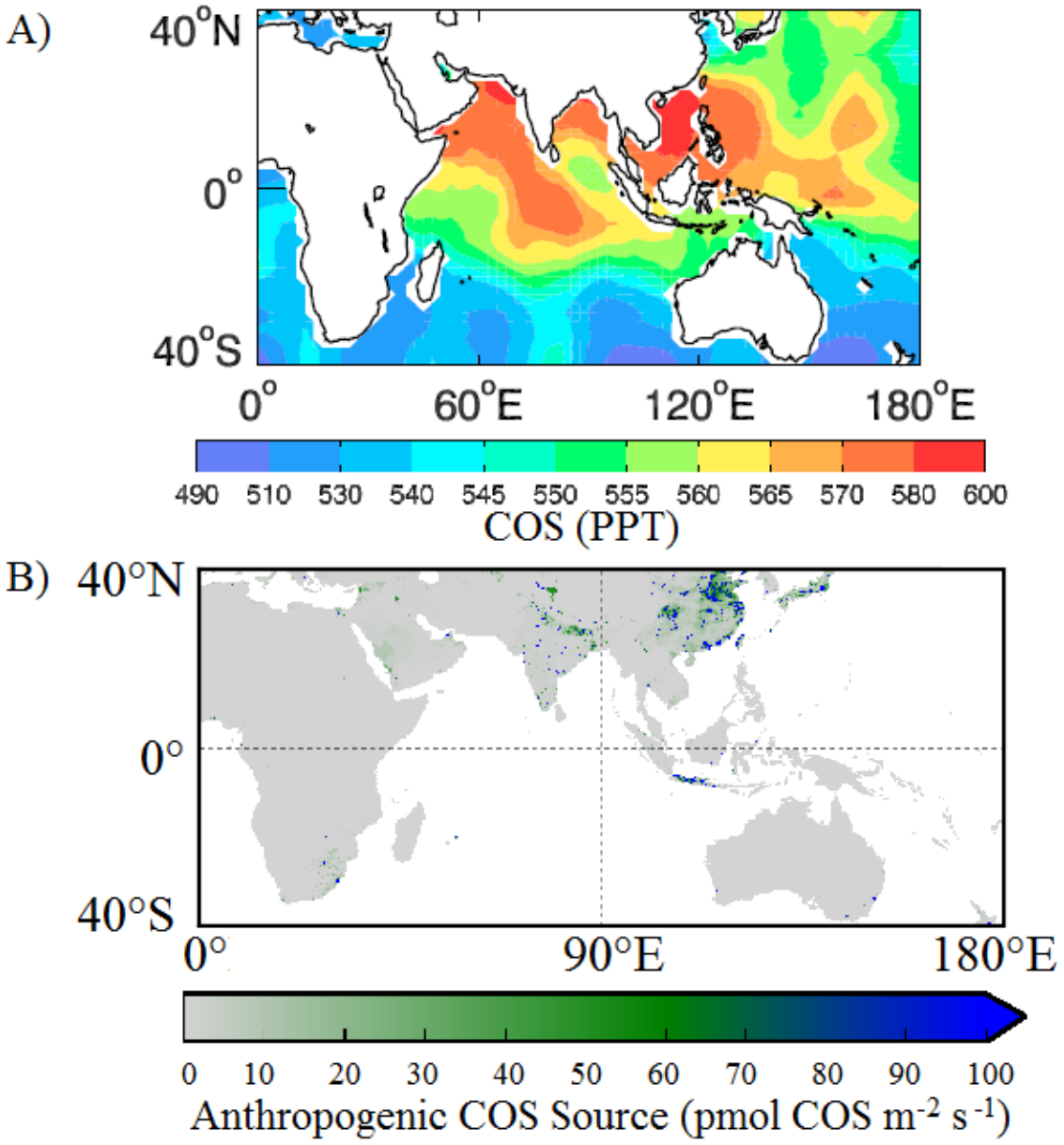

Figure 3-10. A) Free troposphere COS (ppt) for Tropospheric Emissions Spectrometer measurements in June 2006 (top panel) *Portion of the figure obtained from: Kuai et al. (2015), and total estimated anthropogenic COS emissions for 2006 from this study (bottom panel).

Chapter 4: Anthropogenic Sources as an Explanation of the Missing Source of Atmospheric Carbonyl Sulfide

4.1 Abstract

A growing body of work continues to suggest that carbonyl sulfide (COS or OCS) is a potentially important tracer of photosynthesis. Understanding atmospheric COS concentrations and surface fluxes is critical for understanding the role of COS in the sulfur cycle and for using COS as a tracer for photosynthesis. Unfortunately, the global budget of COS is not well understood: there exists a missing source in the atmospheric COS budget that ranges from 280 Gg S y^{-1} to as much as 800 Gg S y^{-1}. Considering high observed COS concentrations in the tropics, researchers have hypothesized that the missing source of atmospheric COS may have an oceanic origin. However, recent studies cast doubt on the ability of the oceanic source to fill the gap in the COS budget due to observed COS under-saturation of ocean surface waters. The hypothesis proposed in this study is that the missing source could be explained by anthropogenic activity and that the high tropical COS concentrations observed by the TES satellite could be due to atmospheric transport of anthropogenically sourced COS. This study shows that simulations of atmospheric COS driven by enhanced anthropogenic sources perform similarly to simulations driven by enhanced ocean sources in comparison to observations. This top-down assessment is further supported by recent bottom-up anthropogenic COS inventories that suggest that anthropogenic sources of COS are likely a significant component of the missing COS source.

4.2 Introduction

Atmospheric COS is a potentially powerful tracer of photosynthesis, stomatal conductance, and evapotranspiration. Quantifying the sources and sinks of atmospheric COS is critical for understanding the sulfur cycle, carbon cycle and for understanding carbon-climate interactions.

Observations from the NOAA global air monitoring network and the NASA Intercontinental Chemical Transport Experiment over North America (INTEX-NA) have inspired a growing body of research aimed at partitioning photosynthesis and respiration fluxes via COS for large spatial scales [*Montzka et al.*, 2007; *Blake et al.*, 2008; *Campbell et al.*, 2008]. Recent work has demonstrated the potential for this COS tracer approach [*Montzka et al.*, 2007; *Campbell et al.*, 2008; *Hilton et al.*, 2015]. COS is consumed by terrestrial vegetation in a process that is closely related to CO_2 uptake by plants, except that COS chemical processes within the plant are irreversible and COS is not respired by plants. This makes observations of COS potentially more useful for understanding photosynthetic fluxes than observations of CO_2 [*Campbell et al.*, 2008]. The lack of respiration of COS, the strong relationship between COS and CO_2 plant uptake, and the spatial separation of

the large sources and sinks of COS would make it ideal for inferring photosynthesis if the confounding sources were well understood [*Campbell et al.*, 2008; *Stimler et al.*, 2010]. However, there exists a large missing source of COS that introduces uncertainty into the COS tracer approach.

The missing COS source is apparent due to the disagreement between top-down and bottom-up COS inventories. Tropospheric measurements over the last two decades show long-term trends that are on the order of 1% yr^{-1} or less, suggesting that global COS sources and sinks are roughly in balance [*Montzka et al.*, 2007; *Kremser et al.*, 2015; *Lejeune et al.*, 2017]. However, bottom-up inventories are largely out of balance, with global sinks that are twice the magnitude of global sources [*Berry et al.*, 2013]. Solving this imbalanced budget requires the discovery of either a missing source or an overestimated sink. An overestimate of the sink is unlikely because the primary uptake mechanism through plants has been verified through a wide range of experiments including analysis of continental vertical drawdown [*Campbell et al.*, 2008], global latitudinal variation [*Berry et al.*, 2013], northern hemisphere seasonal amplitude [*Montzka et al.*, 2007; *Suntharalingam et al.*, 2008], leaf chamber uptake [*Stimler et al.*, 2010], and eddy covariance measurements (e.g. *Maseyk et al.*, (2014a)). A more likely reason for the budget imbalance is a missing source given the relatively large uncertainty of previous source estimates.

Recent studies have focused on the potential for the missing source to be of oceanic origin. Analysis of regional and seasonal variation in tropospheric COS are consistent with a tropical ocean source that could balance the global budget [*Suntharalingam et al.*, 2008; *Berry et al.*, 2013; *Kuai et al.*, 2015]. Furthermore, bottom-up models of the ocean source have confirmed the potential for tropical oceans to account for the missing source [*Launois et al.*, 2015]. However, this large tropical ocean source is not supported by direct observations of the ocean source from ship-based cruise data [*Lennartz et al.*, 2016]. Either the cruise data are too sparse to capture the tropical ocean source or the missing source is not due to the oceans.

Given this uncertainty with the missing ocean source hypothesis, here we explore an alternative hypothesis based on a missing anthropogenic source. Additionally, new bottom-up estimates of the anthropogenic source of atmospheric COS suggests a large upward revision to over 400 Gg Sulfur y^{-1} [*Campbell et al.*, 2015; *Chapter 3*]. The new global estimate of gridded anthropogenic COS source estimates from Chapter 3 use newer emissions factors and industry activity data compared to previous work (which is largely based on data that is now over three decades old) [*Kettle et al.*, 2002]. This new data set proposes a very different picture of global anthropogenic sources of COS and is large enough to suggests that the COS budget may largely be balanced by anthropogenic sources. Furthermore, previous modeling studies with enhanced ocean sources of COS were unable to replicate upper-troposphere high COS concentrations caused by deep convection above southeast Asia that were observed in the Michelson Interferometer for Passive Atmospheric Sounding (MIPAS) data set [*Glatthor et al.*, 2015]. Previous work hypothesized that this missing convected source of COS to the upper-troposphere could be due to incorrect estimates of the plant uptake of COS or a missing continental source that might be

consistent with increased rayon production in China [*Campbell et al.*, 2015; *Glatthor et al.*, 2015]. The latter hypothesis is consistent with the anthropogenic sources of Chapter 3. Lastly, new observations of COS concentrations by the Infrared Atmospheric Sounding Interferometer (IASI) instruments provide a different picture of total column COS than TES observations. In the IASI observations of COS, there are high concentrations of COS over oceans in the Southern Hemisphere (unlike TES observations showing observations of high COS concentrations in the tropics) and dominated by enchantment over China in the Northern Hemisphere [*Anthony Vincent and Dudhia*, 2017]. These findings are also consistent with the anthropogenic inventory of Chapter 3.

Therefore, it is hypothesized here that the missing source could be dominated by anthropogenic activity with a secondary or joint contribution from oceans. This hypothesis is tested by evaluating the agreement between simulated atmospheres driven by enhanced anthropogenic sources or enhanced ocean sources in comparison to MIPAS, TES and NOAA observations.

4.3 Methods

4.3.1 Atmospheric Transport Modeling

The Goddard Earth Observation System Chemical (GEOS-Chem) atmospheric transport model (ATM) is used to test the above hypothesis. All input data (see section 4.3.2) are kept constant between scenarios except for the anthropogenic source and the photochemical ocean source (used to maintain global COS budget balance).

GEOS-Chem is a three-dimensional model driven by meteorological data from the Goddard Earth Observing System with a horizontal resolution of 2° latitude × 2.5° longitude and 47 vertical levels providing 3-hourly results [*Bey et al.*, 2001]. Simulations of atmospheric COS are performed from 2004 to 2006, where the first two years are neglected as spin-up and only the year 2006 is used for analysis and comparisons.

4.3.2 Model Data

Here, the flux parameterization from Berry et al. (2015) that assumes an enhanced ocean source of COS is used for defining surface fluxes within the model parameterization for testing the ocean source hypothesis and as a starting point for parameterizing the model run to test the anthropogenic hypothesis of this study. In model comparisons, throughout, the modeled atmosphere derived the assumptions of Berry et al. (2013) with enhanced ocean sources are referred to as the "Ocean Enhancement" scenario and the modeled atmosphere derived from anthropogenic sources from Chapter 3 and a reduced photochemical ocean sources is referred to as the "Anthropogenic Enhancement" scenario. Table 4-1 summarizes the input data used for each model scenario.

Table 4-1. The sources and sinks of atmospheric COS used in the modeling portion of this study for the Ocean Enhancement and Anthropogenic Enhancement scenarios. Superscripts reference the work responsible for adjacent values. The additional photochemical ocean flux for the Anthropogenic Enhancement scenario is computed in this study to balance the global budget.

Sources (Gg S y^{-1})	**Scenarios**	
	Ocean Enhancement	**Anthropogenic Enhancement**
Direct COS from Oceans	44[a,b]	44[a,b]
Indirect COS from Oceans	246[a,b]	246 [a,b]
Additional Photochemical Ocean Flux	542[b]	270
Anthropogenic	180[a]	453[c]
Biomass Burning	136[b]	136[b]
Soils*		
Sinks		
Destruction by OH Radical	111[d]	111[d]
Uptake by Plants	871[e]	871[e]
Uptake by Soil	166[e]	166[e]

[a][*Kettle et al.*, 2002], [b][*Berry et al.*, 2013], [c][*Chapter 3*], [d][*Kuai et al.*, 2015], [e][*Sellers et al.*, 1986a]

*Soils can also be a source of COS but global estimates are not well characterized [*Maseyk et al.*, 2014b; *Campbell et al.*, 2015].

4.3.2.1 Anthropogenic Sources

Anthropogenic sources of COS are taken directly from Kettle et al. (2002) in the Ocean Enhancement scenario and then replaced with anthropogenic sources from Chapter 3 in the Anthropogenic Enhancement scenario. The Kettle et al. (2002) inventory of anthropogenic sources includes direct and indirect sources of COS (DMS, CS_2) with all anthropogenic sources summing to 180 Gg S y^{-1}. The anthropogenic COS source inventory from Chapter 3 represents a more contemporary state of anthropogenic contributions to atmospheric COS by employing updated emissions factors, industry activity data and, additionally, a more comprehensive spatial scaling technique based on source-specific proxy fluxes. While the Kettle et al. (2002) data set provides estimates for direct and indirect sources of COS, Chapter 3 provide estimates for specific sources: aluminum, industrial and residential coal, rayon yarn and staple, industrial solvents, agricultural Chemicals, titanium dioxide and black carbon pigments, tire wear and pulp and paper. The addition of new sources of COS and the use of more current input data results in a much larger estimate of the total anthropogenic contribution of 453 Gg S y^{-1} (year 2006) to atmospheric COS. Large amounts of the increase in this new estimate are a direct result of increased industrial processes in China which is reflected in the spatial distribution of sources in the Chapter 3 data set.

4.3.2.2 COS Canopy and Soil Sinks

COS canopy and soil sinks are both obtained from the Simple Biosphere Model (SiB) version 4 where the total global plant uptake is 871 Gg S y^{-1} and the soil uptake is 166 Gg S y^{-1} [*Sellers et al.*, 1986b]. It may be important to note that this is a newer version of SiB than used in Berry et al. (2013) for global plant and canopy sinks.

4.3.2.3 Ocean Sources

Ocean emissions taken from Kettle et al. (2002), with slight modifications to the totals following Berry et al. (2013), are applied to both modeling scenarios (the Anthropogenic Enhancement and Ocean Enhancement) for direct and indirect COS emissions from DMS and CS_2 equaling 44, 90 and 156 Gg S y^{-1}, respectively. An additional photochemical ocean source proposed by Berry et al. (2013) is used to balance the COS fluxes after all other fluxes are accounted for in the model. This photochemical COS flux is spatially distributed based on solar insolation. The magnitude of the photochemical ocean source enhancement used in the Anthropogenic Enhancement scenario is 270 Gg S y^{-1} and 600 Gg S y^{-1} for the Ocean Enhancement scenario. The photochemical source used in the Anthropogenic Enhancement scenario is reduced when using the Chapter 3 anthropogenic sources of COS to maintain the observed low annual variability in global concentrations of COS [*Kettle et al.*, 2002; *Montzka et al.*, 2007; *Kuai et al.*, 2015]. Because a photochemical source is included in the model run for the Anthropogenic Enhancement scenario to balance the global COS budget, the ocean source is larger than that of conventional estimates but is still much smaller than in the Ocean Enhancement scenario.

4.3.2.4 Biomass Burning Source

The 2004 Global Fire Emissions Database version 4 (GFEDv4) is used for the spatial distribution of COS emissions from biomass burning [*Randerson et al.*, 2015]. However, because GFEDv4 does not have a specific estimate for the emission of COS from biomass burning, the Berry et al. (2013) estimated total of 136 Gg S y^{-1} is proportionally distributed over the GFEDv4 biomass burning areas.

4.3.2.5 Destruction by OH Radicals

The sink estimate for the destruction of COS by OH radicals in the atmosphere is assumed to be 111 Gg y^{-1} [*Kuai et al.*, 2015].

4.3.3 Observation Data

4.3.3.1 Michelson Interferometer for Passive Atmospheric Sounding (MIPAS)

MIPAS is a satellite remote sensing platform that uses a high spectral resolution limb-sounding instrument to detect trace gases in the atmosphere. Like the TES data described

below, the MIPAS data is smoothed to GEOS-Chem grid, from 5° latitude ×15° longitude to 2° latitude × 2.5° longitude. MIPAS observations are available only at 250 hectopascal (hpa), so it is more useful for making upper-troposphere comparisons. MIPAS provides estimates for the entire globe; however, it is important to note that the data provided over land with high cloud cover and data from above 40°N and below 40°S are characterized with higher levels of uncertainty. Results and conclusions based on data from these uncertain areas should be taken with caution [*Glatthor et al.*, 2015; *Anthony Vincent and Dudhia*, 2017]. While this data set provides multiple years of data, 2006 values are used for comparison.

4.3.3.2 Tropospheric Emissions Spectrometer (TES)

TES data is used here as outlined in Kuai et al. (2015) for the year 2006. TES COS observations are obtained via a satellite based spectral remote sensing platform and are characterized as nadir-viewing column averaged measurements of COS concentrations between 900 hpa and 200 hpa for global oceans between ±40° latitude. Following Kuai et al. (2015), a monthly, TES product is re-gridded onto the GEOS-Chem spatial resolution of 2° latitude × 2.5° longitude, spatially smoothed from the original 20° × 20° grid cells, is used for comparison. TES measurements above 40°N and below 40°S are not currently available because the instrument sensitivity depends on temperature (which are prohibitive at these latitudes) and it is difficult to differentiate between surface emissions and background COS concentrations [*Kuai et al.*, 2015].

4.3.3.3 NOAA ESRL Flask Data

The National Oceanic and Atmospheric Administration (NOAA) Earth Systems Research Laboratory (ESRL) produces flask observation of COS data for the atmospheric dry mole fraction in parts per trillion (ppt) [*Montzka et al.*, 2004, 2007]. Observation data from the following NOAA monitoring stations are used in this study for model comparison: South Pole (SPO, 90°S, 2837 meters above sea level (m asl)), American Samoa (SMO, 14.247°S, 170.564°W, 77 m asl), Mauna Loa, USA (MLO, 19.5362°N, 155.5763°W, 3397 m asl), Cape Kumukahi, USA (KUM, 19.516°N, 154.811°W, 3 m asl), Niwot Ridge, USA (NWR, 40.1°N, 105.5°W, 3475 m asl), Trinidad Head, USA (THD, 41.0°N, 124.1°W, 120 m asl), Wisconsin, USA (LEF, 45.6°N, 90.27°W, 868 m asl; inlet is 396 m above ground), Harvard Forest, USA (HFM, 42.5°N, 72.2°W, 340 m asl; inlet is 29 m above ground), Mace Head, Ireland (MHD, 53.3°N, 9.9°W, 42 m asl), Barrow, USA (BRW, 71.3°N, 156.6°W, 8 m asl), Alert, Canada (ALT, 82.5°N, 62.3°W, 210 m asl), Summit, Greenland (SUM, 72.6°N, 38.4°W, 3200 m asl).

4.4 Results

Atmospheric concentrations of COS modeled by GEOS-Chem, based on the Anthropogenic Enhancement and Ocean Enhancement scenarios, are compared to MIPAS, TES, and NOAA observations of atmospheric COS to the test the underlying hypotheses for closing the global budget of COS and identifying the missing source. Here, we find that

the Anthropogenic Enhancement scenario performs similarly to or slightly better than the Ocean Enhancement scenario for explaining COS observation. This suggests that anthropogenic sources are important for explaining gaps in the global COS budget.

As stated above, previous work has assumed that the missing source of COS is largely due to an unknown ocean source of COS and that anthropogenic COS has remained relatively unchanged for several decades [*Kettle et al.*, 2002; *Berry et al.*, 2013; *Glatthor et al.*, 2015; *Kuai et al.*, 2015]. Below, these assumptions (described in more detail in section 4.3.2) are used to characterize the Ocean Enhancement scenario driven by Kettle et al. (2002) anthropogenic sources and enhanced ocean sources proposed by Berry et al. (2013). For the Anthropogenic Enhancement scenario, the Ocean Enhancement scenario is modified by replacing the anthropogenic sources with that of Chapter 3 and balancing the global budget by reducing ocean sources. For the hypothesis proposed in this study that is characterized by increased anthropogenic sources of COS to hold true, modeled atmospheres from the Anthropogenic Enhancement scenario must perform as well as or better than the Ocean Enhancement scenario in comparison to observations of atmospheric COS. While better agreement of modeled atmospheres from the Anthropogenic Enhancement scenario to observations will obviously support the hypothesis presented here, similar performance, or improvements in some ways and diminished performance in others, demonstrates that anthropogenic sources at least pose strong competition to the ocean source hypothesis. Throughout, four seasons are used for model comparisons and are defined as: March through May (MAM), June through August (JJA), September through November (SON), and December through February (DJF).

The first benchmark for testing the competing hypotheses for the missing source of COS is the MIPAS COS observation data set. Modeled concentrations of COS at approximately 250 hpa from the Anthropogenic Enhancement scenario and the Ocean Enhancement scenario are compared to MIPAS observations which provide data at this pressure level. Figure 4-1 shows the spatial patterns of upper-troposphere COS as the seasonal deviations from the global mean for the Anthropogenic Enhancement scenario (left column), the Ocean Enhancement scenario (center column) and MIPAS observations (right column). Modeled concentrations for this section of the atmosphere more accurately capture spatial trends than modeled concentrations at the level of TES observations (900 hpa to 200 hpa, see the following comparison below). However, both scenarios of modeled concentrations overestimate tropical concentrations in comparison to MIPAS observations. This could be either due to deficiencies in the surface flux parameterization used to drive the GEOS-Chem model or possibly could stem from uncertainty in observed COS over cloudy regions [*Glatthor et al.*, 2015]. However, neglecting this discrepancy, GEOS-Chem simulates COS spatial patterns with exceptional proficiency at 250 hpa for both model scenarios for MAM, JJA and SON. For DJF, both scenarios largely overestimate COS concentrations in comparison to MIPAS observations.

In Figure 4-2 A), the error in the seasonal deviation from the global mean is averaged over the 16 regions of Figure 4-2 B). Errors represent the disagreement from the MIPAS observations for the Anthropogenic Enhancement scenario (left column) and the Ocean

Enhancement scenario (right column). In Figure 4-2 A), shades of blue represent underestimated modeled concentrations and shades of red represent overestimates where darker colors represent higher levels of disagreement with the observations. It is not apparently clear from qualitative analysis that either scenario is superior.

To quantitatively compare model performance and to test the underlying hypotheses of the Anthropogenic Enhancement and Ocean Enhancement scenarios to MIPAS observations, the annual root mean square error (RMSE) is calculated for the error in the deviation from the global mean for the regions in Figure 4-2 B) and are recorded in Table 4-2. The comparison is for the spatial scale of the 16 regions of Figure 4-2 because pixelwise comparisons at fine spatial scales may be unreliable. For example, a simulated plume that is offset by a couple of pixels within the simulated atmosphere in a pixelwise comparison may give a false impression of poor model performance even though overall atmospheric trends are captured in close spatial proximity. Table 4-2 shows that most regions slightly favor the Anthropogenic Enhancement scenario over the Ocean Enhancement scenario except for in regions 12, 15 and 16. Overall, global agreement is better for estimated COS concentrations from the Anthropogenic Enhancement scenario than for the Ocean Enhancement scenario when compared to MIPAS observations.

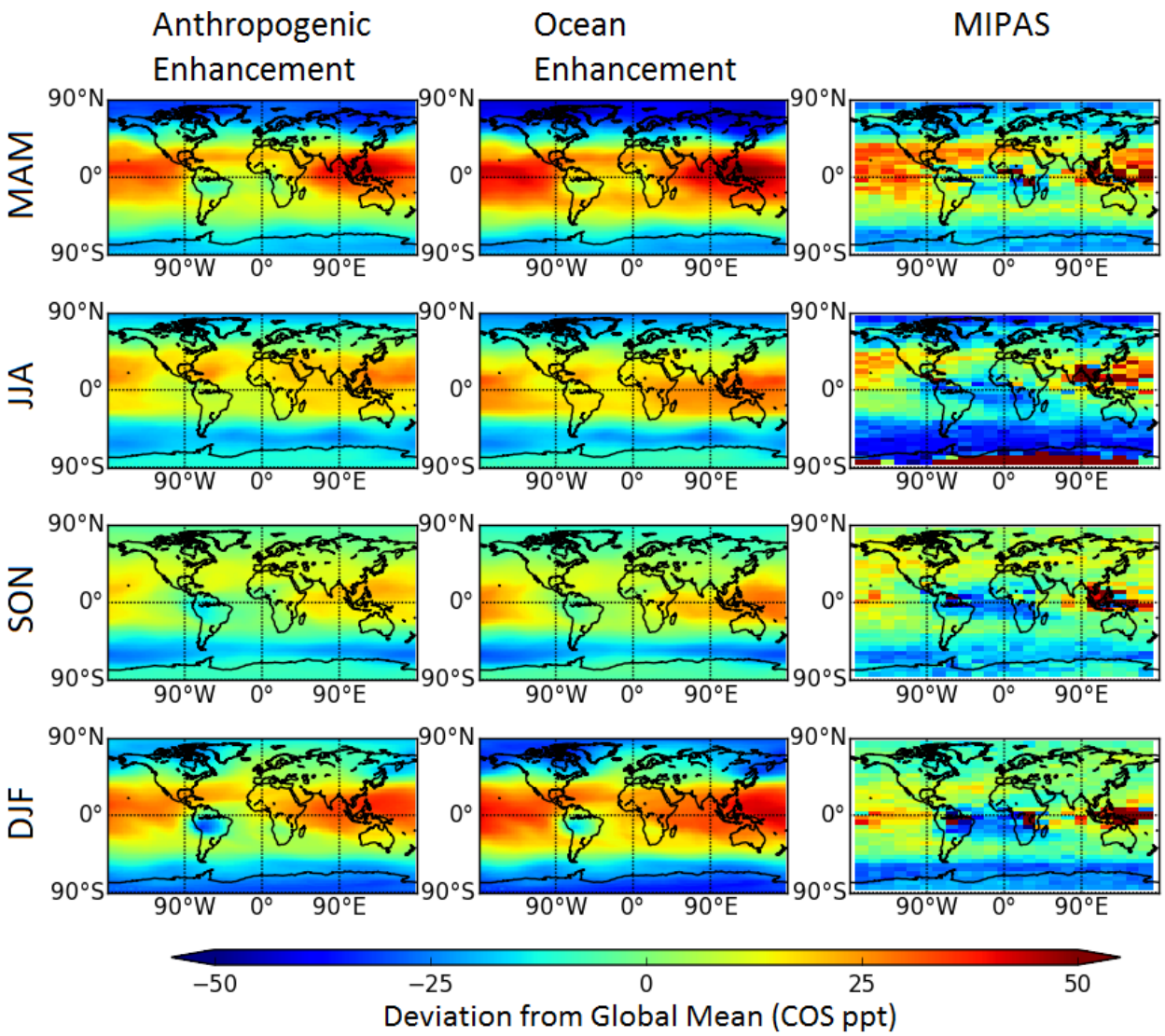

Figure 4-1. Seasonal mean concentrations of COS presented as the deviations from the global mean (COS ppt) from the Anthropogenic Enhancement scenario (left column), the Ocean Enhancement scenario (center column) and MIPAS observations (right column) for March through May (MAM), June through August (JJA), September through November (SON), and December through February (DJF). All data represents COS concentrations at ~250hpa.

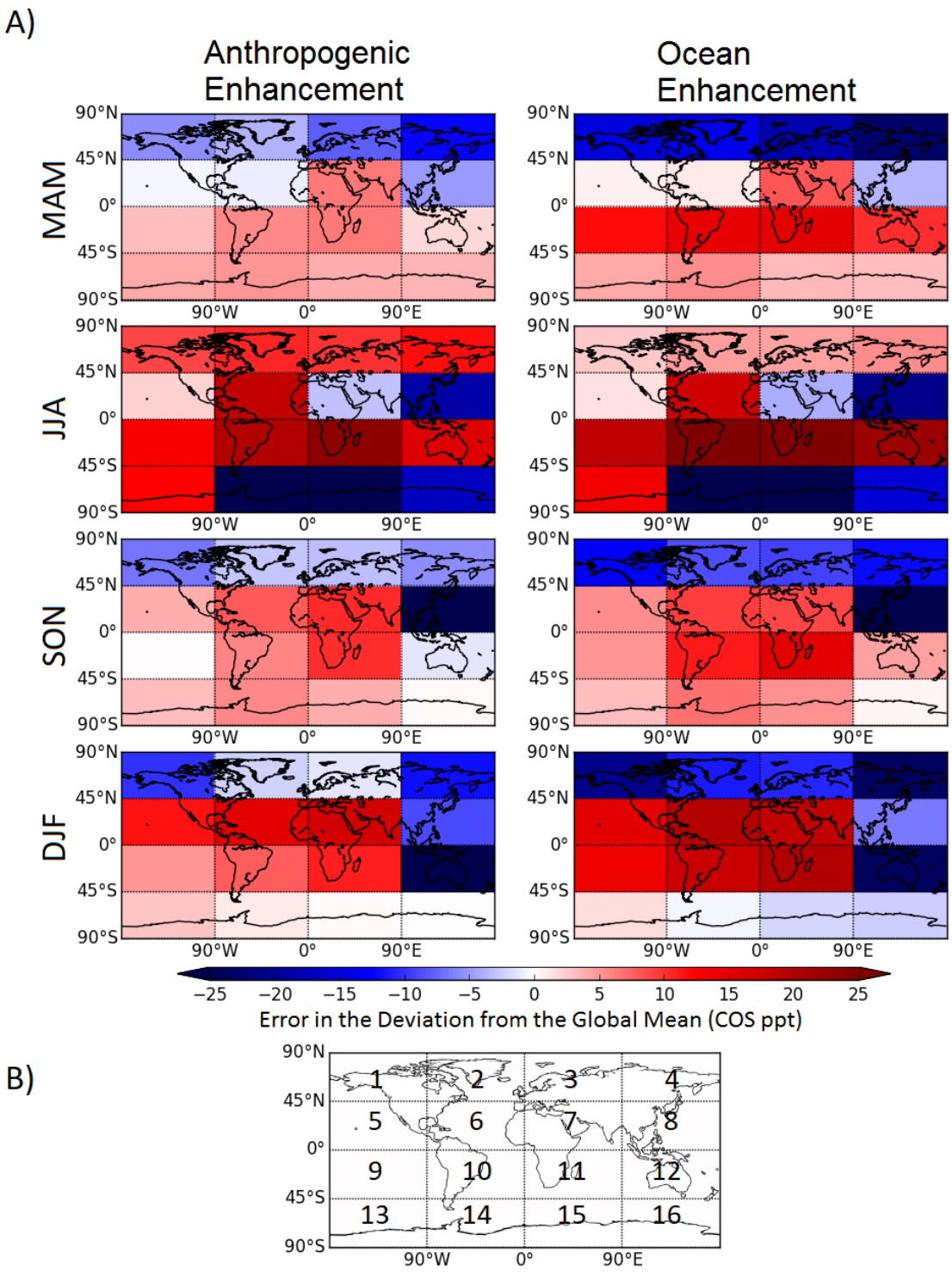

Figure 4-2. A) Error in the modeled seasonal average deviation in COS concentrations from the global mean in comparison to MIPAS observation of atmospheric COS for the Anthropogenic Enhancement scenario (left column) and from the Ocean Enhancement scenario (right column) averaged over B) 16 global regions for March through May (MAM), June through August (JJA), September through November (SON), and December through February (DJF). All data represents COS concentrations at ~250hpa.

Table 4-2. Annual RMSE for the errors in the deviation from the global mean shown in Figure 4-2 A) for the regions shown in Figure 4-2 B).

Region	Anthropogenic Enhancement Scenario	Ocean Enhancement Scenario
1	8.1	14.2
2	5.9	10.3
3	6.6	11.7
4	10.7	17.7
5	6.3	8.1
6	12.7	14.0
7	10.5	11.3
8	17.2	17.8
9	7.3	13.5
10	11.6	18.1
11	14.4	20.8
12	17.9	17.2
13	7.0	7.5
14	24.0	23.3
15	35.6	34.8
16	8.6	8.0

Figure 4-3 compares modeled atmospheric COS concentrations from the Anthropogenic Enhancement scenario (left column) and from the Ocean Enhancement scenario (center column) to TES observations (right column) given as the seasonal mean deviation from global mean COS concentrations (COS ppt) for the vertical column between 900 hpa and 200 hpa and between 40°N and 40°S. Qualitative assessment of Figure 4-3 shows that both parameterizations poorly model Eastern Pacific COS trends. Modeled concentrations from the Anthropogenic Enhancement scenario are biased toward the north and concentrations from the Ocean Enhancement scenario too narrowly concentrated near the equator in comparison to the observations. For this region, surface fluxes from the Anthropogenic Enhancement scenario better characterize areas of high COS in northern latitudes for MAM and SON but the Ocean Enhancement scenario better represents areas of high COS concentrations around the equator, particularly for DJF. Overall, the Ocean Enhancement scenario appears to perform only slightly better for this region. However, poor agreement from both scenarios in comparison to TES observation in the Eastern Pacific does not discount anthropogenic COS sources as a component of the missing source of COS because the only other proposed hypotheses performs poorly as well. It is possible that both enhanced oceans and anthropogenic COS sources might be needed in combination with the addition of other sources or sinks (either additional unknown sources or incorrect estimates of sources already included or all the above) for better model agreement with TES observations in this region. However, if both ocean and anthropogenic sources need enhancement for model agreement with observations, then an additional sink would be required to balance the global budget. As high levels of uncertainty exist within current

estimates of global and regional scale photosynthesis and because it has been proposed that plant uptake could be responsible for historical fluctuations in ice core and firn air COS histories, the plant sink is a logical area of future inquiry [*Montzka et al.*, 2004; *Campbell et al.*, 2008; *Hilton et al.*, 2015, 2017]. In fact, this key uncertainty is a main motivation in developing methodology for using COS as an atmospheric tracer of the carbon cycle.

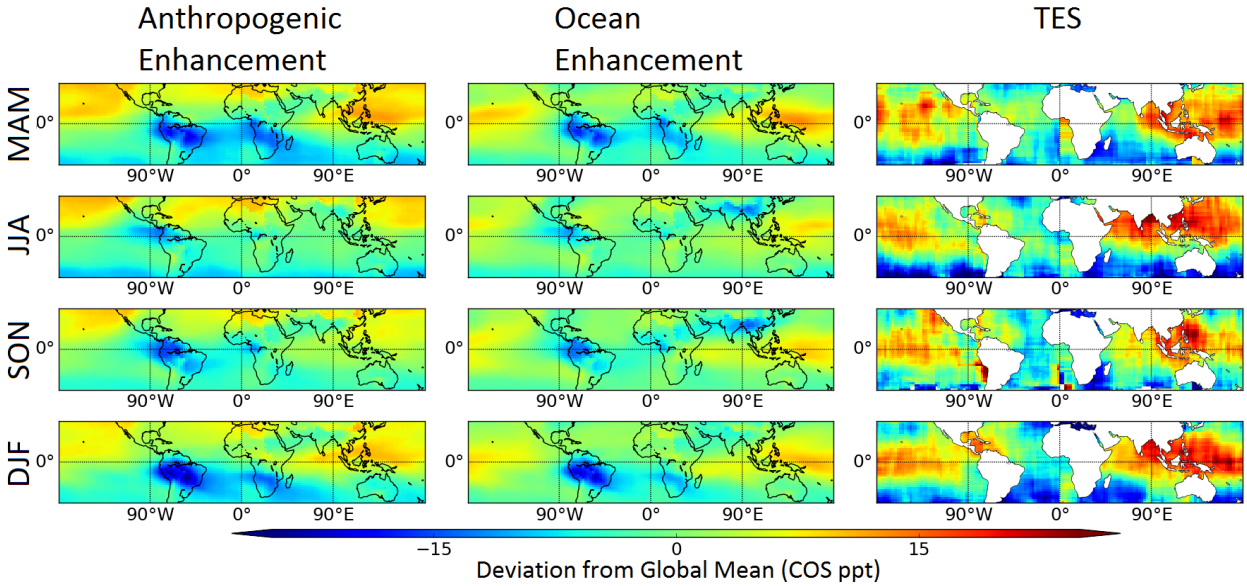

Figure 4-3. Seasonal mean concentrations of COS presented as the deviations from the global mean (COS ppt) from the Anthropogenic Enhancement scenario (left column), anthropogenic sources from the Ocean Enhancement scenario (center column) and TES observations (right column) for March through May (MAM), June through August (JJA), September through November (SON), and December through February (DJF). Values represent an atmospheric column between 200 and 900 hpa.

The oceans to the south and east of Asia have been of particular interest for COS studies, showing high concentrations of atmospheric COS. These areas of observed COS hotspots are compared to modeled atmospheres here because these hotspots have played a large role in the development of the missing ocean source of COS hypothesis [*Kettle et al.*, 2002; *Berry et al.*, 2013; *Glatthor et al.*, 2015; *Kuai et al.*, 2015]. In Figures 4-3 and 4-4, this area of the Western Pacific is shown as the seasonal deviation from the global mean. Here, the model results from the Anthropogenic Enhancement scenario perform better than that of the Ocean Enhancement scenario in reproducing the spatial patterns of TES observed COS enhancement around China and Southeast Asia. While modeled COS concentrations from the Anthropogenic Enhancement scenario miss the mark on some significant observed spatial patterns of COS in this region (e.g. in the Bay of Bengal, hotspots not reaching far enough to the south, and overall poor model agreement for the SON season), the Ocean Enhancement scenario also experiences these deficiencies with the added problem of COS concentrations being spatially biased to the equator.

In Table 4-3, the pixelwise RMSE is computed for the region shown in Figure 4-4 where land points are shown in white to indicate exclusion from the RMSE calculation. For all seasons but MAM, the Anthropogenic Enhancement scenario performs better than the Ocean Enhancement scenario, with a lower RMSE when compared to TES observations. While, qualitatively, the COS hotspots are also better reproduced for MAM (Figures 4-3 and 4-4) in the Anthropogenic Enhancement scenario, this scenario scores lower in the RMSE comparison due to overestimating the magnitude of COS concentrations in northern latitudes where TES observations report very low concentrations. Overall model agreement to TES observations for this region are generally more supportive of surface fluxes assumed in the Anthropogenic Enhancement scenario.

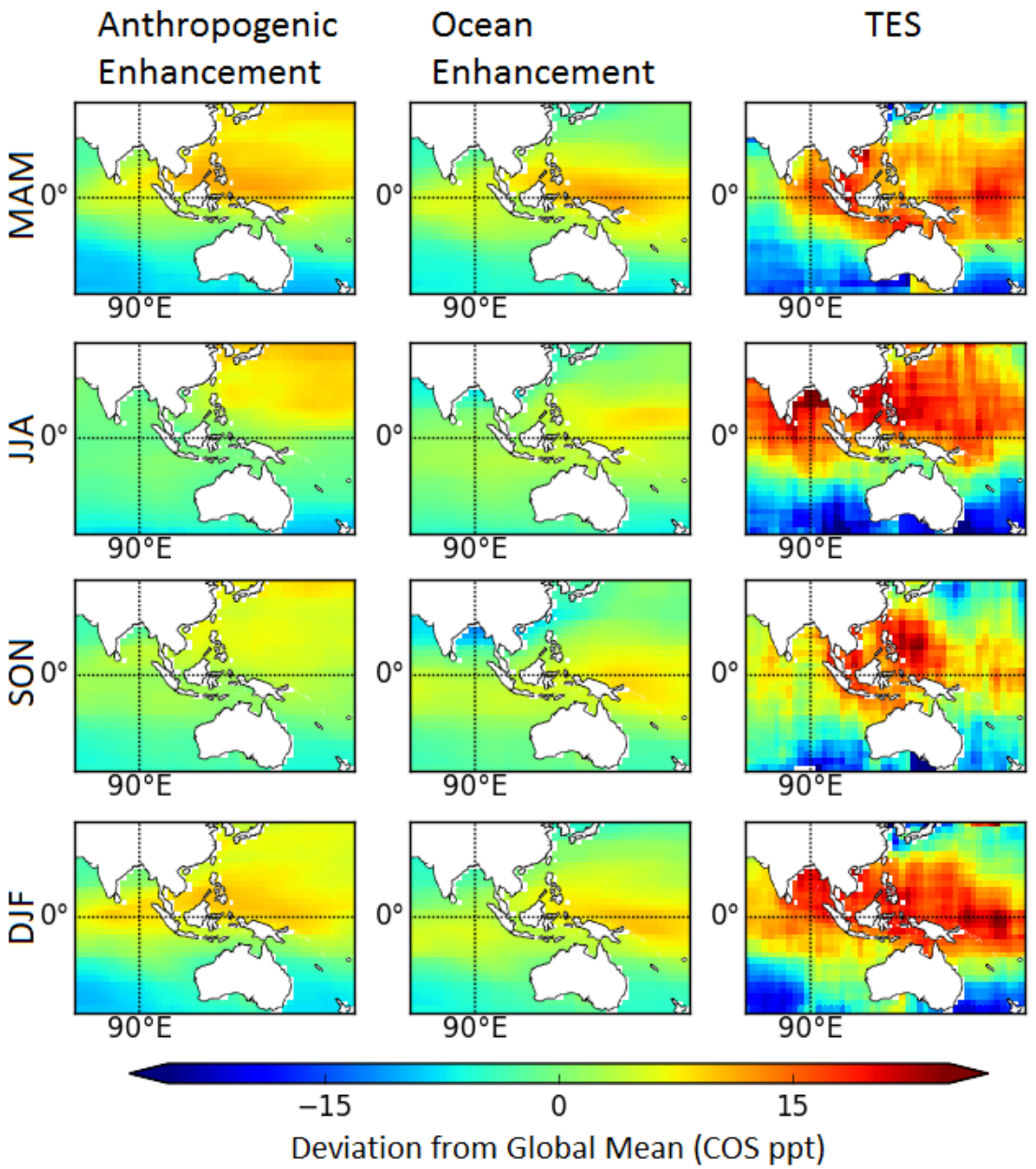

Figure 4-4. Seasonal mean deviations from the global mean (COS ppt) for simulated atmospheric concentrations of COS over Asian tropical oceans. Left column: The Anthropogenic Enhancement scenario, center column: Ocean Enhancement scenario and Right column: TES observations for March through May (MAM), June through August (JJA), September through November (SON), and December through February (DJF). Values represent an atmospheric column between 200 and 900 hpa.

Table 4-3. Seasonal mean pixelwise RMSE of the deviation from the global mean (COS ppt) for modeled concentrations of COS from the Anthropogenic Enhancement scenario and the Ocean Enhancement scenario in comparison to TES observations in the region shown in Figure 4-4. Land areas (white) are excluded.

	RMSE	
Season	**Anthropogenic Enhancement Scenario**	**Ocean Enhancement Scenario**
MAM	9.5	9.0
JJA	11.7	13.5
SON	8.3	9.3
DJF	9.4	9.6

In Figure 4-5 A), the error in the seasonal deviation from the global mean is averaged over the eight regions of Figure 4-5 B). Errors represent the disagreement from the TES observations for the Anthropogenic Enhancement scenario (left column) and the Ocean Enhancement scenario (right column). Modeled concentrations from the Anthropogenic Enhancement scenario perform slightly better for all regions shown in Figure 4-5 except for regions 2 and 3 where the Ocean Enhancement scenario performs much better in region 2. However, for the remaining 6 regions, modeled COS concentrations from the Anthropogenic Enhancement scenario perform better for all seasons with considerably better agreement in region 4 (the approximate region analogous to the region in Figure 4-4 that was used to analyze COS hotspots in tropical Asian oceans which was an important region in the formulation of the ocean source hypothesis).

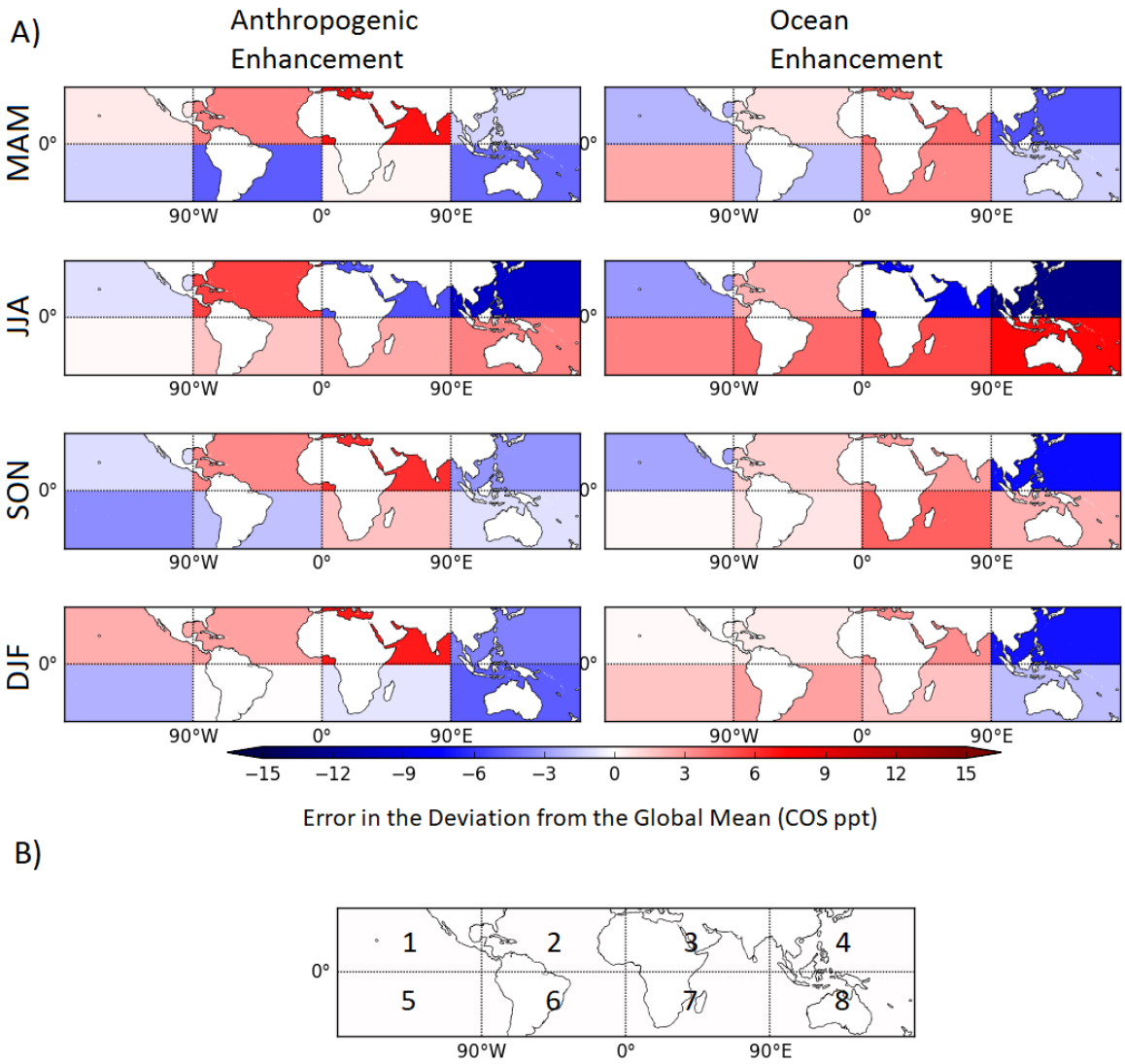

Figure 4-5. A) Error in the modeled seasonal average deviation in COS concentrations from the global mean in comparison to MIPAS observation of atmospheric COS for the Anthropogenic Enhancement scenario (left column) and the Ocean Enhancement scenario (right column) for B) eight global regions for March through May (MAM), June through August (JJA), September through November (SON), and December through February (DJF). Values represent an atmospheric column between 200 and 900 hpa.

Table 4-4 shows the annual RMSE in modeled COS concentrations in comparison to TES observations for the deviation from the global mean. Like the qualitative analysis in Figure 4-5, the results shown in Table 4-4 confirm that the modeled concentrations from the Anthropogenic Enhancement scenario perform better than that of the Ocean Enhancement scenario for all regions except regions 2 and 3, with overall better global agreement.

Table 4-4. Annual RMSE for the errors in the deviation from the global mean shown in Figure 4-5 A) for the regions shown in Figure 4-5 B).

	RMSE	
Region	**Anthropogenic Enhancement Scenario**	**Ocean Enhancement Scenario**
1	1.4	2.3
2	4.0	1.4
3	6.3	5.1
4	5.5	8.4
5	2.1	2.4
6	2.7	2.8
7	1.6	4.0
8	3.8	4.0

Figure 4-6 provides a comparison of monthly average simulated COS concentrations from the Anthropogenic Enhancement scenario (green) and the Ocean Enhancement scenario (blue) to observations of COS from 12 NOAA monitoring stations. The green and blue lines represent a linear fit for the Anthropogenic Enhancement scenario and the Ocean Enhancement scenario, respectively, and the black dashed line represents the one-to-one line that would result from perfect model agreement to observations. The locations of the NOAA observation sites are shown in Figure 4-7. In Figure 4-6, a higher R^2 value indicates that a simulation captures seasonal trends in COS variability well in comparison to observations. Similarly, a regression line with a slope closer to the dashed one-to-one line indicates a simulation that captures a similar magnitude in the seasonal trends. The Anthropogenic Enhancement scenario produces simulations with a higher R^2 value than that of the Ocean Enhancement scenario for 7 out of 12 NOAA sites (ALT, MLO, SUM, KUM, BRW, THD, MHD), and one tie (SPO). Overall, the slope of the regression lines from the Anthropogenic Enhancement scenario and the Ocean Enhancement scenario are similar for most NOAA sites and indicate that the overall model variation is somewhat muted in comparison to observation data. In other words, the slopes of the regression lines indicate that large changes in seasonal COS concentrations are represented by a relatively smaller modeled change for the same location and month. The Anthropogenic Enhancement scenario has regression slopes closer to the one-to-one line at 8 of the 12 NOAA stations (ALT, LEF, SUM, HFM, KUM, BRW, MHD, and NWR); however, in most cases, the difference is quite small. Both models perform particularly well at the MLO and SPO sites, producing slopes close to 1 and high R^2 values. At SPO, modeled results are so similar that the dots from the Anthropogenic Enhancement scenario are eclipsed by the dots from the Ocean Enhancement scenario. Like the MIPAS and TES comparisons, the model performance in comparison to the NOAA observation suggests that higher anthropogenic sources may be a slightly better or complementary explanation for the missing source of COS in comparison to enhanced ocean sources.

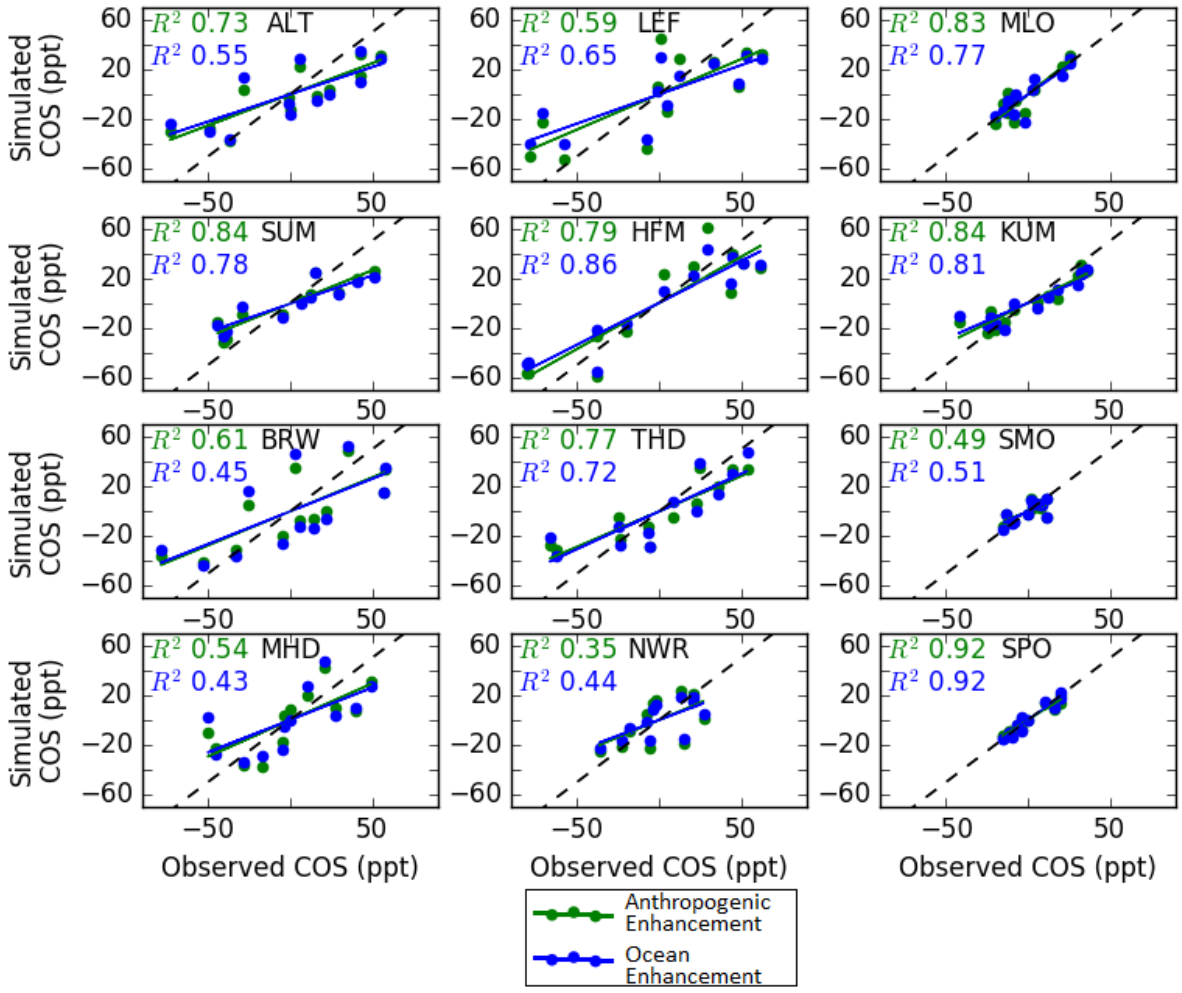

Figure 4-6. A comparison of average monthly simulated atmospheric COS concentrations from the Anthropogenic Enhancement scenario (green) and the Ocean Enhancement scenario (blue) to COS observations at 12 NOAA monitoring stations. Values are shown as the deviation from the annual mean (ppt) for 2006. Green and Blue lines represent a linear regression for each simulation and the black dashed line represents the one-to-one line that would result from a perfect agreement between simulated and observed values.

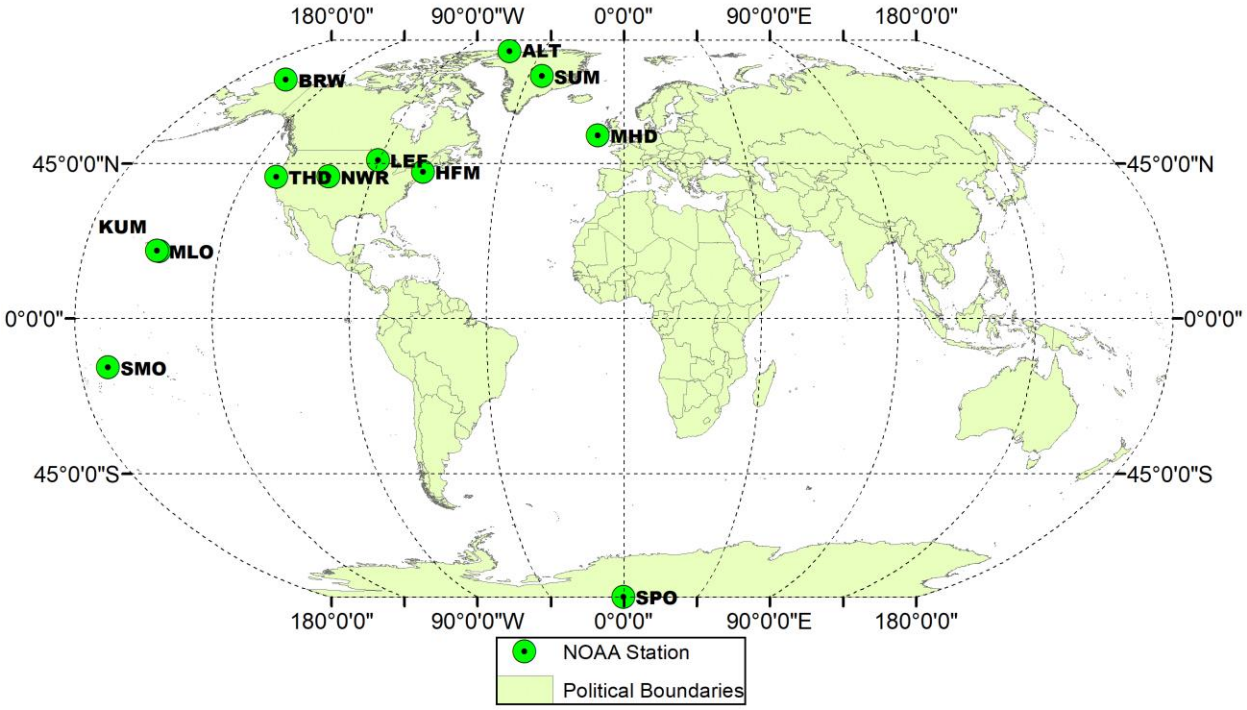

Figure 4-7. Location of NOAA COS monitoring stations (green circles): Alert, Canada (ALT), Summit Greenland (SUM), Barrow, Alaska (BRW), Mace Head, Ireland (MHD), Trinidad Head, California (THD), Niwot Ridge, Colorado (NWR), Cape Kumukahi, Hawaii (KUM), Manua Loa, Hawaii (MLO), American Samoa (SMO), Cape Grim, Australia (CGO), Park Falls, Wisconsin (LEF), South Pole, Antarctica (SPO).

4.5 Discussion

The relatively stable time series of observed atmospheric concentrations of COS and an upward revisions of the global plant sink of COS present a strong case for a missing source of atmospheric COS [*Kettle et al.*, 2002; *Sandoval-Soto et al.*, 2005; *Montzka et al.*, 2007]. It is shown here that compensating for the missing source of COS through anthropogenic sources of COS to the atmosphere provide similar, and in some cases, higher levels of agreement to observations than assuming enhanced ocean sources. Simulations show that the observed areas of high COS concentrations in tropical Asian oceans, a key factor in developing the hypothesis for a missing source of oceanic COS, are better characterized by anthropogenic enhancement than ocean enhancement. This is shown through two estimates of atmospheric concentrations of COS simulated by the GEOS-Chem ATM that is driven by enhanced anthropogenic sources of COS and enhanced ocean sources. These results allow for increased anthropogenic COS sources to be a strong candidate for closing the atmospheric COS budget and provide an intriguing alternate explanation for COS enhancement over tropical Asian oceans. Furthermore, recent revisions of global anthropogenic COS sources, and work that has challenged the missing ocean source hypothesis due to findings of under-saturated ocean surface waters and low global annual direct emissions of COS from oceans further support an anthropogenic explanation to the

missing COS source (*Lennartz et al.*, 2016*; Chapter 3*). However, model deficiencies still exist and with persistent uncertainty in the magnitude and spatial distribution of plant sink of COS, enhanced ocean sources are certainly not ruled out as an additional or complementary explanation of the missing source of COS.

Additional future transport modeling using new characterizations of COS plant uptake, various degrees of anthropogenic, ocean or combined anthropogenic and ocean enhancement, different transport models and meteorological driver data may provide a better representation of observed atmospheric COS and provide additional insights into source balancing. It is also important to note that the anthropogenic sources of COS used here from Chapter 3 in the Anthropogenic Enhancement scenario are not the final version of the anthropogenic sources that are reported in Chapter 3 and overestimated the pulp and paper source by over 100 Gg S y^{-1}. This overestimate of the pulp and paper sources was based on large total pulp and paper COS sources reported in Lee and Brimblecombe (2016). This was part of a preliminary version of Chapter 3 sources of COS before we opted to base our pulp and paper source on the U.S. EPA estimates [*EPA Office of Air Quality Planning and Standards and EPA Office of Air and Radiation*, 2012]. Subsequent modelling studies will use the reduced pulp and paper source that is presented in Chapter 3.

It is also important to note that while MIPAS and TES satellite observations of COS are used as benchmarks for model performance, uncertainty in satellite retrieval methods are relevant and these products require further validation. For example, new methodology for obtaining COS observations from IASI satellite retrievals provide a different picture of total column COS than TES observations, showing high COS over China (TES did not provide over-land estimates), consistent with anthropogenic source estimates of Chapter 3, and showing the largest ocean enhancement to be concentrated in the Southern Hemisphere in contrast with TES observations [*Kuai et al.*, 2015; *Anthony Vincent and Dudhia*, 2017].

While the focus of this study is to evaluate anthropogenic and ocean COS enhancements of COS sources as possible explanations of missing global COS sources, the results of this study also provide some support for the upward revision in anthropogenic COS sources of Chapter 3. Though there are too many confounding factors to make a definitive statement of source validation, the results here are at least encouraging of the Chapter 3 estimate. Furthermore, any favorable model performance in the Ocean Enhancement scenario is likely attributed to the large ocean sources and not the much smaller Kettle et al. (2002) anthropogenic sources. Additionally, the large COS observations near China shown in the IASI observation are consistent with Chapter 3 inventories of anthropogenic sources of atmospheric COS while in contrast with Kettle et al. (2002).

Chapter 5: Conclusion

5.1 Discussion of Results

Here I make estimates of global anthropogenic sources of COS that I assert are an improvement over other estimates for one or more of the following reasons: 1) data is provided in gridded format that is of a finer spatial resolution (0.1 × 0.1 degrees latitude/longitude) than other estimates of anthropogenic COS sources, 2) more sources of anthropogenic COS are considered than ever before in a single gridded data set, 3) the best and most current industry activity and emissions factor data are used as input, 4) a more sophisticated and comprehensive spatial scaling method is used here than ever before applied to anthropogenic sources of COS, and 5) an annual history from 1980 to 2012 is provided, whereas the previous gridded inventory provides only a one year climatological estimate.

The first iteration of this data set (Chapter 2) was limited in comparison to the 5 points of the previous paragraph in a few key areas: the spatial extent was limited to the U.S., an annual history was not provided, and it did not contain the full list of anthropogenic sources found in the global data set of Chapter 3. However, it was still an advancement toward understanding anthropogenic COS sources and is the basis for the methodology of the global source estimate presented in Chapter 3. It also served as a case study for demonstrating how much anthropogenic sources change when using current data and source specific spatial scaling in comparison to the previous gridded data set (which was the only gridded data set available for modeling studies). This U.S. case study of anthropogenic COS sources provides a very different magnitude of sources because more sources are considered and because industry activity data used in previous estimates are from more than three decades ago are not representative of current anthropogenic activity. Additionally, the unique source specific spatial scaling of this study suggests a very different spatial pattern of anthropogenic COS sources in the U.S. Subsequent atmospheric transport modeling of the updated estimates of COS sources from this study and of previous estimates show significantly different spatial patterns of anthropogenic atmospheric COS enhancement. This suggests that using the Kettle inventory likely introduces large interpretation bias when analyzing COS observations. These findings encouraged the effort to create a global data set.

Like the U.S. data set, the global data set, characterized by the five key points discussed above, also demonstrated a very different picture of anthropogenic sources than previous estimates. Therefore, interpretation bias at this spatial scale is also a major concern when using the Kettle inventory.

Lastly, the large upward revision in anthropogenic COS sources in the global data set presented here led me to hypothesize that anthropogenic COS sources might explain the gap in the global COS budget, as opposed to the unknown ocean source hypothesized in

previous work. Anthropogenic COS emerges from atmospheric transport modeling scenarios (one designed to represent the anthropogenic enhancement hypothesis of this study and another for the ocean source enhancement hypothesis) as a strong, novel and alternative or complementary explanation for the missing source of atmospheric COS.

5.2 Future Work

Though the emissions factors used in this study to create the gridded data set of anthropogenic COS sources are the best available, they are still the largest source of uncertainty. Future work can reduce this uncertainty by reevaluating the emissions factors through sampling campaigns and laboratory experimentation. A key source of uncertainty in emissions factors to be addressed in future work stems from regional variation in emissions control standards, industrial processes and fuel composition. Currently, emissions factors are largely derived from relatively few input data. For example, the emissions factors for COS emissions from coal power plants are based only on select observations in the U.S.

Advancements in our ability to make large-scale remote sensing observations of atmospheric COS (e.g. satellites) can be used to better validate the assertions of Chapter 4. Specifically, TES and IASI observations lead to different conclusions about atmospheric COS trends. This problem calls for an advancement in satellite retrieval methods or increased computational power to allow for more complex but more accurate algorithms to be used for the retrieval process. Additionally, more robust and widespread flask sampling of COS could be used to help validate satellite based observation products of atmospheric COS concentrations.

Finally, revisiting the modeling studies of Chapter 4 with different assumptions and surface flux parameterizations could produce new insights into balancing the global budget of atmospheric COS. While Chapters 3 and 4 demonstrated that anthropogenic COS is a more important component of the global budget of atmospheric COS than previously considered and may be the most important source for closing the global budget, atmospheric transport modeling results do not completely explain observed atmospheric COS trends. This could be due to model deficiencies or deficiencies in any of the model input. Future atmospheric transport modeling studies exploring the global budget of atmospheric COS should include different assumptions of the plant uptake of COS (which is highly uncertain) as well as varying combinations of anthropogenic and ocean enhancement. One interesting modification to the ocean source of COS would be to relocate it to the Southern Hemisphere as shown in IASI observations (in modeling studies here, ocean enhancement is centered around the equator in agreement with TES observations). Using alternative atmospheric transport models or meteorological driver data may also produce interesting results.

References

Anthony Vincent, R., and A. Dudhia (2017), Fast retrievals of tropospheric carbonyl sulfide with IASI, *Atmos. Chem. Phys.*, *17*(4), 2981–3000, doi:10.5194/acp-17-2981-2017.

Apodaca, L. E. (2015), *Mineral Commodity Summaries: Sulfur*.

Arneth, A. et al. (2010), Terrestrial biogeochemical feedbacks in the climate system, *Nat. Geosci*, *3*(8), 525–532.

Barnes, I., K. H. Becker, and I. Patroescu (1994), The tropospheric oxidation of dimethyl sulfide: A new source of carbonyl sulfide, *Geophys. Res. Lett.*, *21*(22), 2389–2392, doi:10.1029/94GL02499.

Berry, J. et al. (2013), A coupled model of the global cycles of carbonyl sulfide and CO2 : A possible new window on the carbon cycle, *J. Geophys. Res. Biogeosciences*, *118*(2), 842–852, doi:10.1002/jgrg.20068.

Bey, I., D. J. Jacob, R. M. Yantosca, J. A. Logan, B. D. Field, A. M. Fiore, Q.-B. Li, H.-Y. Liu, L. J. Mickley, and M. G. Schultz (2001), Global modeling of tropospheric chemistry with assimilated meteorology: Model description and evaluation, *J. Geophys. Res.*, *106*, 73–95, doi:10.1029/2001JD000807.

Billesbach, D. P., J. A. Berry, U. Seibt, K. Maseyk, M. S. Torn, M. L. Fischer, M. Abu-Naser, and J. E. Campbell (2014), Growing season eddy covariance measurements of carbonyl sulfide and CO2 relationships in Southern Great Plains winter wheat, *Agric. For. Meteorol.*, *184*, 48–55.

Blagoev, M., and C. Funada (2011), Marketing Research Report: Carbon Disulfide, *CEH*, (625.5000C), 1–65. Available from: https://www.ihs.com/products/chemical-economics-handbooks.html

Blake, N. J., D. G. Streets, J.-H. Woo, I. J. Simpson, and J. Green (2004), Carbonyl sulfide and carbon disulfide: Large-scale distributions over the western Pacific and emissions from Asia during TRACE-P, *J. Geophys. Res.*, *109*(D15), D15S05, doi:10.1029/2003JD004259.

Blake, N. J. et al. (2008), Carbonyl sulfide (OCS): Large-scale distributions over North America during INTEX-NA and relationship to CO2, *J. Geophys. Res.*, *113*(D9), D09S90, doi:10.1029/2007JD009163.

Blonquist, J. M., S. A. Montzka, J. W. Munger, D. Yakir, A. R. Desai, D. Dragoni, T. J. Griffis, R. K. Monson, R. L. Scott, and D. R. Bowling (2011), The potential of carbonyl sulfide as a proxy for gross primary production at flux tower sites, *J. Geophys. Res. Biogeosciences*, *116*(G4), G04019, doi:10.1029/2011JG001723.

Büchel, K. H., H.-H. Moretto, D. Werner, and P. Woditsch (2000), *Industrial Inorganic Chemistry*, 2 edition., Wiley-VCH, Weinheim, Germany.

Campbell, J., A. Zumkehr, J. A. Berry, M. S. Torn, S. Biraud, S. A. Montzka, C. Sweeney, U. H. Seibt, K. S. Maseyk, and I. T. Baker (2013), Regional constraints on GPP using atmospheric carbonyl sulfide simulations and airborne observations, *Am. Geophys. Union*.

Campbell, J. E. et al. (2007), Analysis of anthropogenic CO2 signal in ICARTT using a regional chemical transport model and observed tracers, *Tellus B*, *59*(2), 199–210,

doi:10.1111/j.1600-0889.2006.00239.x.
Campbell, J. E. et al. (2008), Photosynthetic control of atmospheric carbonyl sulfide during the growing season, *Science*, *322*(5904), 1085–1088, doi:10.1126/science.1164015.
Campbell, J. E., M. E. Whelan, U. Seibt, S. J. Smith, J. A. Berry, and T. W. Hilton (2015), Atmospheric carbonyl sulfide sources from anthropogenic activity: Implications for carbon cycle constraints, *Geophys. Res. Lett.*, *42*(8), 3004–3010, doi:10.1002/2015GL063445.
Carmichael, G. R., L. K. Peters, and R. D. Saylor (1991), The STEM-II regional scale acid deposition and photochemical oxidant model—I. An overview of model development and applications, *Atmos. Environ. A.General Top.*, *25*(10), 2077–2090, doi:http://dx.doi.org/10.1016/0960-1686(91)90085-L.
Central Intelligence Agency (2016), The World Factbook, Available from: https://www.cia.gov/library/publications/the-world-factbook/rankorder/2119rank.html
Chin, M., and D. D. Davis (1993), Global sources and sinks of OCS and CS2 and their distributions, *Global Biogeochem. Cycles*, *7*(2), 321–337, doi:10.1029/93GB00568.
Commane, R., L. K. Meredith, I. T. Baker, J. A. Berry, J. W. Munger, S. A. Montzka, P. H. Templer, S. M. Juice, M. S. Zahniser, and S. C. Wofsy (2015), Seasonal fluxes of carbonyl sulfide in a midlatitude forest., *Proc. Natl. Acad. Sci. U. S. A.*, *112*(46), 14162–7, doi:10.1073/pnas.1504131112.
Cox, P. M., R. A. Betts, C. D. Jones, S. A. Spall, and I. J. Totterdell (2000), Acceleration of global warming due to carbon-cycle feedbacks in a coupled climate model, *Nature*, *408*(6809), 184–187.
Crump, E. L. (2000), *Economic Impact Analysis For the Proposed Carbon Black Manufacturing NESHAP*.
D'Allura, A. et al. (2011), Meteorological and air quality forecasting using the WRF-STEM model during the 2008 ARCTAS field campaign, *Atmos. Environ.*, *45*(38), 6901–6910, doi:10.1016/j.atmosenv.2011.02.073.
Dargay, J., D. Gately, and M. Sommer (2007), Vehicle ownership and income growth, worldwide: 1960-2030, *Energy J.*, *28*(4), 143–170, doi:10.2307/41323125.
Dodd, N., M. Cordella, O. Wolf, J. Waidløw, M. Stibold, and E. Hansen (2013), *Revision of the European Ecolabel and Green Public Procurement Criteria for Textile Products*, Sevilla, Spain.
Du, Q. et al. (2016), An important missing source of atmospheric carbonyl sulfide: Domestic coal combustion, *Geophys. Res. Lett.*, *43*(16), 8720–8727, doi:10.1002/2016GL070075.
EPA Office of Air Quality Planning and Standards, and EPA Office of Air and Radiation (2012), *Residual Risk Assessment for the Pulp & Paper Source Category*.
Fiber Economics Bureau (2014), Fiber Organon, , 94–116. Available from: http://www.fibereconomics.com/feb3c.htm
Field, C. B., D. B. Lobell, H. A. Peters, and N. R. Chiariello (2007), Feedbacks of terrestrial ecosystems to climate change, *Annu. Rev. Environ. Resour.*, *32*(1), 1–29, doi:10.1146/annurev.energy.32.053006.141119.
Food and Agriculture Organization (2010), *pulp and paper capacities*, Rome.

Friedlingstein, P. et al. (2006), Climate-carbon cycle feedback analysis: Results from the C4MIP model intercomparison, *J. Clim.*, *19*(14), 3337–3353, doi:10.1175/JCLI3800.1.

Friedlingstein, P., M. Meinshausen, V. K. Arora, C. D. Jones, A. Anav, S. K. Liddicoat, and R. Knutti (2014), Uncertainties in CMIP5 climate projections due to carbon cycle feedbacks, *J. Clim.*, *27*(2), 511–526, doi:10.1175/JCLI-D-12-00579.1.

Gandhi, B. (2005), *Reassessment of one Exemption from the Requirement of a Tolerance for Carbon Black*, Washington D.C.

Glatthor, N. et al. (2015), Tropical sources and sinks of carbonyl sulfide observed from space, *Geophys. Res. Lett.*, *42*(22), 10,082-10,090, doi:10.1002/2015GL066293.

Global Industry Analysts (2011), Global Cellulosic Man-made Fibers Market to Reach 5.16 Million Tons by 2017, According to a New Report by Global Industry Analysts, Inc., *PRWEB*. Available from: http://www.prweb.com/releases/cellulosic_man-made_fiber/rayon_viscose_filament/prweb8831419.htm (Accessed 1 January 2017)

Gullingsrud, A. (2017), *Fashion Fibers + Studio Access.*, Fairchild Books.

Gurney, K. R. et al. (2002), Towards robust regional estimates of CO2 sources and sinks using atmospheric transport models., *Nature*, *415*(6872), 626–30, doi:10.1038/415626a.

Harnisch, J., R. Borchers, P. Fabian, and K. Kourtidis (1995), Aluminium production as a source of atmospheric carbonyl sulfide (COS), *Environ. Sci. Pollut. Res.*, *2*(3), 161–162, doi:10.1007/BF02987529.

Hilton, T. W., A. Zumkehr, S. Kulkarni, J. Berry, M. E. Whelan, and J. E. Campbell (2015), Large variability in ecosystem models explains uncertainty in a critical parameter for quantifying GPP with carbonyl sulphide, *Tellus B*, *67*, doi:10.3402/tellusb.v67.26329.

Hilton, T. W., M. E. Whelan, A. Zumkehr, S. Kulkarni, J. A. Berry, I. T. Baker, S. A. Montzka, C. Sweeney, B. R. Miller, and J. E. Campbell (2017), Peak growing season gross uptake of carbon in North America is largest in the Midwest USA, *Nat. Clim. Chang.*, (May), doi:10.1038/NCLIMATE3272.

Hinds, W. E. (1902), Carbon Bisulphid as an Insecticide, in *Farmers' Bulleting*, p. 28, U.S. Department of Agriculture, Washington D. C.

Huntzinger, D. N. et al. (2012), North American Carbon Program (NACP) regional interim synthesis: Terrestrial biospheric model intercomparison, *Ecol. Model.*, *232*(0), 144–157, doi:http://dx.doi.org/10.1016/j.ecolmodel.2012.02.004.

IARC - World Health Organization (1984), Evaluation of the Carcinogenic Risk of Chemicals to Humans, *IARC Monogr.*, *33*.

IARC - World Health Organization (2010), Some Aromatic Amines, Organic Dyes, and Related Exposures, *IARC Monogr. Eval. Carcinog. Risks to Humans*, *93*, 9–38, doi:10.1007/s10350-006-0552-z.

ICBA (2016a), Carbon Black User's Guide, *Int. Carbon Black Assoc.*, 36. Available from: http://www.carbon-black.org/images/docs/2016-ICBA-Carbon-Black-User-Guide.pdf

ICBA (2016b), What is Carbon Black?, Available from: http://www.carbon-black.org/index.php/what-is-carbon-black (Accessed 17 January 2017)

Intergovernmental Panel on Climate Change (Ed.) (2014), *Climate Change 2013 - The Physical Science Basis*, Cambridge University Press, Cambridge.

Joint Research Centre (2011), Global Emissions EDGAR v4.2, Available from: http://edgar.jrc.ec.europa.eu

Kettle, A. J., U. Kuhn, M. von Hobe, J. Kesselmeier, and M. O. Andreae (2002), Global budget of atmospheric carbonyl sulfide: Temporal and spatial variations of the dominant sources and sinks, *J.Geophys.Res.*, *107*, 4658, doi:10.1029/2002JD002187.

Khalil, M. A. K., and R. A. Rasmussen (1984), Global sources, lifetimes and mass balances of carbonyl sulfide (OCS) and carbon disulfide (CS2) in the earth's atmosphere, *Atmos. Environ.*, *18*(9), 1805–1813, doi:10.1016/0004-6981(84)90356-1.

Kimmerle, F., and L. Noel (1997), COS, CS2 and SO2 emissions from prebake Hall Heroult cells, *Arvida Reasearch Dev. Cent.*, 153–158.

Kjellstrom, E. (1998), A three-dimensional global model study of carbonyl sulfide in the troposphere and the lower stratosphere, *J. Atmos. Chem.*, *29*(2), 151–177, doi:10.1023/A:1005976511096.

Kremser, S., N. B. Jones, M. Palm, B. Lejeune, Y. Wang, D. Smale, and N. M. Deutscher (2015), Positive trends in Southern Hemisphere carbonyl sulfide, *Geophys. Res. Lett.*, *42*(21), 9473–9480, doi:10.1002/2015GL065879.

Kuai, L., J. Worden, S. S. Kulawik, S. A. Montzka, and J. Liu (2014), Characterization of Aura TES carbonyl sulfide retrievals over ocean, *Atmos. Meas. Tech.*, *7*(1), 163–172, doi:10.5194/amt-7-163-2014.

Kuai, L. et al. (2015), Estimate of carbonyl sulfide tropical oceanic surface fluxes using Aura Tropospheric Emission Spectrometer observations, *J. Geophys. Res. Atmos.*, *120*(20), 11,012-11,023, doi:10.1002/2015JD023493.

Kulkarni, S. et al. (2014), Source sector and region contributions to BC and $PM_{2.5}$ in Central Asia, *Atmos. Chem. Phys. Discuss.*, *14*(8), 11343–11392, doi:10.5194/acpd-14-11343-2014.

Launois, T., P. Peylin, S. Belviso, and B. Poulter (2014), A new model of the global biogeochemical cycle of carbonyl sulfide – Part 2: Use of OCS to constrain gross primary productivity of current vegetation models, *Atmos. Chem. Phys. Discuss.*, *14*(20), 27663–27729, doi:10.5194/acpd-14-27663-2014.

Launois, T., S. Belviso, L. Bopp, C. G. Fichot, and P. Peylin (2015), A new model for the global biogeochemical cycle of carbonyl sulfide – Part 1: Assessment of direct marine emissions with an oceanic general circulation and biogeochemistry model, *Atmos. Chem. Phys.*, *15*(5), 2295–2312, doi:10.5194/acp-15-2295-2015.

Lee, C. L., and P. Brimblecombe (2016), Anthropogenic contributions to global carbonyl sulfide, carbon disulfide and organosulfides fluxes, *Earth-Science Rev.*, *160*, 1–18, doi:10.1016/j.earscirev.2016.06.005.

Lejeune, B., E. Mahieu, M. K. Vollmer, S. Reimann, P. F. Bernath, C. D. Boone, K. A. Walker, and C. Servais (2017), Optimized approach to retrieve information on atmospheric carbonyl sulfide (OCS) above the Jungfraujoch station and change in its abundance since 1995, *J. Quant. Spectrosc. Radiat. Transf.*, *186*, 81–95, doi:10.1016/j.jqsrt.2016.06.001.

Lennartz, S. T. et al. (2016), Oceanic emissions unlikely to account for the missing source of atmospheric carbonyl sulfide, *Atmos. Chem. Phys. Discuss.*, *mixi*(September), 1–23, doi:10.5194/acp-2016-778.

Maseyk, K., J. A. Berry, D. Billesbach, J. E. Campbell, M. S. Torn, M. Zahniser, and U. Seibt (2014a), Sources and sinks of carbonyl sulfide in an agricultural field in the Southern Great Plains., *Proc. Natl. Acad. Sci. U. S. A.*, *111*(25), 9064–9, doi:10.1073/pnas.1319132111.

Maseyk, K., J. A. Berry, D. Billesbach, J. E. Campbell, M. S. Torn, M. Zahniser, and U. Seibt (2014b), Sources and sinks of carbonyl sulfide in an agricultural field in the Southern Great Plains., *Proc. Natl. Acad. Sci. U. S. A.*, *111*(25), 9064–9, doi:10.1073/pnas.1319132111.

Maseyk, K. S., U. Seibt, J. A. Berry, D. P. Billesbach, J. Campbell, and M. S. Torn (2012), Strong soil source of carbonyl sulfide in an agricultural field, *AGU Fall Meet. Abstr.*, *1*, 4.

Montzka, S. A., M. Aydin, M. Battle, J. H. Butler, E. S. Saltzman, B. D. Hall, A. D. Clarke, D. Mondeel, and J. W. Elkins (2004), A 350-year atmospheric history for carbonyl sulfide inferred from Antarctic firn air and air trapped in ice, *J.Geophys.Res.*, *109*, D22302, doi:10.1029/2004JD004686.

Montzka, S. A., P. Calvert, B. D. Hall, J. W. Elkins, T. J. Conway, P. P. Tans, and C. Sweeney (2007), On the global distribution, seasonality, and budget of atmospheric carbonyl sulfide (COS) and some similarities to CO2, *J. Geophys. Res.*, *112*(D9), D09302, doi:10.1029/2006JD007665.

OICA (2016), Vehicles in use, *OICA*. Available from: http://www.oica.net/category/vehicles-in-use/ (Accessed 9 September 2016)

Peyton, T. O., R. V. Steele, and W. R. Mabey (1978), *Carbon disulfide, carbonyl sulfide: literature review and environmental assessment*, Environmental Protection Agency, Office of Health and Ecological Effects, Washington.

Pos, W. H., and H. Berresheim (1993), Automotive tire wear as a source for atmospheric OCS and CS2, *Geophys. Res. Lett.*, *20*(9), 815–817, doi:10.1029/93GL00972.

Protoschill-Krebs, G., C. Wilhelm, and J. Kesselmeir (1996), Consumption of carbonyl sulfide (COS) by higher plant carbonic anhydrase (CA), *Atmos. Environ.*, *30*(18), 3151–3156.

Ramankutty, N., and J. A. Foley (1999), Estimating Historical Changes in Land Cover: North American Croplands from 1850 to 1992, *Glob. Ecol. Biogeogr.*, *8*(5), 381–396.

Ramankutty, N., A. T. Evan, C. Monfreda, and J. A. Foley (2008), Farming the planet: 1. Geographic distribution of global agricultural lands in the year 2000, *Global Biogeochem. Cycles*, *22*, 19.

Randerson, J. T., G. R. van der Werf, L. Giglio, G. J. Collatz, and P. S. Kasibhatla (2015), Global Fire Emissions Database, Version 4, (GFEDv4), *ORNL DAAC*, doi:10.3334/ORNLDAAC/1293. Available from: https://daac.ornl.gov/VEGETATION/guides/fire_emissions_v4.html (Accessed 31 March 2017)

Sandoval-Soto, L., M. Stanimirov, M. von Hobe, V. Schmitt, J. Valdes, A. Wild, and J. Kesselmeier (2005), Global uptake of carbonyl sulfide (COS) by terrestrial

vegetation: Estimates corrected by deposition velocities normalized to the uptake of carbon dioxide (CO2), *Biogeosciences*, *2*(2), 125–132.

Sellers, P. J., Y. Mintz, Y. C. Sud, A. Dalcher, P. J. Sellers, Y. Mintz, Y. C. Sud, and A. Dalcher (1986a), A Simple Biosphere Model (SIB) for Use within General Circulation Models, *J. Atmos. Sci.*, *43*(6), 505–531, doi:10.1175/1520-0469(1986)043<0505:ASBMFU>2.0.CO;2.

Sellers, P. J., Y. Mintz, Y. C. Sud, A. Dalcher, P. J. Sellers, Y. Mintz, Y. C. Sud, and A. Dalcher (1986b), A Simple Biosphere Model (SIB) for Use within General Circulation Models, *J. Atmos. Sci.*, *43*(6), 505–531, doi:10.1175/1520-0469(1986)043<0505:ASBMFU>2.0.CO;2.

Smith, S. J., J. Van Aardenne, Z. Klimont, R. J. Andres, A. Volke, and S. D. Arias (2011), Anthropogenic sulfur dioxide emissions : 1850 – 2005, , 1101–1116, doi:10.5194/acp-11-1101-2011.

Stimler, K., S. A. Montzka, J. A. Berry, Y. Rudich, and D. Yakimir (2010), Relationships between carbonyl sulfide (COS) and CO2 during leaf gas exchange, *New Phytol. Trust*, *186*(4), 869–878.

Suntharalingam, P., A. J. Kettle, S. M. Montzka, and D. J. Jacob (2008), Global 3-D model analysis of the seasonal cycle of atmospheric carbonyl sulfide: Implications for terrestrial vegetation uptake, *Geophys. Res. Lett.*, *35*(19), L19801, doi:10.1029/2008GL034332.

Susa, D., and J. Haydary (2013), Sulphur distribution in the products of waste tire pyrolysis, *Chem. Pap.*, *67*(12), 1521–1526, doi:10.2478/s11696-012-0294-4.

The World Bank (2016), Population, total, *World Bank Open Data*. Available from: http://data.worldbank.org/ (Accessed 9 September 2016)

U.S. Energy Information Administration (2003), *Annual Energy Review 2002*, U.S. Department of Energy, Washington, D.C.

U.S. Energy Information Administration (2013), *International Energy Statistics*, Washington D.C.

U.S. Environmental Protection Agency (2003), *Compilation of Air Pollutant Emission Factors, Stationary Point and Area Sources, AP-42*, Washington, D.C.

U.S. Geological Survey (2012), USGS Minerals Information: Aluminum, Available from: http://minerals.usgs.gov/minerals/pubs/commodity/aluminum/

U.S. Geological Survey (2013), 2012 Minerals Yearbook: Aluminum, , 5.1-5.21. Available from: https://minerals.usgs.gov/minerals/pubs/commodity/aluminum/myb1-2012-alumi.pdf

U.S. Geological Survey (2015), Mineral Commodity Summaries: Titanium Dioxide, Available from: https://minerals.usgs.gov/minerals/pubs/commodity/titanium/

United Nations Statistics Division (2016a), Energy Statistics Database, Available from: http://unstats.un.org/unsd/energy/edbase.htm (Accessed 1 January 2017)

United Nations Statistics Division (2016b), Industry Statistics Database, Available from: http://unstats.un.org/unsd/industry//ics_intro.asp (Accessed 1 January 2016)

Utne, I., K. A. Paulsen, and J. Thonstad (1998), The Emission of Carbonyl Sulphide from prebake and Söderberg Aluminium Cells, *Light Met.*, 293–301.

Vainio, E., A. Brink, N. DeMartini, M. Hupa, H. Vesala, K. Tormonen, and T. Kajolinna

(2010), In-furnace measurement of sulfur and nitrogen species in a recovery boiler, *J. Pulp Pap. Sci.*, *36*(3–4), 135–142.

Wang, L., F. Zhang, and J. Chen (2001), Carbonyl sulfide derived from catalytic oxidation of carbon disulfide over atmospheric particles., *Environ. Sci. Technol.*, *35*(12), 2543–2547.

Wang, Y. et al. (2016), Towards understanding the variability in biospheric CO_2 fluxes: using FTIR spectrometry and a chemical transport model to investigate the sources and sinks of carbonyl sulfide and its link to CO_2, *Atmos. Chem. Phys.*, *16*(4), 2123–2138, doi:10.5194/acp-16-2123-2016.

Watts, S. F. (2000), The mass budgets of carbonyl sulfide, dimethyl sulfide, carbon disulfide and hydrogen sulfide, *Atmos. Environ.*, *34*(5), 761–779, doi:10.1016/S1352-2310(99)00342-8.

Whelan, M. E., T. W. Hilton, J. A. Berry, M. Berkelhammer, A. R. Desai, and J. E. Campbell (2016), Carbonyl sulfide exchange in soils for better estimates of ecosystem carbon uptake, *Atmos. Chem. Phys.*, *16*(6), 3711–3726, doi:10.5194/acp-16-3711-2016.

Zumkehr, A., and J. E. Campbell (2013), Historical U.S. cropland areas and the potential for bioenergy production on abandoned croplands, *Environ. Sci. Technol.*, *47*(8), 3840–3847.

Zumkehr, A., T. W. Hilton, M. Whelan, S. Smith, and J. E. Campbell (2017), Gridded anthropogenic emissions inventory and atmospheric transport of carbonyl sulfide in the U.S., *J. Geophys. Res. Atmos.*, doi:10.1002/2016JD025550.